



Government of  
Western Australia

Department of  
**Mines and Petroleum**

**REPORT  
129**

**SEDIMENTOLOGICAL AND STRUCTURAL  
EVOLUTION OF THE MOUNT RAGGED FORMATION,  
NORNALUP ZONE, ALBANY-FRASER OROGEN,  
WESTERN AUSTRALIA**

by P-J Waddell



Curtin University



**Geological Survey of Western Australia**



Government of **Western Australia**  
Department of **Mines and Petroleum**

**REPORT 129**

# **SEDIMENTOLOGICAL AND STRUCTURAL EVOLUTION OF THE MOUNT RAGGED FORMATION, NORNALUP ZONE, ALBANY–FRASER OROGEN, WESTERN AUSTRALIA**

by  
P-J Waddell

Perth 2014



**Geological Survey of  
Western Australia**



**Curtin University**

**MINISTER FOR MINES AND PETROLEUM**  
**Hon. Bill Marmion MLA**

**DIRECTOR GENERAL, DEPARTMENT OF MINES AND PETROLEUM**  
**Richard Sellers**

**EXECUTIVE DIRECTOR, GEOLOGICAL SURVEY OF WESTERN AUSTRALIA**  
**Rick Rogerson**

#### **REFERENCE**

**The recommended reference for this publication is:**

Waddell, P-J 2014, Sedimentological and structural evolution of the Mount Ragged Formation, Nornalup Zone, Albany–Fraser Orogen, Western Australia: Geological Survey of Western Australia, Report 129, 116p.

**National Library of Australia Cataloguing-in-Publication entry:**

**Author:** Waddell, Peter-Jon, author.  
**Title:** Sedimentological and structural evolution of the Mount Ragged Formation, Nornalup Zone, Albany-Fraser Orogen, Western Australia / Peter-Jon Waddell.  
**ISBN:** 9781741685329 (ebook)  
**Subjects:** Sedimentation and deposition--Western Australia--Albany-Fraser Orogen.  
Seismites--Western Australia--Albany-Fraser Orogen.  
Sedimentary structures--Western Australia--Albany-Fraser Orogen.  
Sediments (Geology)--Western Australia--Albany-Fraser Orogen.  
**Other Authors/Contributors:** Geological Survey of Western Australia  
**Dewey Decimal Classification:** 551.809941

**ISSN 0508–4741**

Grid references in this publication refer to the Geocentric Datum of Australia 1994 (GDA94). Locations mentioned in the text are referenced using Map Grid Australia (MGA) coordinates, Zone 51. All locations are quoted to at least the nearest 100 m.

#### **About this publication**

This Report is an MSc thesis researched, written and compiled through an ongoing collaborative project between the Geological Survey of Western Australia (GSWA) and Curtin University. Although GSWA has provided field and sample support for this project, the scientific content of the Report, and the drafting of figures, has been the responsibility of the author. No editing has been undertaken by GSWA.

#### **Disclaimer**

This product was produced using information from various sources. The Department of Mines and Petroleum (DMP) and the State cannot guarantee the accuracy, currency or completeness of the information. DMP and the State accept no responsibility and disclaim all liability for any loss, damage or costs incurred as a result of any use of or reliance whether wholly or in part upon the information provided in this publication or incorporated into it by reference.

#### **Published 2014 by Geological Survey of Western Australia**

This product is published in digital format (PDF) and is available online at <[www.dmp.wa.gov.au/GSWApublications](http://www.dmp.wa.gov.au/GSWApublications)>.

#### **Further details of geological publications and maps produced by the Geological Survey of Western Australia are available from:**

Information Centre  
Department of Mines and Petroleum  
100 Plain Street  
EAST PERTH WESTERN AUSTRALIA 6004  
Telephone: +61 8 9222 3459 Facsimile: +61 8 9222 3444  
[www.dmp.wa.gov.au/GSWApublications](http://www.dmp.wa.gov.au/GSWApublications)

**Cover photograph:** The prominent ridges of the Mount Ragged Formation protrude through the surrounding plain of Cape Arid National Park. Photo by Peter-Jon Waddell.

**Sedimentological and structural evolution  
of the Mount Ragged Formation,  
Nornalup Zone, Albany-Fraser Orogen,  
Western Australia**

By

Peter-Jon Waddell

Student Number: 9033018

Geology Project 604

MSc (Geology)

Department of Applied Geology  
WA School of Mines  
Curtin Univerisity



## **Abstract**

The Mount Ragged Formation is located in the eastern Nornalup Zone of the Albany-Fraser Orogen, Western Australia. To characterise the sedimentological and structural development of the Mount Ragged Formation it was necessary to conduct geological field mapping, interpret aerial photography and aeromagnetic datasets, perform facies and sedimentary petrography analysis, perform structural analysis on field data, and compare Geological Survey of Western Australia Warox basement datasets gathered from rocks of the Nornalup Zone in the vicinity of the Mount Ragged Formation.

Based on new geochronological age data obtained from U-Pb zircon analysis the maximum deposition age of the protolith sediments for the Mount Ragged Formation is  $1314 \pm 19$  Ma, which indicates deposition may have started during Stage I (c. 1345-1260 Ma) of the Albany-Fraser Orogeny. New geochronological age data constrains the magmatic age of crystallisation of the Scott Rock monzogranite to  $1175 \pm 12$  Ma. The truncation of the Mount Ragged Formation by the Scott Rock monzogranite constrains the minimum age for the deposition of Ragged Basin sediments to  $1175 \pm 12$  Ma.

The sediments of the Ragged Basin are considered to have been deposited within a shallow intracratonic basin by a large fluvial system dominated by a shifting complex of sandy braided channels. The gradual coarsening upwards sequence of lithofacies suggests the depositional setting was a distal fluvial environment characterised by channel migration and abandonment changing to a proximal fluvial environment characterised by rapid periods of sedimentation and coarser deposits.

In view of the structural data and field observations presented herein, in conjunction with the interpretation of aeromagnetic imagery, the Mount Ragged Formation, rather than representing an echelon pair of northeast-trending synclines as previously thought (Lowry and Doepel 1974), represents a zone where regional strain was partially accommodated through the deformation and subsequent emplacement of fault-bound metasedimentary packages.

## **Acknowledgements**

The author wishes to thank Dr. Nick Timms from Curtin University, Department of Applied Geology for supervision throughout the project. His advice and enthusiasm for the project was greatly valued.

Thanks to Dr. Catherine Spaggiari from the Geological Survey of Western Australia, Department of Mines and Petroleum for initiating the project, as well as organising logistical support and providing advice throughout the project.

Thanks also to the numerous staff of the Geological Survey of Western Australia for their assistance in many aspects of the project. In particular thanks to: Mr. Stewart Jefferys for provision of gridded aerial photographs for fieldwork; Mr. Ray Addenbrooke and Mr. Conrad Salay for organising the loan of survey vehicles and their assistance in vehicle preparation, equipment and field logistics; Ms. Ostiane Massiani for her assistance in fieldwork and for managing the field camps; Mr. John Kirk for assistance and advice on producing digital maps and other GIS queries; Dr. Chris Kirkland and Dr. Michael Wingate for making the effort to get geochronological analysis of samples relevant to this study completed in time for inclusion in this report.

Thanks also to the Department of Parks and Wildlife (DPaW) for permission to work in the Cape Arid National Park and to the staff of the DPaW Esperance office for their advice during the planning of fieldwork.

Further thanks to staff at Curtin University, Department of Applied Geology for their assistance throughout my time at the university whilst undertaking geological study. In particular: Dr. Ian Fitzsimons and Dr. Katy Evans for always making themselves available at short notice to discuss geology; Mrs. Annette Labrooy for help with administrative queries and problems; and Dr. Chris Clark for supplying Figure 5. included herein.

Finally the author wishes to thank everyone who assisted in and provided camaraderie during fieldwork. In particular, special thanks to Ms. Ostiane Massiani and Dr. Peter Russell for their willingness to repeatedly hike through such densely vegetated, steep terrain whilst cheerfully dealing with each new scenario encountered at every location.

## Table of Contents

1.0	Introduction.....	1
1.1	Objectives .....	1
1.2	Significance .....	1
1.3	Previous investigations .....	3
1.4	Affirmation of research .....	4
2.0	Regional Geology .....	5
2.1	Tectonic setting of the Albany-Fraser Orogen .....	5
2.2	Tectonic subdivisions of the Albany-Fraser Orogen .....	5
2.2.1	Northern Foreland.....	5
2.2.1.1	Munglinup Gneiss.....	7
2.2.1.2	Barren Basin Sediments.....	8
2.2.1.2.1	Stirling Range Formation.....	8
2.2.1.2.2	Mount Barren Group.....	10
2.2.1.2.3	Woodline Formation.....	12
2.2.2	Kepa Kurl Booya Province.....	13
2.2.2.1	Biranup Zone .....	13
2.2.2.2	Fraser Zone .....	14
2.2.2.3	Nornalup Zone .....	15
2.2.2.4	Arid Basin Sediments .....	16
2.2.2.4.1	Malcolm Metamorphics.....	18
2.2.2.4.2	Paragneissic rocks from the western Nornalup Zone .....	18
2.2.2.4.3	Gwynne Creek Gneiss .....	19
2.2.2.4.4	Metasedimentary rocks of the Fraser Range Metamorphics .....	19
2.2.2.5	Recherche and Esperance Supersuites.....	20
2.2.2.6	Ragged Basin Sediments .....	21
2.2.2.6.1	Salisbury Gneiss .....	21
2.2.2.6.2	Mount Ragged Formation.....	22
2.3	Tectonic history of the Albany-Fraser Orogen.....	23
2.3.1	Biranup Orogeny .....	23
2.3.2	Albany-Fraser Orogeny .....	23
3.0	Methods and analytical procedures.....	25
3.1	Local setting .....	25
3.2	Fieldwork.....	25
3.3	Sampling.....	28
3.4	Geophysical datasets.....	29

3.5	Stereographic projection of structural data.....	29
4.0	Mapping and field observations.....	31
4.1	Sedimentary rocks (Mount Ragged Formation).....	31
4.1.1	Sedimentary log descriptions.....	31
4.1.2	Lithofacies analysis of the Mount Ragged Formation .....	40
4.1.2.1	Facies A: Metapelite to laminated metasilstone .....	42
4.1.2.2	Facies B: Planar-laminated, fine-grained metasandstone .....	42
4.1.2.3	Facies C: Cross-bedded, medium-grained quartzite .....	43
4.1.2.4	Facies D: Coarse-grained quartzite.....	44
4.1.2.5	Facies E: Quartz gritstone to pebble conglomerate .....	44
4.1.2.6	Facies summary .....	45
4.2	Igneous rocks (Prominent local Nornalup Zone outcrop) .....	46
4.2.1	Gora Hill.....	46
4.2.2	Junana Rock.....	46
4.2.3	Juranda Rockhole .....	46
4.2.4	Outcrop northeast of Gora Hill.....	47
4.2.5	Pine Hill.....	47
4.2.6	Scott Rock.....	47
4.2.7	She-oaks Hill .....	48
4.2.8	Wolgrah Hill.....	48
4.3	Geophysical interpretation .....	48
4.4	Structural data .....	50
4.4.1	Mica Hill.....	50
4.4.2	Mount Esmond .....	52
4.4.3	Mount Ragged .....	53
4.4.4	Russell Range .....	54
4.5	Metamorphism .....	55
4.6	Detrital zircon U-Pb geochronology .....	60
5.0	Discussion.....	61
5.1	Depositional environment of the Ragged Basin sediments.....	61
5.2	Regional-scale structural architecture of the Mount Ragged Formation ....	63
5.2.1	Aeromagnetic interpretation .....	63
5.3	Structural history of the Mount Ragged Formation .....	65
5.4	Timing constraints for the development of the Mount Ragged Formation.	71
5.5	Controls on sedimentary basin style .....	73
5.6	Summary of the tectonic evolution of the Mount Ragged Formation .....	75

5.7 Future investigations .....	78
6.0 Conclusion .....	79
7.0 References.....	81
Appendices List.....	84
Appendix 1 .....	85
Figure A1.1: Aerial photograph of Mica Hill .....	85
Figure A1.2: Aerial photograph of Mount Esmond, Mount Dean and Brook Peak .....	86
Figure A1.3: Aerial photograph of Mount Ragged.....	87
Figure A1.4: Aerial photograph of Russell Range.....	88
Appendix 2 .....	89
Table A2.1: Mount Ragged Formation sample catalogue .....	89
Appendix 3 .....	90
Figure A3.1: Russell Range sedimentary log.....	90
Appendix 4 .....	92
Map of GSWA Warox sites in the vicinity of the Mount Ragged Formation ...	92
Table A4.1: GSWA Warox sites in the vicinity of the Mount Ragged Formation .....	93
Appendix 5 .....	96
Figure A5.1: Aeromagnetic image of Mount Ragged Formation (reduction to pole; normal).....	96
Figure A5.2: Aeromagnetic image of Mount Ragged Formation (reduction to pole, first vertical derivative; sun angle northwest) .....	97
Appendix 6 .....	98
Figure A6.1: Geological map of Mica Hill .....	98
Figure A6.2: Geological map of Mount Esmond.....	99
Figure A6.3: Geological map of Mount Ragged.....	100
Figure A6.4: Geological map of Russell Range.....	101
Appendix 7 .....	102
Figure A7.1: Mica Hill structural data .....	102
Figure A7.2: Mount Esmond structural data.....	103
Figure A7.3: Mount Ragged structural data.....	104
Figure A7.4: Russell Range structural data.....	105

## List of figures

Figure 1. Previous interpretation of the structural relationship in the northern part of the Mount Ragged Formation.....	4
Figure 2. Crustal elements of easternmost Gondwana.....	6
Figure 3. Geological map of the Albany-Fraser Orogen showing the main lithotectonic units.....	7
Figure 4. Time-spaced plot showing age relationships between the Northern Foreland, Biranup Zone, Fraser Zone and Nornalup Zone.....	9
Figure 5: Tectonic model of the Albany-Fraser Orogeny.....	17
Figure 6. 1:100,000 aerial photographs of the project area.....	26
Figure 7. Surface geology of the Mount Ragged Formation and surrounding area.....	27
Figure 8. Location map and legend for Mount Ragged sedimentary logs.....	33
Figure 9a. Mount Ragged sedimentary log 1.1.....	34
Figure 9b. Mount Ragged sedimentary log 1.2.....	35
Figure 10a. Mount Ragged sedimentary log 2.1.....	36
Figure 10b. Mount Ragged sedimentary log 2.2.....	37
Figure 11a. Mount Ragged sedimentary log 3.1.....	38
Figure 11b. Mount Ragged sedimentary log 3.2.....	39
Figure 12. Sedimentary structures common to the Mount Ragged Formation.....	40
Figure 13. Plane-polarised light and cross-polarised light images of Mount Ragged formation facies.....	41
Figure 14. a) Metapelite schist and metasilstone beds; b) Andalusite-bearing metasilstone.....	42
Figure 15. Fine-grained, planar laminated metasandstone.....	43
Figure 16. a) Tangential toe-sets in planar cross-bedded medium-grained quartzite; b) Truncated cross-beds in medium-grained quartzite.....	43
Figure 17. Poorly-sorted, coarse-grained quartzite.....	44
Figure 18. Well-sorted, pebble conglomerate quartzite.....	45
Figure 19. Aeromagnetic image of Mount Ragged Formation and surrounds (reduction to pole; sun angle directly overhead).....	49
Figure 20. Folded cross-beds in coarse-grained quartzite.....	51
Figure 21. Chaotic bedding in coarse-grained quartzite, inferred to be a synform hinge zone.....	52
Figure 22. Small-scale S-folds in medium-grained, quartzite.....	54
Figure 23. Deposition and metamorphic setting of Mount Ragged Formation.....	55
Figure 24. Photomicrographs of characteristic mineral assemblages and features in metasediments from the Mount Ragged Formation.....	57
Figure 25. a) Andalusite-bearing metapelite schist; b) Andalusite crystals with reaction rims in metapelite schist.....	58

Figure 26. Quartz veins a) Small-scale folded and sheared quartz veins in andalusite-bearing metapelite; b) Post deformation, quartz vein tension-gash array in medium-grained quartzite .....	58
Figure 27. Viridine-bearing quartz vein between beds of medium-grained quartzite....	59
Figure 28. Photomicrographs of plane-polarised light images of various forms of viridine.....	59
Figure 29. Basement map of Mount Ragged Formation project area .....	64
Figure 30. Diagrammatic cross-sections demonstrating the relationship between fold and thrust faults .....	68
Figure 31. Photographs of suspected displacement features in the Mount Ragged Formation .....	70

### **List of tables**

Table 1. Primary characteristics of the facies units of the Mount Ragged Formation ...	45
Table 2. Summary of SHRIMP sample locations, preliminary ages of magmatic crystallisation of igneous outcrop in the vicinity of the Mount Ragged Formation.....	60
Table 3. Summary of SHRIMP sample locations, and preliminary maximum deposition ages of Mount Ragged Formation metasedimentary rocks .....	60
Table A2.1 (Appendix 2). Mount Ragged Formation sample catalogue .....	89
Table A4.1 (Appendix 4). Geological Survey of Western Australia Warox sites in the vicinity of the Mount Ragged Formation .....	93

### **Plates**

Plate 1: Compilation of structural data for the Mount Ragged Formation
--

## **1.0 Introduction**

### **1.1 Objectives**

To determine the sedimentological and structural evolution of the Mount Ragged Formation within the Nornalup Zone of the Albany-Fraser Orogen, Western Australia.

Through studying the sedimentological and structural evolution of the Mount Ragged Formation this investigation attempts to determine the sedimentary fill style of the formation's basin, as well as how stratigraphic intervals have been influenced by the tectonic setting during and/or after deposition.

Background information considered relevant to this project includes the comparison of the different metasedimentary formations located within the Albany-Fraser Orogen, and determine whether similarities exist in their depositional fill, structural development and deformation in association with fold-thrust belts.

To achieve the objectives to characterise the sedimentological and structural development of the Mount Ragged Formation of the Nornalup Zone it was necessary to:

- conduct geological field mapping,
- interpret aerial photography and other digital geophysical datasets,
- perform facies and structural analysis on field data,
- perform petrography analysis on samples from the Mount Ragged Formation, and
- compare GSWA Warox basement datasets gathered from rocks of the Nornalup Zone in the vicinity of the Mount Ragged Formation

### **1.2 Significance**

It is anticipated that through detailed study of the sedimentological and structural evolution of the Mount Ragged Formation information critical to the formation's evolution and development can be ascertained. This will facilitate current studies been undertaken by the Geological Survey of Western Australia (GSWA) to understand and describe the development of the Albany-Fraser Orogen.

Recent research led by the Geological Survey of Western Australia focused in the Mesoproterozoic Albany-Fraser Orogen has led to much re-interpretation of its

development. The Albany-Fraser Orogeny is divided into two stages of tectonic activity (Stage I: continental collision between c. 1345-1260 Ma and Stage II: intracratonic reactivation between c. 1215-1140 Ma) (Clark *et al.* 2000; Bodorkos & Clark 2004b), though magmatic rocks deformed in the Zanthus Event (c. 1680 Ma) also form a large component of the orogen (Kirkland *et al.* 2011a). The southern and southeastern margin of Yilgarn Craton of Western Australia are characterised by the presence of outliers of Proterozoic quartz-rich metasedimentary rocks. The spatial distribution of these metasedimentary rocks along the margin of the orogen suggests that their formation was related to tectonic activity along the margin of the Yilgarn Craton, when it was reworked during the Paleoproterozoic Biranup Orogeny and the Mesoproterozoic Albany-Fraser Orogeny (Spaggiari *et al.* 2011).

Previous interpretations considered the former Biranup Complex to be an allochthonous terrane of Archean and Proterozoic crust accreted to the Yilgarn Craton during the Albany-Fraser Orogeny (Myers 1990; Nelson *et al.* 1995; Myers *et al.* 1996; Clark *et al.* 2000). Similarly, some of the Paleoproterozoic metasedimentary rocks (i.e. the Mount Barren Group) of the Albany-Fraser Orogen were also thought to represent synorogenic sedimentary packages allochthonous to the Yilgarn Craton (Nelson *et al.* 1995; Myers 1995b; Witt 1998). However, based on similarities in lithology, protolith age (Spaggiari *et al.* 2009) and Lu-Hf data (Kirkland *et al.* 2011a, 2011b) the southern margin of the Yilgarn Craton is now interpreted as a reworked, autochthonous terrane and the Paleoproterozoic metasedimentary rock sequences as autochthonous to the Yilgarn Craton (Hall *et al.* 2008; Kirkland *et al.* 2011a; Spaggiari *et al.* 2011).

Though having variable provenance, these Paleoproterozoic metasedimentary rock sequences are linked by the same sedimentary cycle forming inboard remnants of a large basinal system along the craton margin (Hall *et al.* 2008; Spaggiari *et al.* 2009, 2011). The Mesoproterozoic metasedimentary rocks (Salisbury Gneiss and Mount Ragged Formation) of the Albany-Fraser Orogen, whilst having no obvious analogue to the Paleoproterozoic metasedimentary rocks in the western portion of the orogen, are also considered autochthonous having being derived from the Albany-Fraser Orogen during a period of extension and erosion between Stages I and II (c. 1260-1215 Ma) of the Albany-Fraser Orogeny (Clark *et al.* 2000; Bodorkos & Clark 2004b; Spaggiari *et al.* 2011). However, there are no detailed studies of the sedimentary fill and structural architecture of the Mount Ragged Formation, and consequently little is known about the style of sedimentary basin in

which the metasediments were originally deposited, or about their subsequent deformation history.

In particular, this project will yield information that will facilitate studies comparing the depositional fill and structural development of metasedimentary formations located within the Albany-Fraser Orogen and their deformation in fold and thrust belts. Ongoing studies by GSWA into the Albany-Fraser Orogen have been focusing on (a) the various sediment cycles that occurred during orogenic events through the erosion of the different tectonic units of the Albany-Fraser Orogen; and (b) if and how the emplacement of the metasedimentary formations may be related to a common tectonic structure (in e.g. a regional fold-thrust belt setting), despite their different provenance. In the current GSWA model, sediments of the Mount Ragged Formation are considered part of a unique package of sediments belonging to a third cycle of sedimentation that occurred after stage I of the Albany-Fraser Orogeny in the recently termed the Ragged Basin (Spaggiari *et al.* 2011).

### **1.3 Previous investigations**

Lowry and Doepel (1974) interpreted the exposures of the Mount Ragged Formation as belonging to an echelon pair of northeast-trending synclines (Figure 1). The western limb of a northern syncline is formed by Mount Ragged and Russell Range. The eastern limb is formed by Mount Esmond, Mount Dean and Brook Peak, with Mica Hill and the Diamonds Hill making up the southern portion of the structure.

The absence of surface outcrop in the vicinity of this proposed syncline makes the hypothesis of Lowry and Doepel (1974) hard to prove. Likewise, the insufficiency of outcrop around the southern exposures of the Mount Ragged Formation (i.e. Mica Hill and Diamonds Hill) similarly makes it hard to substantiate the existence of a large-scale fold structure. Furthermore, the presence of the Scott Rock monzogranite, which occurs within Lowry and Doepel's (1974) proposed syncline, complicates this theory. New geochronology, presented herein, as well as the cross-cutting relationship this monzogranite intrusion has with the Mount Ragged Formation provide salient evidence for disproving the theory that the Mount Ragged Formation is a single large-scale syncline.

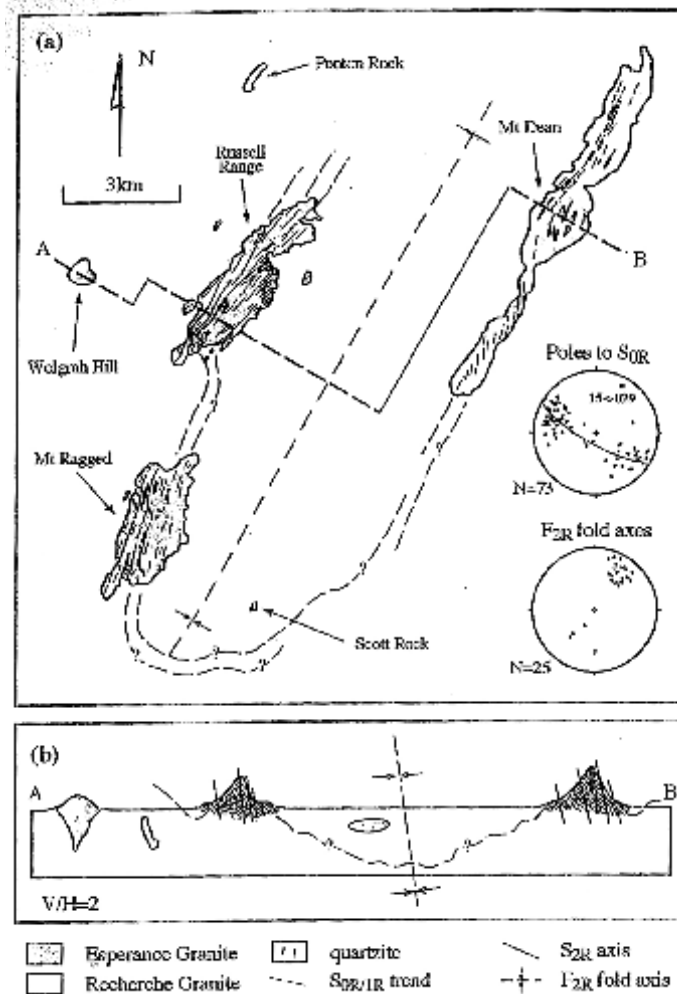


Figure 1. Previous interpretation of the structural relationship in the northern part of the Mount Ragged Formation (Page 74, Clark 1999). a) Outcrop map with bedding trends marked. The apparent double-plunge of small fold structures is an artefact of topography. The large-scale syncline is as inferred by Lowry and Doepel (1974). b) Interpretive cross-section through A-B (to scale). The large-scale fold is consistent with the structural data and the style of smaller folds but cannot be proven to exist from the limited outcrop. Granitic rocks intrude the core of the inferred fold.

#### 1.4 Affirmation of research

All aerial photographs were provided by and used with the permission of the Western Australian Land Information Authority trading as Landgate. All geophysical images and Warox site information were provided by the Geological Survey of Western Australia. Samples were collected during fieldwork or provided by GSWA from D.Clark's PhD thesis (Clark 1999). Thin sections were prepared by Spectrum Petrographics Inc. Age data presented was provided by GSWA and referenced as such, unless referenced as otherwise. All other data, observations and results were attained by the author, unless referenced as otherwise.

## **2.0 Regional Geology**

### **2.1 Tectonic setting of the Albany-Fraser Orogen**

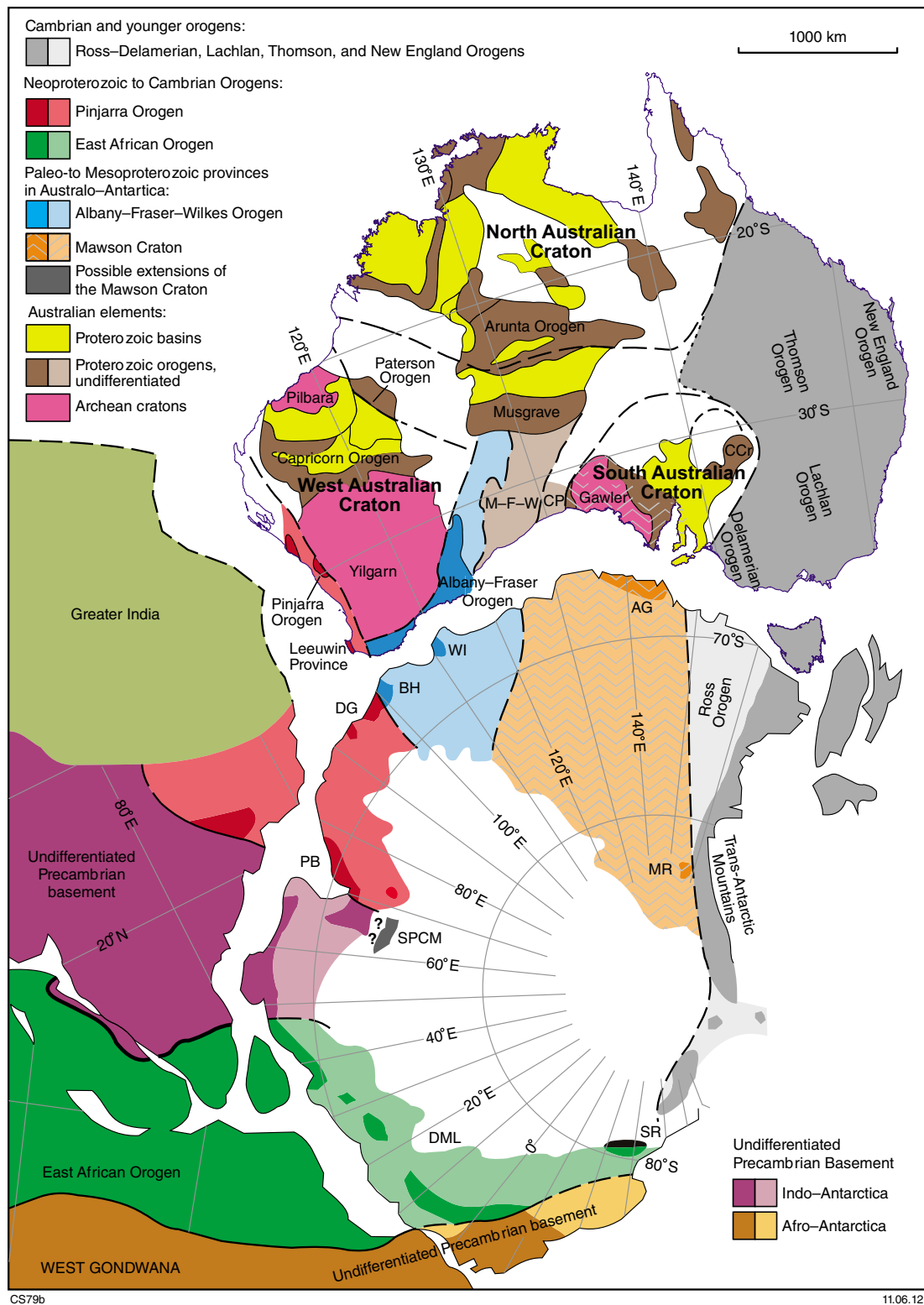
The Albany-Fraser Orogen consists of Proterozoic rocks that outcrop along the southern coast of Western Australia. The orogen is an arcuate orogenic belt adjoining the southern and southeastern margins of the Archaean Yilgarn Craton. The belt represents the Mesoproterozoic continental-continental collision between the combined North and West Australian Cratons and the combined South Australian and East Antarctic Cratons (Myers *et al.* 1996; Fitzsimons 2003; Bodorkos & Clark 2004b; Fitzsimons & Buchan 2005) (Figure 2). The orogen is considered to have developed as the south- and southeastern margins of the Yilgarn Craton were reworked during the Paleoproterozoic Biranup Orogeny (Kirkland *et al.* 2011a) and the Mesoproterozoic Albany-Fraser Orogeny (Clark *et al.* 2000; Bodorkos & Clark 2004b). The Albany-Fraser Orogeny is divided into two tectonic events; Stage I (c. 1345-1260 Ma) representing continental collision and Stage II (c. 1215-1140 Ma) interpreted as representing intracratonic reactivation (Clark *et al.* 2000; Bodorkos & Clark 2004a, b; Spaggiari *et al.* 2009).

Based on geophysical and structural interpretations, combined with geochronology, the orogen has been subdivided into several lithotectonic units (Beeson *et al.* 1988; Myers 1985, 1990, 1995b; Spaggiari *et al.* 2009, 2011; Kirkland *et al.* 2011a, 2011b). These lithotectonic units include the Northern Foreland, the Kepa Kurl Booya Province, and the Recherche and Esperance Supersuites. The Kepa Kurl Booya Province is further subdivided into the Biranup Zone, the Fraser Zone and the Nornalup Zone (Spaggiari *et al.* 2009) (Figure 3).

### **2.2 Tectonic subdivisions of the Albany-Fraser Orogen**

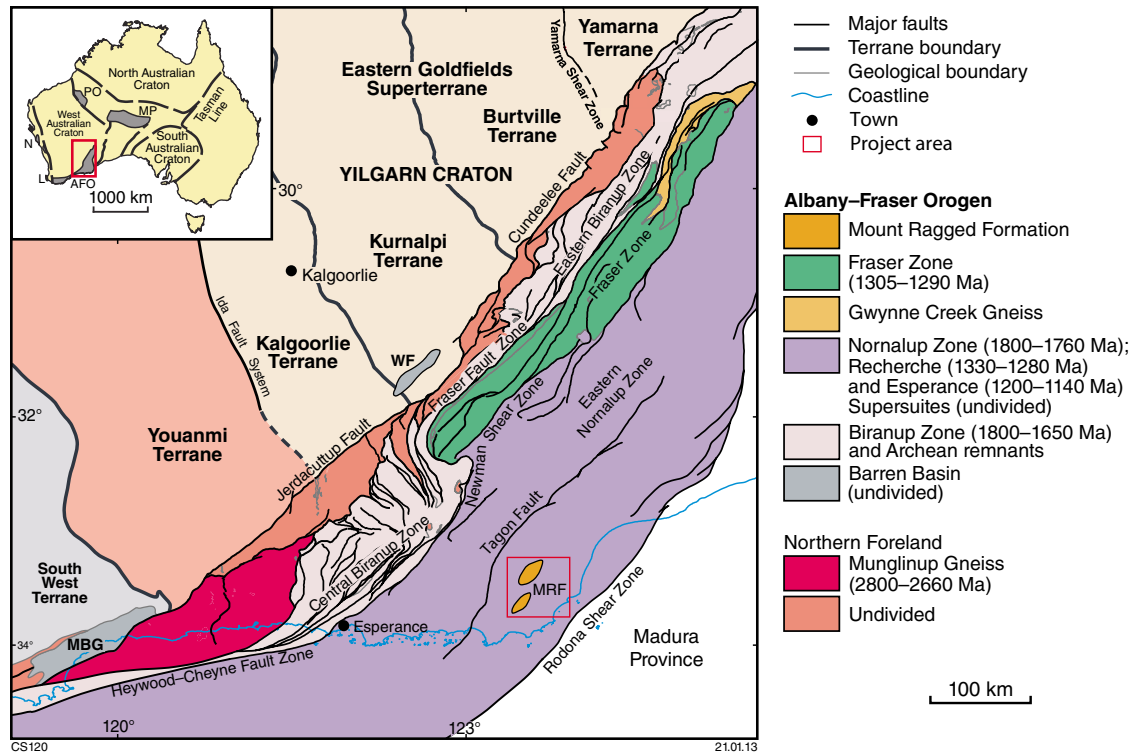
#### **2.2.1 Northern Foreland**

The northernmost lithotectonic unit of the Albany-Fraser Orogen is the Northern Foreland (Figure 3). It represents the southern and southeastern margin of the Yilgarn Craton that was reworked during the Albany-Fraser Orogeny, indicating its close association with the collisional orogenic belt (Myers 1990; Spaggiari *et al.* 2009). The Northern Foreland is dominated by the Munghlinup Gneiss (Section 2.2.1.1). Also included in the Northern Foreland are Late Proterozoic metasedimentary packages (Section 2.2.1.2).



**Figure 2. Crustal elements of easternmost Gondwana. (Spaggiari *et al.* 2009 – modified from references cited therein).**

Where paler and darker shades of the same colour are shown, the paler shade indicates large areas without outcrop where crustal element is inferred. AG, Terre Adélie-King George V Land; BH, Bungar Hills; CC, Coompana Complex (concealed by the Officer and Eucla Basins); CCr, Curnamona Craton; DG, Denman Glacier region; DML, Dronning Maud Land; M-F-W, Madura, Forrest and Waigen Complexes (undivided; concealed by the Officer and Eucla Basins); MR, Miller Range; PB, Prydz Bay; SPCM, southern Prince Charles Mountains; SR, Shackleton Range; WI, Windmill Islands.



**Figure 3. Geological map of the Albany-Fraser Orogen showing the main lithotectonic units. (Spaggiari *et al.* 2009 – adapted from Tyler & Hocking 2001; Fitzsimons & Buchan 2005 and Geological Survey of Western Australia 2007). MBG, Mount Barren Group; MRF, Mount Ragged Formation; SRF, Stirling Range Formation; WF, Woodline Formation.**

The Yilgarn Craton margin that was reworked in the Northern Foreland reflects a reduction in strain and metamorphic grade with increasing northward distance from the orogen, or exhumation of shallower crustal levels. Metamorphic conditions in the Northern Foreland vary from high- to moderate-strain, ductile deformation at amphibolite-granulite facies (Munглиnup Gneiss and southern sections of the Mount Barren Group) to moderate- to low-strain, brittle to semi brittle, greenschist to amphibolite facies (Beeson *et al.* 1988; Myers 1995a; Jones 2006; Spaggiari *et al.* 2009).

### 2.2.1.1 Munглиnup Gneiss

The Munглиnup Gneiss consists of 3000–2600 Ma orthogneisses metamorphosed to amphibolite-granulite facies, interlayered with lenses of metamorphosed mafic rocks, with minor banded metachert (jaspilite), amphibolite schist, serpentinite, and metamorphosed ultramafic rocks (Beeson *et al.* 1988; Myers 1990; Spaggiari *et al.* 2009).

Initially the Munglinup Gneiss was considered a gneissic unit derived from Archean granite, granodiorite, tonalite, and pegmatite within the former Biranup Complex (Myers 1995b). This description correlated with the interpretation that the former Biranup Complex was an allochthonous terrane of Archean and Proterozoic crust accreted to the Yilgarn Craton during the Albany-Fraser Orogeny (Myers *et al.* 1996). However, based on similarities in lithology, protolith age (Spaggiari *et al.* 2009) and Lu-Hf data (Kirkland *et al.* 2011a, 2011b) the Munglinup Gneiss is now interpreted as a reworked portion of the Yilgarn Craton southern margin. Geochronological analysis further supports the protolith of the orthogneiss component being of Yilgarn Craton origin; four phases of granitic magmatism dated at c. 2709, 2680, 2660, and 2630 Ma are equivalent to typical ages of granite magmatism in the Yilgarn Craton (Spaggiari *et al.* 2011 and references cited therein).

#### 2.2.1.2 Barren Basin Sediments

Within the Northern Foreland are a series of Late Proterozoic fault-bound, metasedimentary packages belonging to the Stirling Range Formation, Mount Barren Group and Woodline Formation, as well as isolated occurrences of quartzite and metaconglomerate in the northeast (Thom *et al.* 1984; Muhling & Brakel 1985; Hall *et al.* 2008; Spaggiari *et al.* 2009, 2011). Collectively they are considered to represent the sedimentary units of the Barren Basin and belong to the initial cycle of sedimentation that took place prior to the Albany-Fraser Orogeny (Spaggiari *et al.* 2011) (Figure 4).

The Yilgarn Craton forms the basement for these metasedimentary successions. They are interpreted as inboard remnants of a major system of related or linked basins that evolved along and distal to the margin of the Craton, but with variable provenance (Hall *et al.* 2008; Spaggiari *et al.* 2009, 2011). The evolution of the Barren Basin system, in which cycle one sediments were deposited, is considered to have occurred in a rift- or back-arc setting, along an active margin during the Biranup Orogeny (Spaggiari *et al.* 2011).

##### 2.2.1.2.1 Stirling Range Formation

The Stirling Range Formation is situated approximately 80 kilometres north-northeast of Albany, WA, in the Stirling Range National Park. The Formation is approximately 1600 metres thick and consists of quartzite, shale, slate and phyllite (Muhling & Brakel 1985).

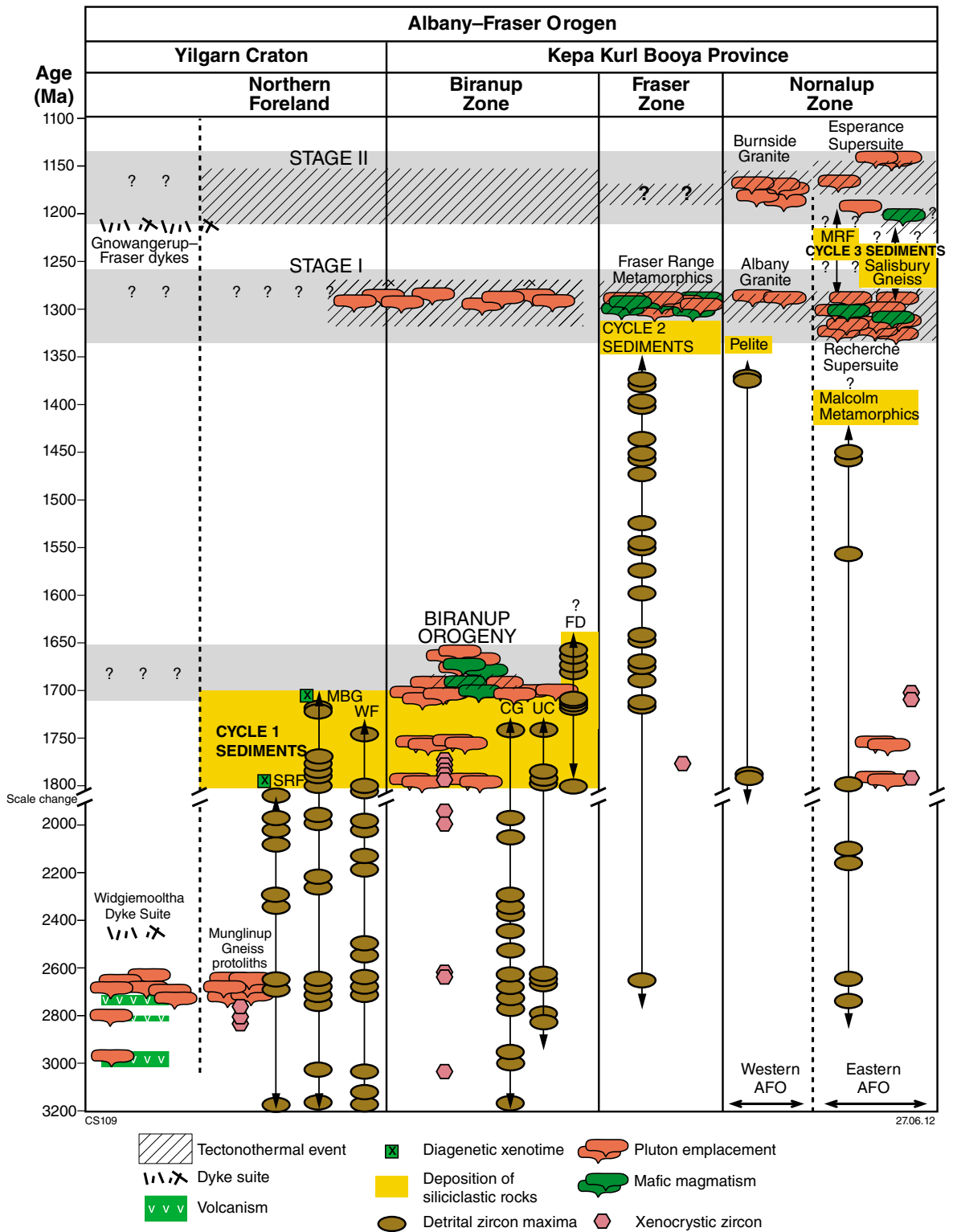


Figure 4. Time-spaced plot showing age relationships between the Northern Foreland, Biranup Zone, Fraser Zone and Nornalup Zone. (Spaggiari *et al.* 2011 – adapted from Fitzsimons & Buchan 2005; Spaggiari *et al.* 2009). MBG, Mount Barren Group; MRF, Mount Ragged Formation; SRF, Stirling Range Formation; WF, Woodline Formation.

Despite the lack of a completely exposed section for the entire formation, the Stirling Range Formation has been informally divided into three lithological units. The basal unit consists of a pink, fine-grained, well-sorted quartz arenite. Based on the consistent direction of tabular cross-bedding, which are common features, the paleocurrent direction is towards the southeast (Muhling & Brakel 1985). The middle unit is dominated by fine- and medium-grained, quartz arenite interbedded with thin beds of slate and phyllite. The middle unit is gradationally overlain by the uppermost unit as light-coloured, medium-grained quartz arenite begins to dominate (Muhling & Brakel 1985).

U-Pb SHRIMP dating of detrital zircons and diagenetic xenotime from the Stirling Range Formation indicated deposition occurred between a maximum age of  $2016 \pm 6$  Ma (Rasmussen *et al.* 2002) to minimum age  $1800 \pm 14$  Ma (Rasmussen *et al.* 2004). Based on a variety of sedimentary structures and paleocurrent analysis a tide-dominated, shallow-marine environment is considered to be the depositional setting (Cruse 1991; Cruse & Harris 1994).

The beds of the Stirling Range Formation are incorporated into the long limbs of large, asymmetric first-generation folds that gently dip southwards; these have been refolded by large-scale, open folds along east-west axes (Muhling & Brakel 1985). The metasediments of the formation have been metamorphosed to sub-greenschist to lower-greenschist facies. U-Th-Pb analysis of monazite overgrowths from interbedded sandstone and shale units within the Stirling Range Formation indicated metamorphism occurred around  $1215 \pm 20$  Ma (Rasmussen *et al.* 2002), which supports earlier Rb-Sr dates of 1312 Ma to 1126 Ma (Turek & Stephenson 1966).

#### 2.2.1.2.2 Mount Barren Group

The Mount Barren Group is located in the Fitzgerald River National Park, WA covering a strike length of about 120 kilometres, from Bremer Bay to east of Ravensthorpe, and lie approximately 100 km east of the Stirling Range Formation.

Consisting of a series of low hills comprised of Paleoproterozoic metasedimentary rocks, the Mount Barren Group comprises a thick succession (>1.2 km) of conglomerate, sandstone, mudrock and dolostone. The Group is divided into three formations: the Steere Formation; the Kundip Quartzite; and the Kybulup Schist (Thom & Chin 1984).

The Steere Formation is the lowermost unit and non-conformably overlies Archaean Manyutup Tonalite of the Yilgarn Craton (Thom *et al.* 1984); however, Witt (1997) proposed that the basal contact is a thrust fault. The basal portion consists of a thin basal conglomerate with clasts of quartzite, chert, banded-iron formation, and felsic volcanic rocks. Overlying these are several metres of bedded, pebbly sandstone and four metres of dolomitic limestone (Thom *et al.* 1984; Witt 1997). The Kundip Quartzite is predominantly composed of massive to coarsely bedded orthoquartzite, interbedded with mica- and magnetite-bearing quartzites and mudstones. The Kybulup Schist is the uppermost unit and consists of primarily thinly bedded pelitic and psammitic rocks of variable metamorphic grade. U-Pb SHRIMP dating of diagenetic xenotime determined a date for early diagenesis of unconsolidated sediments at  $1693 \pm 4$  Ma, which is interpreted as being closest to the depositional age for the Mount Barren Group (Vallini *et al.* 2002; 2005).

The metasedimentary rocks of the Mount Barren Group consist of lower-greenschist to upper-amphibolite facies. Structural examinations conclude that the Mount Barren Group is part of a northwest-vergent fold and thrust belt (Thom *et al.* 1984; Myers 1990; Witt 1998), with increased complexity in the south and southeast where the higher grade rocks occur (Witt 1998; Dawson *et al.* 2003). Within the Mount Barren Group folding and refolding is widespread on all scales, and thrust sheets occur within the group, further complicating sequences (Myers 1990; Fitzsimons & Buchan 2005). Kyanite-bearing, amphibolite facies rocks yielded SHRIMP U-Pb ages of  $1206 \pm 6$  Ma for xenotime and  $1194 \pm 4$  Ma for monazite, and this is interpreted as coinciding with peak thermal metamorphic conditions for the Mount Barren Group (Dawson *et al.* 2003).

Lithofacies associations of the Mount Barren Group are indicative of a small, possibly fault-bound basin (Dawson *et al.* 2002). The Mount Barren Group has been interpreted as a delta to shallow-marine sequence, with the Steere Formation representing fluvial or fluvial-deltaic sediments, the Kundip Quartzite representing a delta plain or upper delta-front, and the Kybulup Schist representing a lower delta-front, possibly with an upper prograding section (Witt 1997; 1998; Dawson *et al.* 2002; Vallini *et al.* 2002, 2005; Spaggiari *et al.* 2009).

### 2.2.1.2.3 Woodline Formation

This 50 kilometre long, north-easterly trending belt of quartz-rich metasedimentary rocks form a series of heavily vegetated low hills. They lie approximately 95 kilometres southeast of Kambalda, WA, and 350 kilometres to the northeast of the Mount Barren Group.

The Woodline Formation is over 250 metres thick. Sequences are dominated by mature, quartz-rich sandstone units interbedded with siltstones. The base of the formation is composed of white to light grey quartz-rich, well bedded sandstone, interbedded with pebble conglomerate. The basal sandstone unit displays predominantly planar-laminar bedding through coarse sandstone-granular conglomerate changing upwards to co-sets of 0.5-1.2 metre thick cross-beds, pebbly-conglomerates grading to medium sandstones, weakly bedded medium to coarse sandstones, and infrequent, thinly bedded, matrix-supported chert breccia. The lowermost unit is overlain by three, quartz-rich sandstone units, which include minor amounts of granular-pebble conglomerate, interbedded with laterally extensive, massive siltstone, tens of metres thick. Matrix- to clast-supported chert breccia and pebble-cobble conglomerates form minor units within various sequences of the unit (Hall *et al.* 2008).

The formation is mildly deformed and occupies a syncline. Beds are folded into open, upright north-easterly trending folds, contain a weak to moderately developed axial-planar cleavage and have been metamorphosed to lower-greenschist facies (Hall *et al.* 2008). Shallow dipping thrust faults also occur in the formation.

The dominance of mature quartz-rich sequences, in combination with the absence of any volcanic rocks, suggests proto-sources for the Woodline Formation were eroded Yilgarn Craton sediments, particularly the Eastern Goldfields Superterrane and the Youanmi Terrane. A paleoflow direction from the northwest further supports provenance derived from Yilgarn Craton sediments. Deposition occurred along a passive margin by fluvial processes transporting sediments in a south to south-easterly direction to a deltaic/continental shelf with long-shore currents. The depositional setting is interpreted as a distal fluvial environment changing to a marine-dominated setting between 1737 Ma and 1620 Ma (Hall *et al.* 2008).

### 2.2.2 Kepa Kurl Booya Province

The term Kepa Kurl Booya Province (Spaggiari *et al.* 2009) replaces the term Biranup Complex (Myers 1990, 1995b), and refers to major tectonic units that wrap around the southern and southeastern reworked margin of the Yilgarn Craton. Spaggiari *et al.* (2009) defined the Province as the crystalline basement of the Albany-Fraser Orogen; specifically the distinct crustal components affected by, and possibly amalgamated by, Stage I tectonism.

The former interpretation for the Province was provided by Myers (1990), who considered the Albany-Fraser Orogen to be composed of two main tectonic units; the inboard Biranup Complex and the outboard Nornalup Complex. The Biranup Complex consisted of an intensely deformed, component (later defined as the Dalyup Gneiss, Coramup Gneiss and Munglinup Gneiss) (Myers 1995b), and included the Fraser Complex (Myers 1985). Subsequently, the c. 2709-2630 Ma Munglinup Gneiss and the c. 1300 Ma Fraser Complex were removed from the Biranup Complex (Myers 1995b; Spaggiari *et al.* 2009; Kirkland *et al.* 2011a).

Spaggiari *et al.* (2009) subdivided the Kepa Kurl Booya Province into three major zones based on variable protolith ages and geological histories; the Biranup Zone (formerly the Biranup Complex, Myers 1990), the Fraser Zone (formerly the Fraser Complex, Myers 1985), and the Nornalup Zone (formerly the Nornalup Complex, Myers 1990). The granitic rocks of the Recherche (c. 1330-1280 Ma) and Esperance (c. 1200-1140 Ma) Supersuites intrude the southeastern portion of the Biranup Zone and most of the Nornalup Zone. The latter also being locally overlain by Mesoproterozoic cover rocks (Spaggiari *et al.* 2009).

#### 2.2.2.1 Biranup Zone

The Biranup Zone is primarily composed of mid-crustal rocks that form a belt around the southern and southeastern Yilgarn Craton margin (Myers 1990; Spaggiari *et al.* 2009) (Figure 3). The northern margin of the Biranup Zone is separated from the Northern Foreland (Munglinup Gneiss) though a series of west-east linked structural contacts; the Miller Point Thrust, the Bremer Fault, the Southern Ocean Shear Zone and Red Island Fault Zone (Spaggiari *et al.* 2009 and references cited therein). To the southwest the Biranup Zone is tectonically interlayered with the Northern Foreland (Spaggiari *et al.* 2011). In the south the Heywood-Cheyne Fault Zone separates the Biranup Zone from the

Nornalup Zone, whilst in the southeast the Fraser Fault separates the Biranup Zone from the Mesoproterozoic Fraser Zone (Spaggiari *et al.* 2009, 2011).

Intensely deformed orthogneisses, paragneisses and metagabbros dominate the Biranup Zone, with rock ages ranging between c. 1760 and 1620 Ma (Nelson *et al.* 1995; Kirkland *et al.* 2011b; Spaggiari *et al.* 2011). The main components of the Biranup Zone are the Dalyup and Coramup Gneisses, though the two are difficult to distinguish and are primarily subdivided by the presence of paragneissic rocks in the Coramup Gneiss (Spaggiari *et al.* 2009).

The Biranup Zone was originally considered an exotic terrane accreted to the Yilgarn Craton during the Albany-Fraser Orogeny (Nelson *et al.* 1995; Clark *et al.* 2000; Spaggiari *et al.* 2009). This in part was due to a lack of evidence in the southern Yilgarn for a Paleoproterozoic magmatic or tectonothermal event that corresponded with Biranup Zone rock ages (Spaggiari *et al.* 2009). However, recent studies have indicated that the Biranup Zone may have formed in-situ, along the Yilgarn Craton margin (Kirkland *et al.* 2011a).

Supporting this autochthonous interpretation is the presence of Archean granite fragments within the Biranup Zone that display ages typical of Yilgarn Craton granites (Spaggiari *et al.* 2011). Furthermore, the near-coeval sedimentation, deformation and magmatism of a suite of rocks in the eastern Biranup Zone, along with geochemical analysis in the area that indicates a tholeiitic series, suggests that the Biranup Zone evolved in a back-arc setting on the Yilgarn Craton margin (Kirkland *et al.* 2011a). During Stages I and II of the Albany-Fraser Orogeny this back-arc was later compressed and tectonically dismembered (Kirkland *et al.* 2011b).

#### 2.2.2.2 Fraser Zone

The Fraser Zone is dominated by high grade, metagabbroic rocks. Geophysical analysis indicates a northeasterly trending unit, approximately 425 kilometres long and 50 kilometres wide (Figure 3). The Fraser Zone is fault-bound by the Fraser Fault Zone along the northwestern edge and southern tip, and by the Newman Shear Zone and Boonderoo Fault along its southeastern edge (Spaggiari *et al.* 2011).

Originally termed the Fraser Complex by Doepel (1973), with specific reference to Fraser Range, the unit was interpreted as an upfaulted wedge of lower crust. Myers (1985) proposed the mafic rocks of the complex were part of a large, stratiform intrusion, though

subsequent review (Condie & Myers 1999) interpreted the Fraser Complex as representing remnants of multiple oceanic magmatic arcs, rather than a single layered intrusion. Spaggiari *et al.* (2009) suggested the terms Fraser Zone and Fraser Range Metamorphics to overcome the ambiguity of the tectonic setting.

The Fraser Zone is dominated by the Fraser Range Metamorphics (Spaggiari *et al.* 2009). The rocks within this unit have been dated at c. 1300 Ma and predominantly consist of metagabbros, interlayered with sheets of granitic material and slivers of pelitic, semipelitic and calcic metasedimentary rocks. Deposition of the metasedimentary sequences is considered to have preceded mafic and felsic magmatic intrusion. The Fraser Range Metamorphics have undergone high temperature metamorphism to granulite facies, with some evidence of localised regression to amphibolite facies (Spaggiari *et al.* 2011 and references cited therein).

Zircon dating of quartz metasandstone deposited around  $1466 \pm 17$  Ma, now interlayered with amphibolite and pyroxene granulite, indicates that early metamorphism in the Fraser Zone occurred around  $1304 \pm 7$  Ma (Spaggiari *et al.* 2011 and references cited therein). Similarly, other geochronological data from the unit suggests metamorphism is associated with Stage I tectonothermal activity. Spaggiari *et al.* (2011) propose that the Fraser Zone represents a structurally modified, mid- to deep-crustal 'hot zone', formed by the repeated intrusion of gabbroic magma into quartzofeldspathic country rock, within either a magmatic arc, back-arc, or rift setting.

#### 2.2.2.3 Nornalup Zone

The Nornalup Zone is the southern- and easternmost lithotectonic unit of the Albany-Fraser Orogen (Figure 3). The Nornalup Zone may continue offshore, but due to the extent of granitic intrusion by the Recherche and Esperance Supersuites this has been difficult to ascertain. In the east the Nornalup Zone is obscured by Cenozoic rocks of the overlying Eucla Basin (Spaggiari *et al.* 2009 and references cited therein). The southwest margin of the Nornalup Zone is separated from the Biranup Zone by the Heywood-Cheyne Fault Zone, whilst the northwestern margin is separated from the Biranup and Fraser Zones are by the Newman Shear Zone and Boonderoo Fault (Spaggiari *et al.* 2009, 2011). In the east the Rodona Shear Zone separates the Nornalup Zone from the Madura Province.

The Nornalup Zone has only two distinctly recognisable units; the Malcolm Metamorphics (formerly the Malcolm Gneiss, Myers 1995b) in the east, and paragneissic rocks (Myers

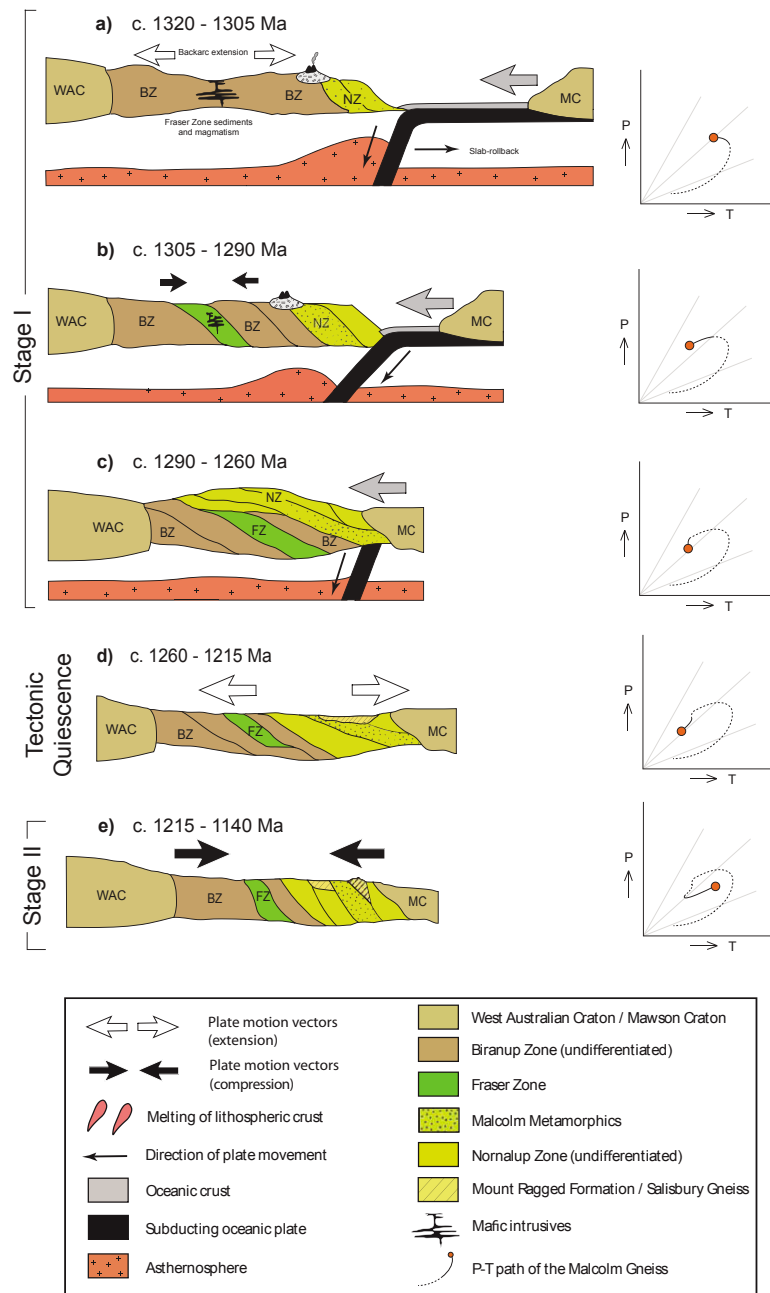
1995b, Clarke 1999) in the west. The sediments of these units are considered to have been deposited in the Arid Basin during a second cycle of sedimentation (Section 2.2.2.4). Dominating throughout the Nornalup Zone are the granitic intrusions of the Recherche and Esperance Supersuites (Section 2.2.2.5) (Spaggiari *et al.* 2011).

Clark *et al.* (2000) identify five deformation episodes within the eastern Nornalup Zone (Figure 5): 1) formation of a first gneissic fabric in the Malcolm Metamorphics (D<sub>1</sub>); 2) transposition of that fabric into a second composite recumbent fabric and foliation of Recherche Supersuite (D<sub>2</sub>); 3) open upright folding (D<sub>3</sub>); 4) deformation and high grade metamorphism of the Salisbury Gneiss, foliation development and folding of the Mount Ragged Formation, and reactivation of the Malcolm Metamorphics in discrete shear zones (D<sub>4</sub>); and 5) a second generation of open folding (D<sub>5</sub>). Clark *et al.* (2000) consider the development of foliation and folding of the Mount Ragged Formation to correlate with the Salisbury Gneiss (D<sub>4</sub>) deformation episode.

#### 2.2.2.4 Arid Basin Sediments

Within the Fraser and Nornalup Zones there are several metasedimentary packages that have maximum depositional ages younger than the Biranup Orogeny. The protoliths of these metasedimentary successions were affected by Stage I tectonothermal activity during the Albany-Fraser Orogeny; they are termed Arid Basin sediments and belong to a second cycle of sedimentation that took place during Stage I of the Albany-Fraser Orogeny (Spaggiari *et al.* 2011) (Figure 4). The majority of dated Arid Basin sediments contain Biranup Zone-aged detritus, indicating its nearness as a source.

The Arid Basin sediments include: the Malcolm Metamorphics of the eastern Nornalup Zone (formerly the Malcolm Gneiss, Myers 1995b), paragneissic rocks from the western Nornalup Zone (Myers 1995b, Clarke 1999), the Gwynne Creek Gneiss (Spaggiari *et al.* 2011), and the metasedimentary rocks of the Fraser Range Metamorphics (Spaggiari *et al.* 2011).



**Figure 5: Tectonic model of the Albany-Fraser Orogeny (Modified from Adams 2012, Figure 8.3 - adapted from Bodorkos & Clark 2004b); P-T graphs display an estimate of the P-T conditions during each stage; Dotted lines indicate conditions from the previous stage. a) Slab-rollback resulted in extension of the Biranup Zone enabling the formation of a backarc basin for the protoliths of the Fraser Range to be deposited; b) Extension ceases and compression begins where the backarc basin is thickened. Peak metamorphism in the Fraser Zone occurs between c. 1291-1266 Ma. F3 folding in the Nornalup Zone may have commenced during this period; c) Thrusting of the Nornalup Zone over the Biranup and Fraser Zones saw peak metamorphic conditions in the Fraser Zone and the formation of F3 tight, closed folds within the Nornalup Zone; d) Sediments shed off the thickened orogen were deposited in shallow intracratonic basins unconformably overlying pre-1300 Ma Nornalup Zone rocks; e) Renewed NW-directed compression resulted in intracratonic reactivation of the orogen which included metamorphism to lower amphibolites facies in the Malcolm Metamorphics, as well as the formation of shear zones and a late folding event (F5).**

#### 2.2.2.4.1 Malcolm Metamorphics

The Malcolm Metamorphics are located in the eastern Nornalup Zone approximately 175 kilometres east of Esperance, Western Australia. The Malcolm Metamorphics outcrop along a series of narrow coastal exposures from Point Malcolm in the north southwards to Cape Pasley.

The Malcolm Metamorphics consist predominantly of siliclastic metasedimentary rocks, and also includes orthogneiss, mafic amphibolitic schist, quartzofeldspathic gneiss and minor calc-silicate rocks of possible volcanic origin (Clark 1999; Spaggiari *et al.* 2009). Muscovite-biotite psammites dominate the metasedimentary sequences, with a lesser component of garnet-biotite-sillimanite pelitic rocks that are locally magmatic (Clark 1999).

The Malcolm Metamorphics appear to be the oldest sedimentary succession in the Nornalup Zone (Spaggiari *et al.* 2011). Based on geochronology analysis of detrital zircon, the maximum depositional age for the Malcolm Metamorphics sedimentary protolith is  $1560 \pm 40$  Ma (Spaggiari *et al.* 2011).

Rocks of the Malcolm Metamorphics unit were metamorphosed at low-pressure, high-temperature conditions (4-5 kbar, 750-800°C), which is considered to have occurred in conjunction with the intrusion by  $1330 \pm 14$  Ma and  $1314 \pm 21$  Ma rocks from the Recherche Supersuite during Stage I of the Albany-Fraser Orogeny (Clark *et al.* 2000).

#### 2.2.2.4.2 Paragneissic rocks from the western Nornalup Zone

In the south west of the Nornalup Zone, in the vicinity of Albany Western Australia, paragneiss metasedimentary rocks occur. Included amongst the paragneisses are garnet-sillimanite migmatitic rocks and quartzites (Spaggiari *et al.* 2009 and references cited therein). Analyses on migmatitic rocks have yielded detrital zircons with ages of 1750-1720 Ma. The maximum depositional age of the paragneiss is considered to be between 1360 and 1310 Ma with metamorphism occurring between  $1314 \pm 5$  Ma and  $1304 \pm 3$  Ma (Spaggiari *et al.* 2009 and references cited therein).

#### 2.2.2.4.3 Gwynne Creek Gneiss

The Gwynne Creek Gneiss is located between the Biranup and Fraser Zones, in the north eastern portion of the Albany-Fraser Orogen. Its location is approximately 360 kilometres east-northeast of Kalgoorlie, Western Australia, fringing the north eastern margin of the Fraser Zone.

The Gwynne Creek Gneiss is dominated by psammitic gneiss interlayered with thin layers of semipelitic gneiss. The unit also include layers of finely laminated quartzofeldspathic gneiss with parallel layers of leucosomes and minor metagranite, metamafic and meta-ultramafic rocks (Spaggiari *et al.* 2011).

Analysis of samples from the semipelitic gneiss indicates a maximum depositional age ranged from  $1533 \pm 11$  Ma to  $1483 \pm 12$  Ma (Spaggiari *et al.* 2011 and references cited therein). However, a significant detrital component, from the semipelitic gneiss, also yielded a date of 1675 Ma, as well as a smaller proportion at c. 1739 and 1607 Ma.

Based on dating of overgrowths in zircon grains, metamorphism has been interpreted as occurring between 1270 and 1193 Ma (Kirkland *et al.* 2011a), though this could also indicate minimum deposition ages (Spaggiari *et al.* 2011). The Gwynne Creek Gneiss is interpreted as containing a significant proportion of material with Biranup Zone provenance (Spaggiari *et al.* 2011). Geochronology indicates that deposition occurred after the Biranup Orogeny and that protolith sediments were affected by tectonothermal activity during Stage I, and quite possibly Stage II, of the Albany-Fraser Orogeny.

#### 2.2.2.4.4 Metasedimentary rocks of the Fraser Range Metamorphics

The Fraser Range Metamorphics occur along a northeast-southwest metagabbro dominated belt known as Fraser Range. Fraser Range is about 100 kilometres east of Norseman, Western Australia. The belt is over 185 kilometres long and approximately 32 kilometres wide (Myers 1985).

The Fraser Range Metamorphics (Spaggiari *et al.* 2009) are predominantly high-grade metagabbroic rocks, interlayered with sheets of granitic material and slivers of metasedimentary rock. The metagabbroic layers are typically separated by quartzofeldspathic layers which are considered to be either granites or metasedimentary layers, or both (Spaggiari *et al.* 2011). The metasedimentary sequences consist of layers of

pelitic, semipelitic and calcic rocks. In the southern portion of the Fraser Zone pelitic and semipelitic rocks dominate the metasedimentary sequences. In the northern areas the metasedimentary sequences have calc-silicate affinities, which possibly represent metamorphosed marls or volcanoclastic protoliths (Spaggiari *et al.* 2011). Metasedimentary rocks are most common along the north western side of the Fraser Zone. Here the metasedimentary sequences are interlayered with mafic layers, that were likely dykes or sills related to the main gabbroic intrusion. The deposition of the metasedimentary rocks is considered to have occurred before the intrusion of mafic and felsic magmatic rocks, which occurred during Stage I of the Albany-Fraser Orogeny (Spaggiari *et al.* 2011).

#### 2.2.2.5 Recherche and Esperance Supersuites

The Recherche and Esperance Supersuites predominantly represent voluminous Mesoproterozoic granitic intrusions that occur throughout the major lithotectonic units of the Albany-Fraser Orogen. Both suites mark two major magmatic events that coincide with Stages I and II of the Albany-Fraser Orogeny (Spaggiari *et al.* 2009).

The Recherche Supersuite (formerly Recherche Granite of Myers 1995b; Nelson *et al.* 1995; Clarke 1999) is dated at c. 1330-1280 Ma (Spaggiari *et al.* 2011). From within the eastern Nornalup Zone, Clarke (1999) identified two distinct varieties of granitic rocks; a biotite-hornblende monzogranitic gneiss, with rare calc-silicate boudins, being the dominant variety, and a peraluminous, garnet-bearing granodiorite gneiss, absent of hornblende. Also included within the suite are syn-plutonic mafic and aplite ( $1313 \pm 16$  Ma) intrusions with features indicative of magma mixing (Myers 1995b; Clarke 1999; Clark *et al.* 2000). Igneous rocks of the suite have a gneissic fabric and were metamorphosed to amphibolite or granulite facies during either Stage I or II, or both (Myers 1995b; Nelson *et al.* 1995; Clark *et al.* 2000). Whilst most abundant in the Nornalup Zone, the Recherche Supersuite is also present in the Biranup Zone, as well as one occurrence in the Munglinup Gneiss (Spaggiari *et al.* 2011). Spaggiari *et al.* (2011) consider this indicative of a spatial connection stitching the Northern Foreland and the Kepa Kurl Booya Province, and the Biranup and Nornalup Zones, together during Stage I of the Albany-Fraser Orogeny. In the west Nornalup Zone granitic rocks of the Recherche Supersuite become less abundant (Fitzsimons & Buchan 2005).

The Esperance Supersuite (formerly Esperance Granite of Myers 1995b; Nelson *et al.* 1995) is dated at c. 1200-1140 Ma (Spaggiari *et al.* 2011). It consists of strongly magnetic

plutons. The igneous rocks of the Esperance Supersuite were metamorphosed to greenschist and amphibolite facies. Whilst occasionally being locally mylonitic or showing some foliation, the rocks of this suite in general display less deformation than rocks of the Recherche Supersuite (Myers 1995b; Nelson *et al.* 1995). Whilst present in other lithotectonic units of the Albany-Fraser Orogen, the suite is most abundant in the Nornalup Zone, indicating voluminous granitic magmatism occurred throughout the region (Spaggiari *et al.* 2011). Emplacement and deformation of the Esperance Supersuite is considered to be constrained to Stage II of the Albany-Fraser Orogeny (Nelson *et al.* 1995; Clark *et al.* 2000; Spaggiari *et al.* 2011).

#### 2.2.2.6 Ragged Basin Sediments

Overlying areas of the Nornalup Zone are covered by sequences of Mesoproterozoic metasedimentary rocks. The protoliths of these metasedimentary successions were deposited in a third cycle of sedimentation after Stage I of the Albany-Fraser Orogeny and are termed Ragged Basin sediments (Spaggiari *et al.* 2011) (Figure 4).

Only two metasedimentary packages have their protoliths allocated to the Ragged Basin setting. They are the Mount Ragged Formation (Spaggiari *et al.* 2009) and the Salisbury Gneiss (Clark *et al.* 2000). Despite being situated within the Madura Province the Salisbury Gneiss is considered part of the Ragged Basin. Analysis of zircon crystals collected from Mount Ragged quartzites have been interpreted as detrital grains (Clark *et al.* 2000), derived from granitic rocks of the Recherche Supersuite (Spaggiari *et al.* 2011). Based on mineralogy and the clean, mature nature of quartzose sediments the deposition environment for Ragged Basin sediments has been interpreted as a shallow intracratonic basin (Clark *et al.* 2000; Bodorkos & Clark 2004a, 2004b).

##### 2.2.2.6.1 Salisbury Gneiss

The Salisbury Gneiss is located on an isolated series of islands approximately 165 kilometres southeast of Esperance, Western Australia. The unit was named Salisbury Gneiss (Clark 1999) after Salisbury Island, though refers collectively to the offshore islands southeast of the Rodona Shear Zone that extend to the edge of the continental shelf.

From geochronological analysis Clark *et al.* (2000) infer that the unit differs from the Malcolm Metamorphics, and is separated from them by the Rodona Shear Zone. Despite the scarcity of geological data owing to their remote offshore location, the unit is considered part of the Nornalup Zone (Spaggiari *et al.* 2011).

Based on the geological description recorded from Salisbury Island, the Salisbury Gneiss is dominated by metapelitic gneisses and mafic granulite, with subordinate outcrops of porphyritic granite-gneiss and two-pyroxene metagabbro (Clark 1999). The sediments of the Salisbury Gneiss protolith are considered to have been derived from the Albany-Fraser Orogen during a period of extension and erosion (1260-1215 Ma) after Stage I of the Albany-Fraser Orogeny (Bodorkos & Clark 2004b; Spaggiari *et al.* 2011) (Figure 5d).

Rocks of the Salisbury Gneiss record high-grade metamorphism to granulite facies under conditions of 800°C and  $\geq 5$  kbar (Bodorkos & Clark 2004a). Dating of the zircon cores from migmatitic leucosomes, derived from partial melting of the metapelitic gneiss, indicated the onset of crystallisation at  $1214 \pm 8$  Ma (Clark *et al.* 2000). Zircon rim analysis from the migmatitic leucosomes yielded a date of  $1182 \pm 13$  Ma, and is considered to represent decompression from peak metamorphic temperatures (Clark *et al.* 2000; Spaggiari *et al.* 2011). Also indicating retrogression from granulite facies is the presence of strongly deformed amphibolite margins in the metagabbro components, whilst the cores remained relatively undeformed (Clark 1999). Clark *et al.* (2000) proposed that retrogression overprinting occurred during uplift and westward movement of the Salisbury Gneiss unit along the Rodona Shear Zone.

#### 2.2.2.6.2 Mount Ragged Formation

In the eastern portion of the Nornalup Zone prominent hills composed of quartz-rich metasedimentary rocks form the Mount Ragged Formation. The sequence was originally described by Clarke *et al.* (1954) and in the past has been referred to as the Mount Ragged Beds (Lowry & Doepel 1974) and Mount Ragged Schist (Myers 1995b). The term Mount Ragged Formation was proposed by Spaggiari *et al.* (2009). It includes sequences of massive grey quartzite and quartz-muscovite schist, with minor, sporadic components of quartz-pebble conglomerate and pelitic schist.

As this study investigates the Mount Ragged Formation a more detailed account of the sedimentary and structural evolution of formation occurs in subsequent sections.

## 2.3 Tectonic history of the Albany-Fraser Orogen

In the history of the Albany-Fraser Orogen three major tectonic events have been recognised. These are the Paleoproterozoic Biranup Orogeny, which includes the c. 1680 Ma Zanthus Event (Kirkland *et al.* 2011a; Spaggiari *et al.* 2011), and the Mesoproterozoic Albany-Fraser Orogeny, which is divided into two stages; Stage I (c. 1345-1260 Ma) representing continental collision and Stage II (c. 1215-1140 Ma) representing intracratonic reactivation (Clark *et al.* 2000; Bodorkos & Clark 2004a, b; Spaggiari *et al.* 2009). The dominant control on the preserved crustal architecture of craton-directed, fault-bound thrust slices of largely mid-crustal, high grade rocks are primarily due to these tectonic events, especially Stage II (Spaggiari *et al.* 2011 and references cited therein).

### 2.3.1 Biranup Orogeny

Based on present geochronology, the Biranup Orogeny occurred during the Paleoproterozoic between c. 1760 and 1650 Ma and involved a period of extensive magmatism, sedimentary basin formation and high temperature metamorphism and deformation, referred to as the Zanthus Event (Kirkland *et al.* 2011a). However, the Biranup Orogeny may have begun earlier than 1760 Ma if deposition of the Stirling Range Formation at c. 1800 Ma and c. 1800 Ma zircon inheritance ages are considered. The Biranup Orogeny marks a period of active margin process along the southern and southeastern Yilgarn Craton margin that eventually lead to its modification. It includes rocks of the Northern Foreland and the Biranup Zone (Spaggiari *et al.* 2011).

During the Biranup Orogeny at c. 1680 Ma a period of migmatization associated with northeast-southwest directed crustal shortening occurred. This period is referred to as the Zanthus Event (Kirkland *et al.* 2011a). The Zanthus Event is constrained by dating of folded migmatitic leucosomes in Biranup Zone hornblende-biotite-garnet granitic gneisses at c.  $1676 \pm 6$  Ma and cross-cutting axial planar leucosomes within the same gneisses at c.  $1679 \pm 6$  Ma (Kirkland *et al.* 2011a).

### 2.3.2 Albany-Fraser Orogeny

The Albany-Fraser Orogeny occurred during the Mesoproterozoic and is divided into Stage I (c. 1345-1260 Ma) and Stage II (c. 1215-1140 Ma) (Clark *et al.* 2000; Bodorkos & Clark 2004a). This orogeny event is considered responsible for the tectonic shortening of the

Biranup and Fraser Zones, and the reworking of the Yilgarn Craton margin to produce the Northern Foreland (Kirkland *et al.* 2011b).

Stage I of the Albany-Fraser Orogeny is generally considered to have begun in response to continental-continental collision between the combined North and West Australian (Yilgarn) Cratons and the combined South Australian and East Antarctic (Mawson) Cratons (Myers *et al.* 1996; Fitzsimons 2003; Bodorkos & Clark 2004b; Fitzsimons & Buchan 2005). During Stage I tectonothermal activity dominated, with voluminous mafic and felsic magmatism. This resulted in the evolution of the magmatic rocks of the Fraser Zone and the Recherche Supersuite, which accompanied high temperature metamorphism and deformation (Clark 1999; Bodorkos & Clark 2004a, b). Spaggiari *et al.* (2011) interpret the c. 1300 Ma granitic intrusions of the Recherche Supersuite to signify a spatial connection between the Northern Foreland and the lithotectonic units of the Kupa Kurl Booya Province by the end of Stage I of the Albany-Fraser Orogeny.

During the period between Stage I and II (1260-1215 Ma) of the Albany-Fraser Orogeny uplift and erosion of the Nornalup Zone and the Recherche Supersuite occurred. This resulted in the deposition of the sediments for the Salisbury Gneiss and Mount Ragged Formation protoliths (Clark *et al.* 2000; Bodorkos & Clark 2004b; Spaggiari *et al.* 2011).

Stage II of the Albany-Fraser Orogeny is interpreted as representing intracratonic reactivation involving the reworking of crustal material (Clark *et al.* 2000; Bodorkos & Clark 2004a, b; Spaggiari *et al.* 2009). Extensive high temperature metamorphism, evident across the Biranup Zone, and in the Munglinup Gneiss, Gwynne Creek Gneiss and Recherche Supersuite, indicates the reactivation during Stage II occurred in an intra-continental setting (Spaggiari *et al.* 2011). Accompanying the reactivation was the development of major, predominantly, thrust faults (i.e. Jerdacuttup Fault, Cundeelee Fault, Red Island Shear Zone) that separate the various lithotectonic units. Similarly, the development of internal fault-bound successions and fold-thrust sequences, such as those evident in the Stirling Range Formation and the Mount Barren Group, are also considered to have occurred during Stage II (Rasmussen *et al.* 2002; Dawson *et al.* 2003; Spaggiari *et al.* 2009, 2011). Coinciding with the end of Stage II of the Albany-Fraser Orogeny was the magmatic intrusion of the c. 1140 Ma granitic Esperance Supersuite (Kirkland *et al.* 2011b).

### **3.0 Methods and analytical procedures**

#### **3.1 Local setting**

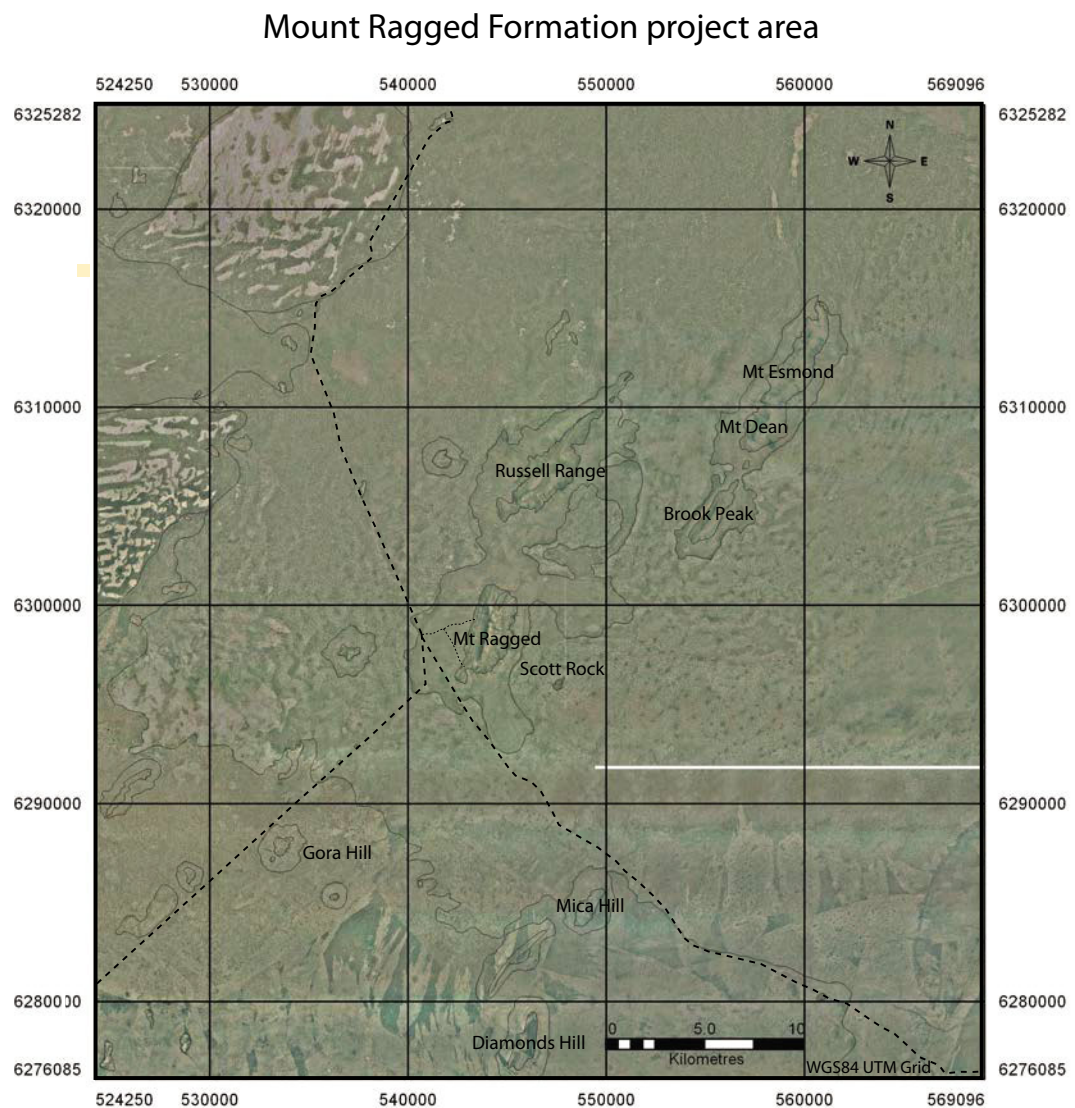
Outcrops of the Mount Ragged Formation can be recognised on aerial photographs as a series of densely vegetated, isolated, high ridges along northeast-southwest trending axes, dominated by Proterozoic quartz-rich metasedimentary rocks (Figure 6; Appendix 1). In its entirety the surface expression of the formation is referred to as the Russell Range which is subdivided into four zones of prominent hills and ridges. The range takes its name from the westernmost ridge – Russell Range. Immediately due south is the highest ridge; Mount Ragged which attains a height of 594 metres at Tower Peak. The easternmost ridge consists of Brook Peak, Mount Dean and Mount Esmond. A series of low hills consisting of Diamonds Hill, Hill 62 and Mica Hill, approximately 15 kilometres due south of Mount Ragged, constitute the southern extent of the formation (Figure 7). The summits of these low, rounded hills ( $\approx 250$  m) correspond to wave-cut benches on the more persistent ridges to the north (Russell Range, Mount Ragged, Brook Peak, Mount Dean and Mount Esmond) and are thought to indicate past sea-levels during the Eocene and Miocene (Lowry 1970). Colluvium and talus splay out from the ranges and form the lower slopes. A variable mosaic of dense heath and thicket dominate all aspects of the range, including the uppermost mountain slopes. The dominant plant species across the formation are *Allocasuarina humilis*, *Banksia armata* var. *armata*, *B. speciosa*, *B. media*, *Callitris preissii*, *Calothamnus quadrifidus*, *Dillwynia pungens*, *Eucalyptus incrassata*, *Isopogon buxifolius* and *Kunzea baxteri* (Beard 1975).

The dominant feature surrounding the Mount Ragged Formation is a calcareous plain, approximately 150 metres above sea level. The plain is variably covered by a thin veneer of loam-clay, silt and sand which contains indurated sheet and nodular calcrete. Southwards towards the coast the sand content increases. The area is dominated by low, open mallee woodland with a low understorey consisting of scrub-heath and sedges.

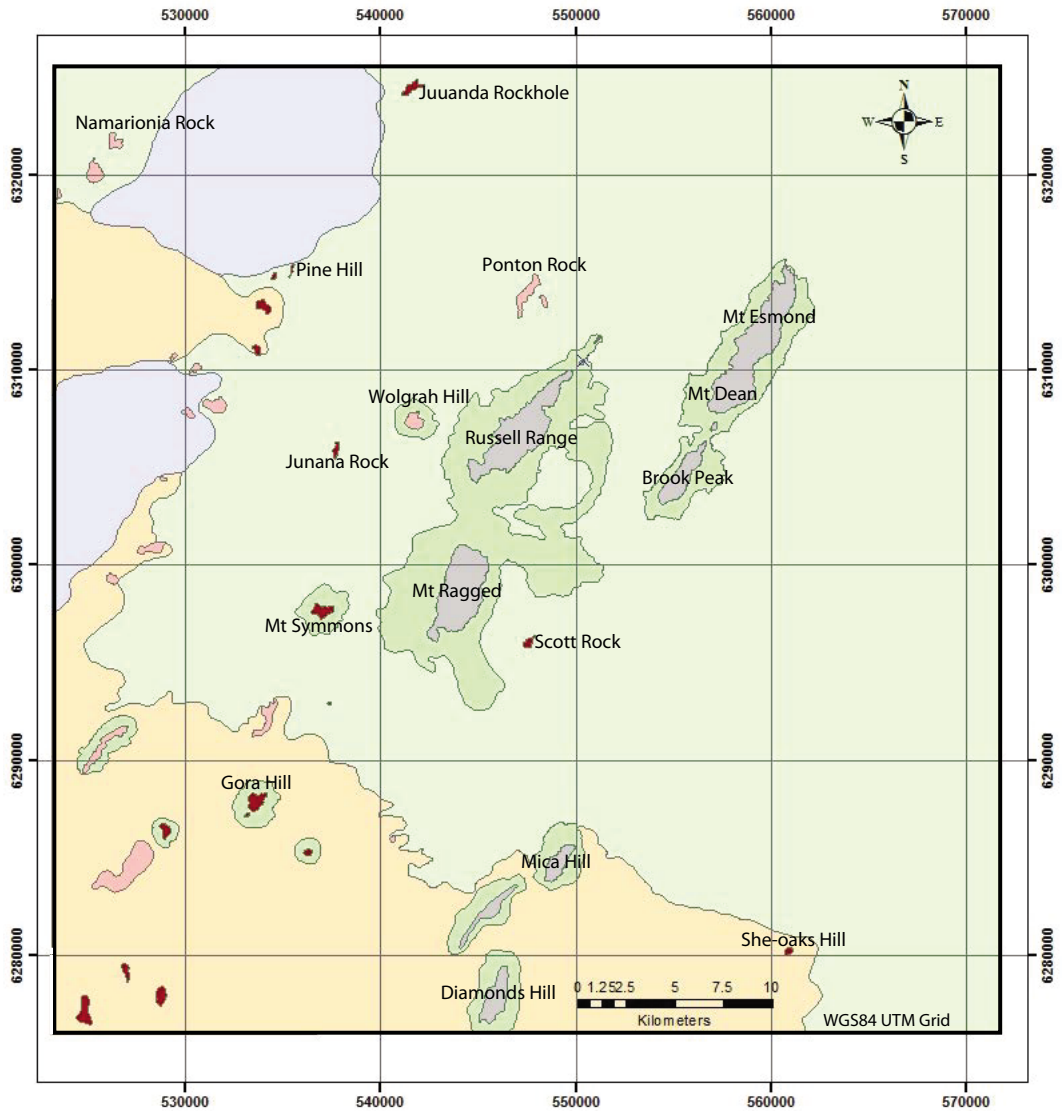
#### **3.2 Fieldwork**

Fieldwork was conducted over four consecutive weeks in October and November 2012 in the Cape Arid National park, approximately 165 kilometres east-northeast of Esperance, WA. The project area is located between 524,250mE and 570,000mE and 627,6000mN and 632,5300mN (Figure 6). The area within these co-ordinates also includes the GSWA Warox sites referred to later in this report. Locations of samples and geological

measurements were recorded by a global positioning system (GPS) with the geodetic reference datum WGS84. Universal Transverse Mercator (UTM) was used to provide the position format and grid co-ordinates were recorded as eastings and northings corresponding to the Map Grid of Australia (MGA). The project area is located in Zone 51H. The aerial photographs used in this investigation corresponded to the Buraminya, Malcolm, Mount Dean and Sandy Bight 1:100,000 map sheets, which all occur within the Malcolm 1:250,000 map sheet. All aerial photographs are dated January 2009.



**Figure 6. 1:100,000 aerial photographs of the project area. The aerial photographs correspond to the Buraminya, Malcolm, Mount Dean and Sandy Bight 1:100,000 map sheets and are dated January 2009**



**Lithological Legend**

- Lake deposits: Sand, Silt and Clay; Saline and Gypsiferous
- Colluvium: clay, sand and rock fragments; slope deposits
- Residual and eolian loam-clay, silt and sand containing sheet and nodular calcrete
- Sand: White and yellow sand; in places containing limonite pisoliths; contains yellow clay beneath surface
- Psammitic Schist (Mount Ragged Formation)
- Monzogranite
- Metagranite

Figure 7. Surface geology of Mount Ragged Formation and surrounding area

As the hills and ridges of the Mount Ragged Formation are of variable size mapping was undertaken at different scales to suit the specific locality. Access to the field area is via Fisheries Road, east of Esperance, approximately 100 kilometres into the Cape Arid National Park and then northeast along the unsealed Balladonia Road for 50 kilometres. Access to Mica Hill was via the Gora Track. For all unsealed roads a four-wheel drive was required. All sites other than the lower western slopes of Mount Ragged typically required a considerable hike to encounter insitu outcrop.

For this study of the Mount Ragged Formation four areas were selectively traversed. They are Mica Hill, Mount Esmond, Mount Ragged and Russell Range. Due to time constraints and poor accessibility because of dense vegetation and steep terrain Diamonds Hill, Mount Dean and Brook Peak were not visited during the field period specific to this study. Similarly, due to accessibility only the southern half of Russell Range and the northernmost flanks and ridge of Mount Esmond were traversed during the fieldwork period.

In conjunction with poor accessibility the formation is characterised by large distances between outcrop and exposures are typically poor. Due to weathering and/or deformation sedimentary and structural features commonly are poorly defined or ambiguous. These were the main limiting factors to fieldwork.

### **3.3 Sampling**

Eighteen rock samples were collected from the Mount Ragged Formation during the fieldwork period. The location of samples is shown on aerial photographs in Appendix 1, in the sample catalogue in Appendix 2, Table A2.1 and on geological maps in Appendix 6. All samples were collected from insitu rock by using a geo-pick to provide unweathered surfaces when possible, with the exception of three samples (MRF\_03, MRF\_06 and MRF\_017) that were collected as loose, float material due to opportunity, uniqueness and/or rarity. Sample locations were recorded using a GPS, using MGA Datum WGS84.

From the eighteen rock samples, twenty-six thin sections were prepared. Due to interesting features and visible crystals some rock samples were cut into more than one piece to enable thin-sections from different aspects from the one rock sample to be produced.

### **3.4 Geophysical datasets**

Several aeromagnetic datasets were used in this study. These were collected in 2008 with 400 m line spacing, and are available from the GSWA website (<http://www.dmp.wa.gov.au>). Measurements of the magnetic intensity within rocks acquired during airborne aeromagnetic surveys provided the base magnetic datasets from which to later make geophysical interpretations. Magnetic intensity is measured in nanoTesla (nT) and provides an indication of the magnetisation of a particular rock in proportion to the earth's magnetic field, which is termed magnetic susceptibility. Magnetic susceptibility primarily depends on magnetite content, though pyrrhotite and maghemite are also important to a lesser extent (Spaggiari 2008). Three aeromagnetic images created from these datasets were used to provide a spatial indication of the geophysical properties of the subsurface features in the vicinity of the Mount Ragged Formation.

Aeromagnetic data was processed using Intrepid and ERMapper to enhance the visual appearance of datasets. Two forms of data manipulation provided the best methods for viewing the subsurface features within the Mount Ragged Formation project area; *Reduction to Pole (RTP)* and *First Vertical Derivative (IVD)*. Reduction to pole of magnetic data results in magnetic anomalies being placed in their correct positions making them more suitable for map drawing. Processing to the first vertical derivative emphasises gradients in the data. Magnetic trend lines (formlines) and subsurface geological units were identified in poorly exposed basement areas from two reduction to pole images (RTP-normal and RTP-sun directly overhead) and one reduction to pole, first vertical derivative image (RTP-IVD-sun angle from the northwest). This aeromagnetic interpretation was then used in conjunction with field and Warox data, resulting in a benchmarked geophysical interpretation (Section 4.3).

### **3.5 Stereographic projection of structural data**

To graphically display and interpret field data collected information was analysed using stereographic techniques, in particular equal area stereographic projections. To assist with data processing the software package GEOrient© version 9.2 (February 26, 2004) was used. This program is a 32-bit, windows 95/98/NT specific version and is registered to Dr. RJ Holcombe, Department of Earth Sciences, The University of Queensland, Queensland, 4072, Australia.

GEOrient© plots geological structural orientation diagrams such as equal area stereographic projections or rose diagrams. For the Mount Ragged Formation structural orientation data, recorded in excel spreadsheets linked to GPS software, was converted to text files to enable processing with the GEOrient© program. As well as single data sets, data from multiple files was also merged to form single data sets and overlaid using different symbols to allow comparison (i.e. Bedding-Cleavage intersections and meso-scale fold hinges; the mean principal orientation of fold hinges and the mean cleavage plane).

Structural data has been described using conventional classification terms for such features as fold hinge and axial plane attitude or orientation, interlimb angle and fold shape (McClay 1987; Twiss & Moores 2007).

## **4.0 Mapping and field observations**

Geological maps of the four study sites of the Mount Ragged Formation are provided within this report (Appendix 6). These areas are Mica Hill, Mount Esmond, Mount Ragged and Russell Range.

### **4.1 Sedimentary rocks (Mount Ragged Formation)**

The base of the Mount Ragged Formation is not exposed on any of the ridges. Similarly, the lowermost units are rarely exposed but where observed, in deep gullies eroding through the lower colluvial slopes, it consists of fine to medium-grained quartzites, muscovite-bearing quartzites and psammitic schists infrequently interspersed with thin pelitic layers. The majority of the rocks exposed in the Mount Ragged Formation are hard, pink or grey coloured quartzites interspersed with minor amounts of muscovite-bearing quartzite. The formation predominantly consists of medium-grained quartzites, with grain size diameters typically ranging between 0.25 and 1 mm. There are also sporadic beds of quartz-pebble conglomerate which occurred most frequently on the upper ridges and scree slopes of Mount Ragged. On all the ridges, the sedimentary beds of the Mount Ragged Formation typically dip steeply to the southeast.

Thin layers of pelitic schists were observed infrequently along the lower western flanks of Mount Ragged and Russell Range. Pelitic layers ranged from being several metres wide and over tens of metres in length down to millimetre-scale lenses. These contain various metamorphic assemblages, and will be described in more detail in Section 4.5.

#### **4.1.1 Sedimentary log descriptions**

Three sections of continuous outcrop with no fold hinges on Mount Ragged were used for sedimentary logging, primarily to characterise the lithological variability that is typical of the Mount Ragged Formation.

- Mount Ragged Sedimentary Log 1 (MGA 543073, 6297623 WGS84) was logged from west to east along a 24 metre vertical cliff section of gently dipping strata exposed in an east-west orientated gully in the southwest of Mount Ragged (Figure 8). This locality is at approximately 215 metres above sea-level and is considered to represent some of the lowermost exposed stratigraphy of the Mount Ragged Formation.





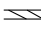
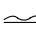

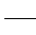


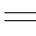

- Mount Ragged Sedimentary Log 2 (MGA 543123, 6297078 WGS84) was logged up a 23 metre near vertical cliff section of gently dipping strata just below the wave-cut bench in the southwest of Mount Ragged (Figure 8). This locality is at approximately 240 metres above sea-level and provided a good, exposed section of rock prior to the ridge slopes becoming obscured by boulders, talus and vegetation.
- Mount Ragged Sedimentary Log 3 (MGA 544109, 6299230 WGS84) was logged from west to east along a 20 metre vertical cliff section of steeply dipping rocks exposed along the south side of Tower Peak, Mount Ragged (Figure 8). This locality is at approximately 490 metres above sea-level and is considered to represent the uppermost exposed stratigraphy of the Mount Ragged Formation.

Amongst the lowermost topographic units of Mount Ragged (and Russell Range) thin mudstone and siltstone interbeds are infrequently interspersed between fine- to medium-grained quartzites (Figures 9, 12b, 14a & b). These finely laminated layers are now preserved as metamorphosed metapelites and metasilstones. The vast majority of sediments that dominant the Mount Ragged lithological units are medium-grained, well-sorted, planar cross-bedded sandstones now preserved through metamorphism as quartzite (Figure 16). The uppermost topographic strata units are dominated by poorly-sorted quartz-pebble conglomerates (Figure 17) interspersed with thick beds of well-sorted granular, quartz-dominated gritstones (Figure 18). As with the underlying topographic sequences these units have also been metamorphosed to quartzite.

Common sedimentary structures observed during logging and traversing included normal grading as well as fining up sequences; planar and trough cross-bedding, and rip-up clasts (Figures 9, 10, 12a, b, c & d, 16a & b). Less common sedimentary structures included massive bedding, planar laminar bedding, channels and scoured surfaces, and ripple marks (Figures 10, 11, 12e, 12f, & 15). Sedimentary structures identified that assisted in determining the way-up of strata included dewatering and load structures, graded bedding, ripples, scoured surfaces and channels, truncation of cross-beds and cross-laminae (Figures 12e & 16b). The most common way-up structure was the truncation of cross-beds.

A fourth sedimentary log undertaken on Russell Range (MGA 545717E, 6305538 WGS84) indicated that lithofacies and sedimentary structures were similarly comparable to those on Mount Ragged (Appendix 3).

### Legend for Sedimentary Log Symbols

 Mudstone / shale	 Trough cross-bedding	 Flaser bedding
 Siltstone	 Planar cross-bedding	 Ripples
 Sandstone	 Plane bedding	 Rip-up mud clasts
 Coarse sandstone / gritstone	 Parallel lamination	 Fining upwards

### Location Map for Mount Ragged Sedimentary Logs

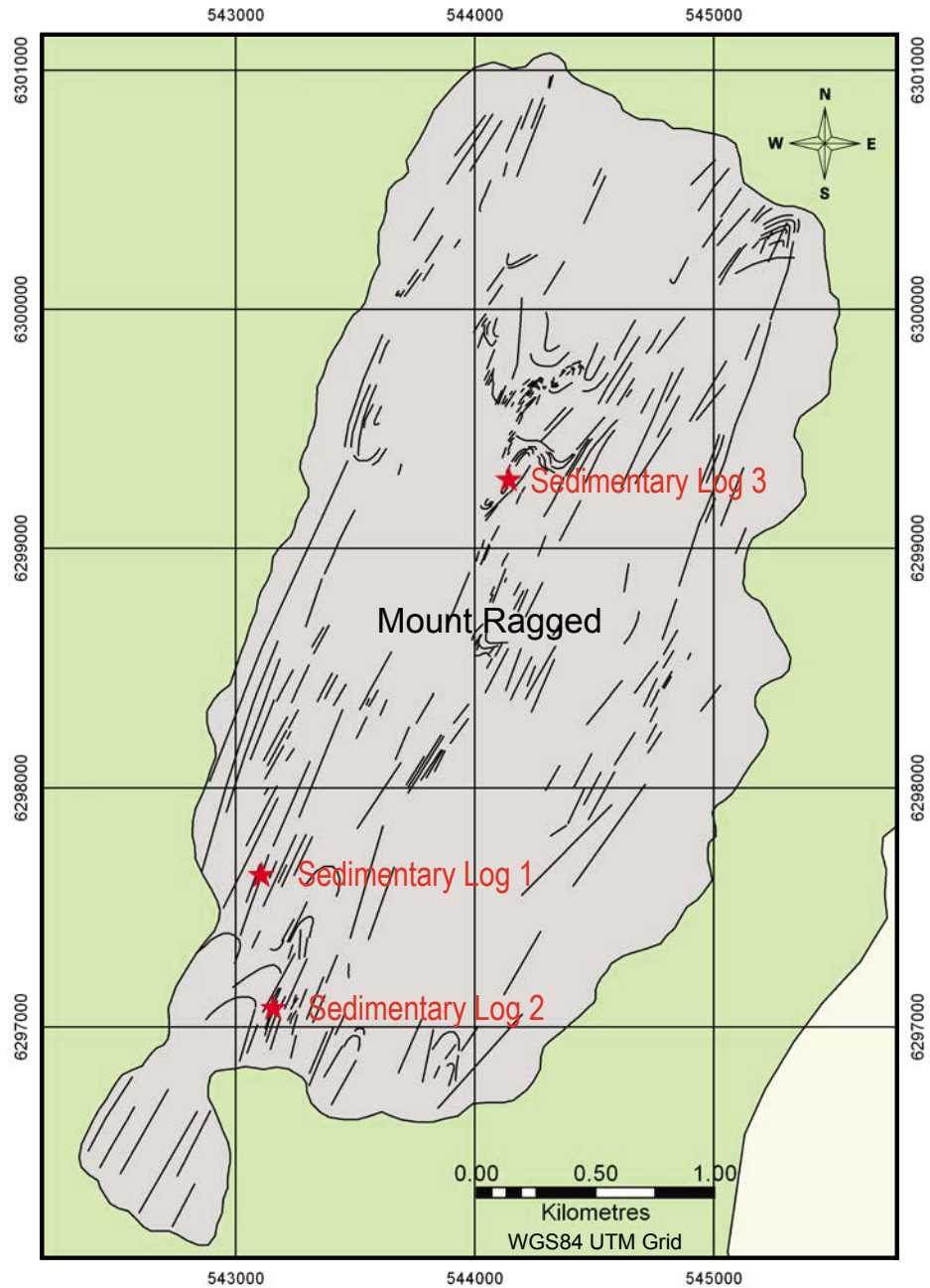


Figure 8. Location map and legend for Mount Ragged sedimentary logs

# Mount Ragged Sedimentary Log 1 - Cliff section, southwest Mt Ragged

Name: P. Waddell / O. Massiani

Date: 24 October 2012

Location: 51H 0543073 6297623 WGS84 (~215 m/asl) Log Sheet: 1 (of 2)

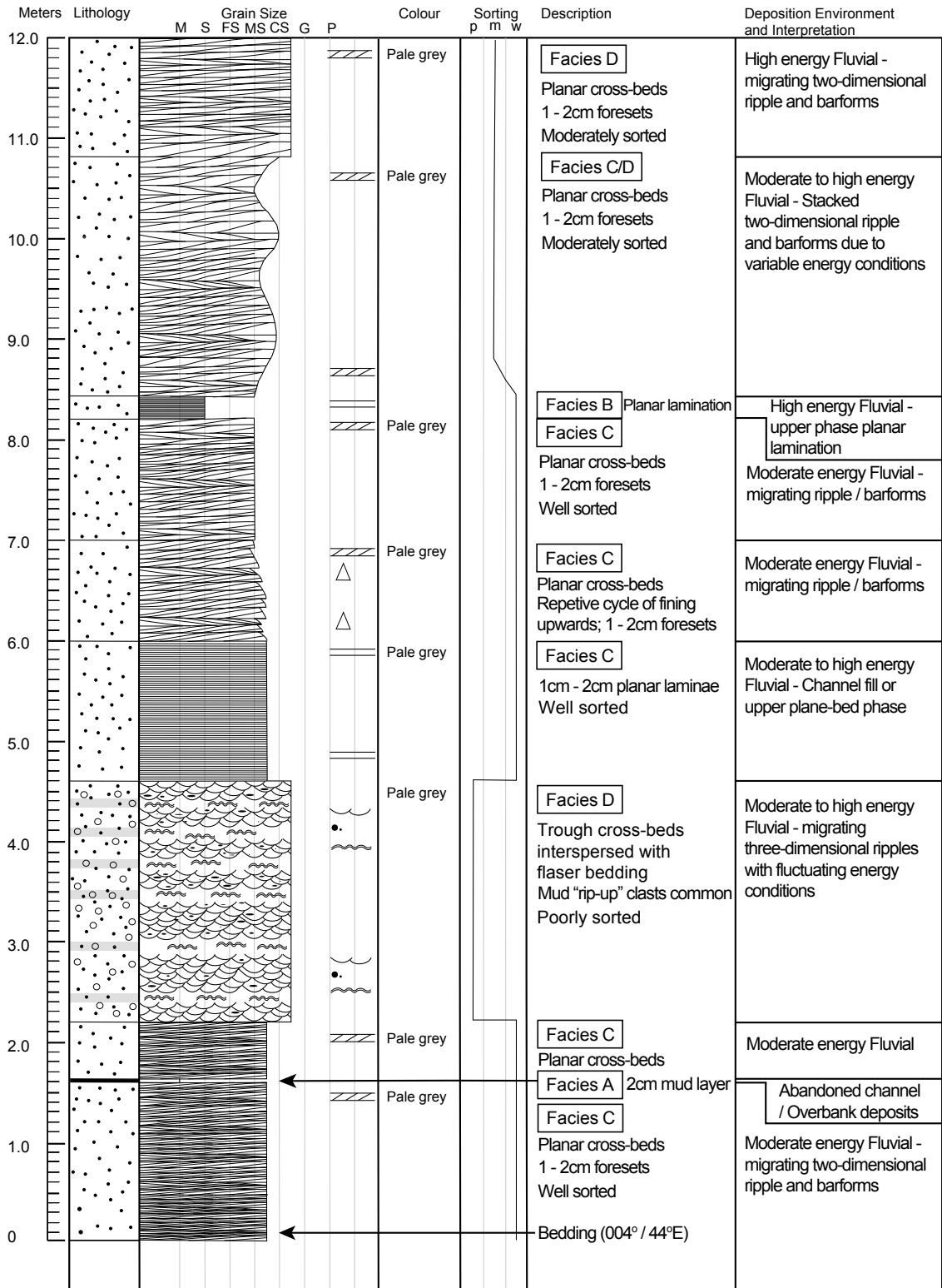


Figure 9. a) Mount Ragged Sedimentary Log 1; log sheet 1.

Mount Ragged Sedimentary Log 1 - Cliff section, southwest Mt Ragged

Name: P. Waddell / O. Massiani

Date: 24 October 2012

Location: 51H 0543073 6297623 WGS84 (~215 m/asl) Log Sheet: 2 (of 2)

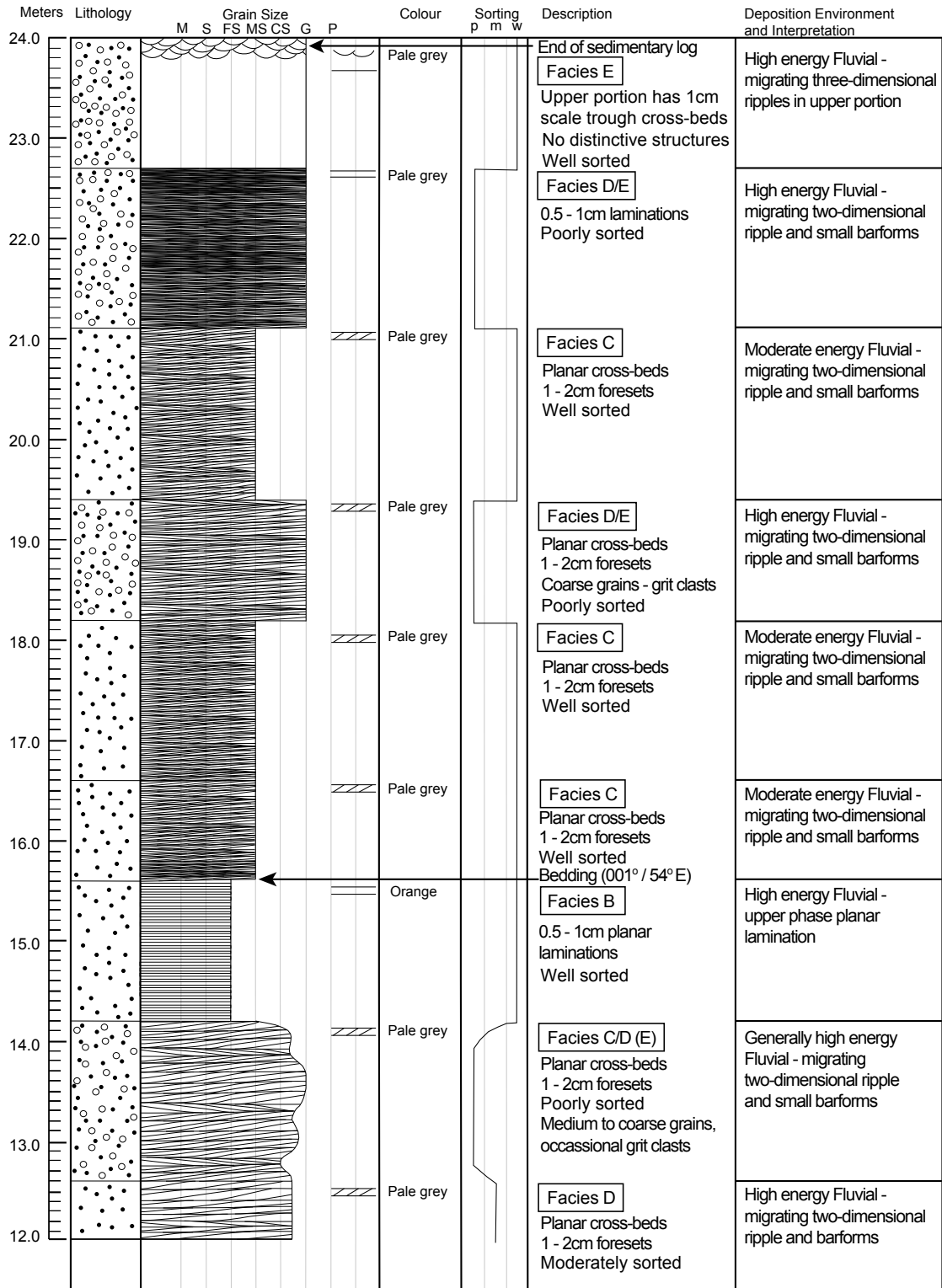


Figure 9. b) Mount Ragged Sedimentary Log 1; log sheet 2.

# Mount Ragged Sedimentary Log 2 - Cliff section, southwest Mount Ragged

Name: P. Waddell / N. Timms

Date: 18 October 2012

Location: 51H 0543123 6297078 WGS84 (~240 m/asl) Log Sheet: 1 (of 2)

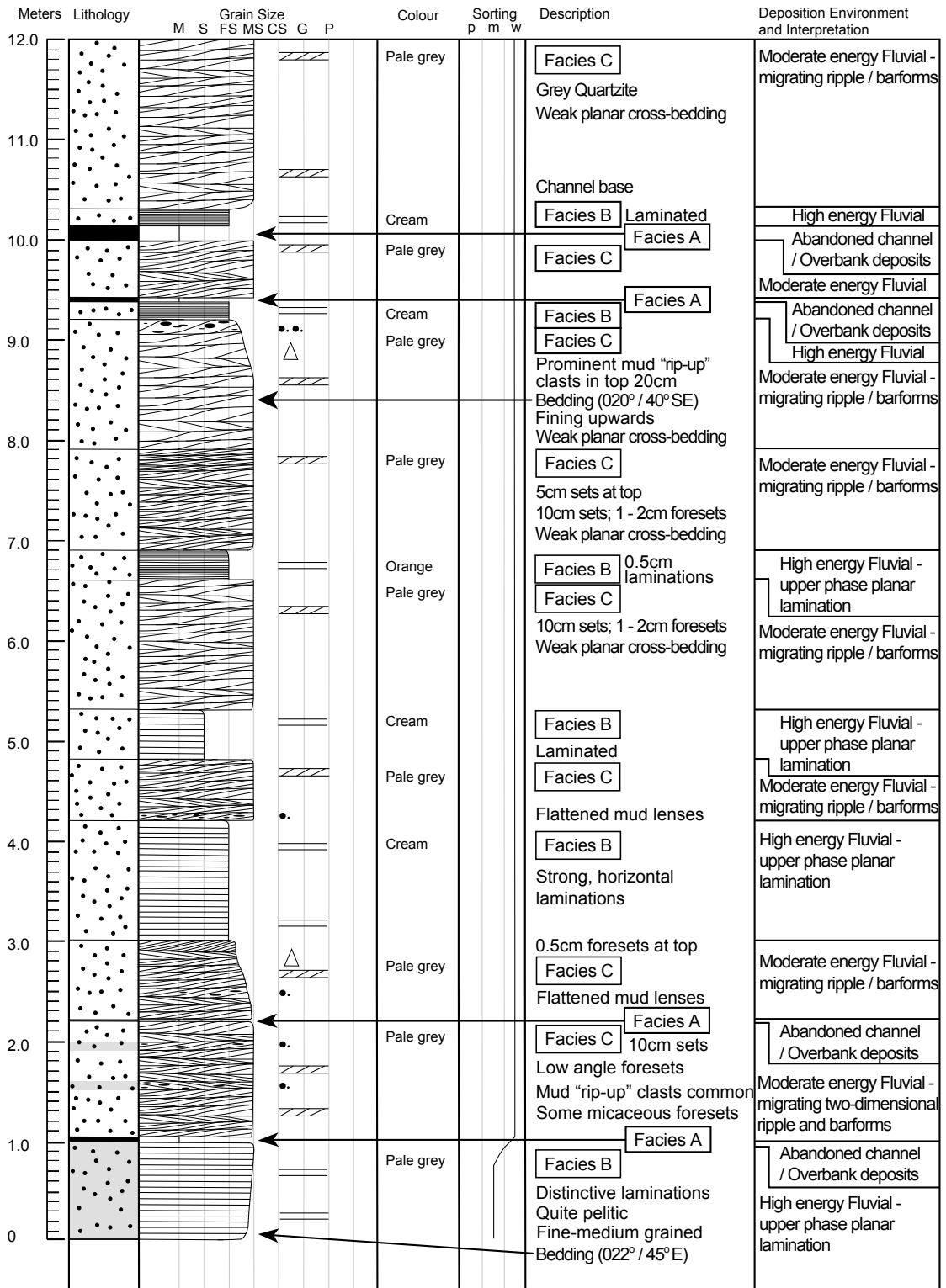


Figure 10. a) Mount Ragged Sedimentary Log 2; log sheet 1.

# Mount Ragged Sedimentary Log 2 - Cliff section, southwest Mount Ragged

Name: P. Waddell / N. Timms

Date: 18 October 2012

Location: 51H 0543123 6297078 WGS84 (~240 m/asl) Log Sheet: 2 (of 2)

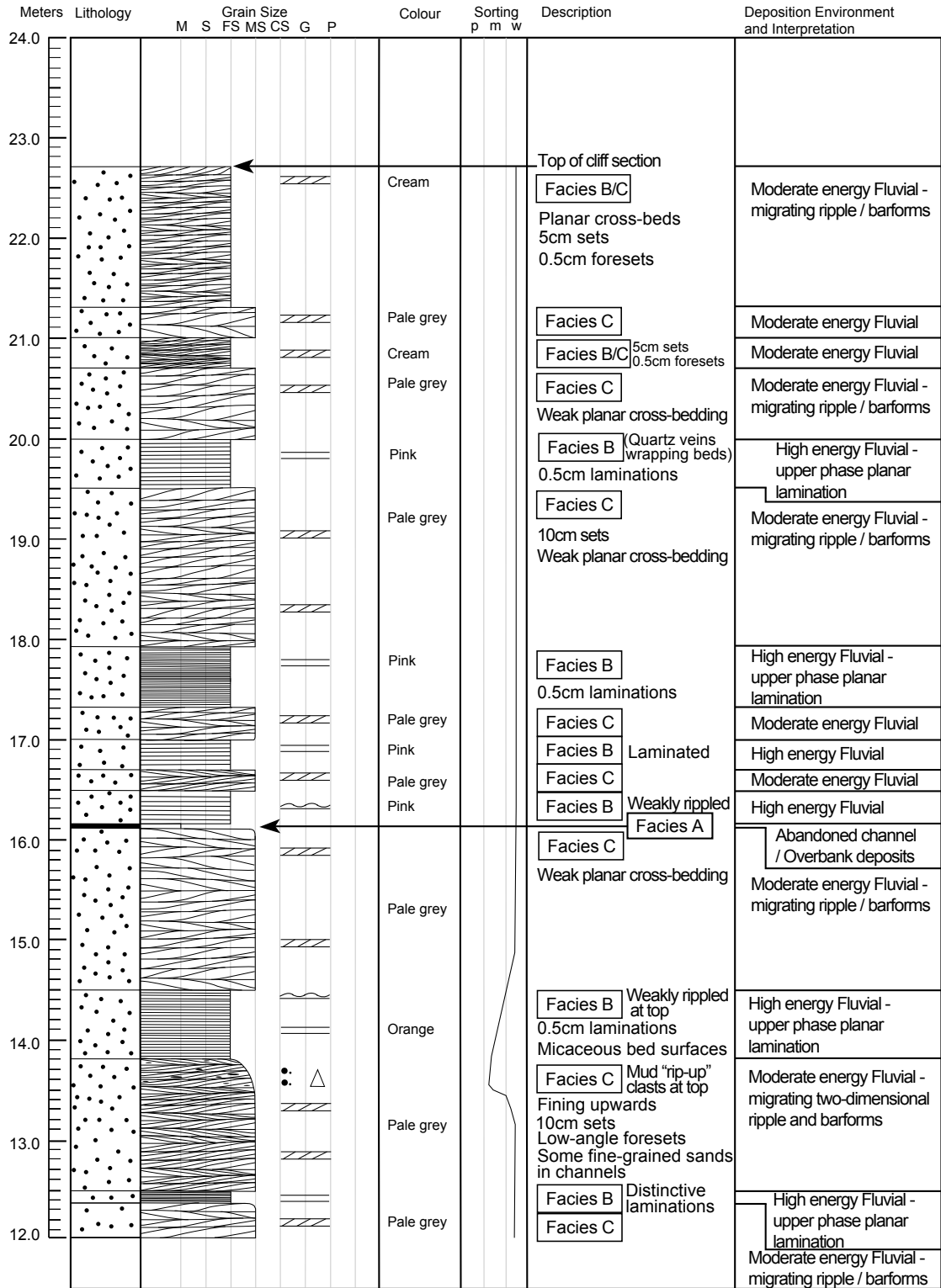


Figure 10. b) Mount Ragged Sedimentary Log 2; log sheet 2.

# Mount Ragged Sedimentary Log 3 - Cliff section, south side of Tower Peak

Name: P. Waddell / N. Timms

Date: 21 October 2012

Location: 51H 0544109 6299230 WGS84 (~490 m/asl) Log Sheet: 1 (of 2)

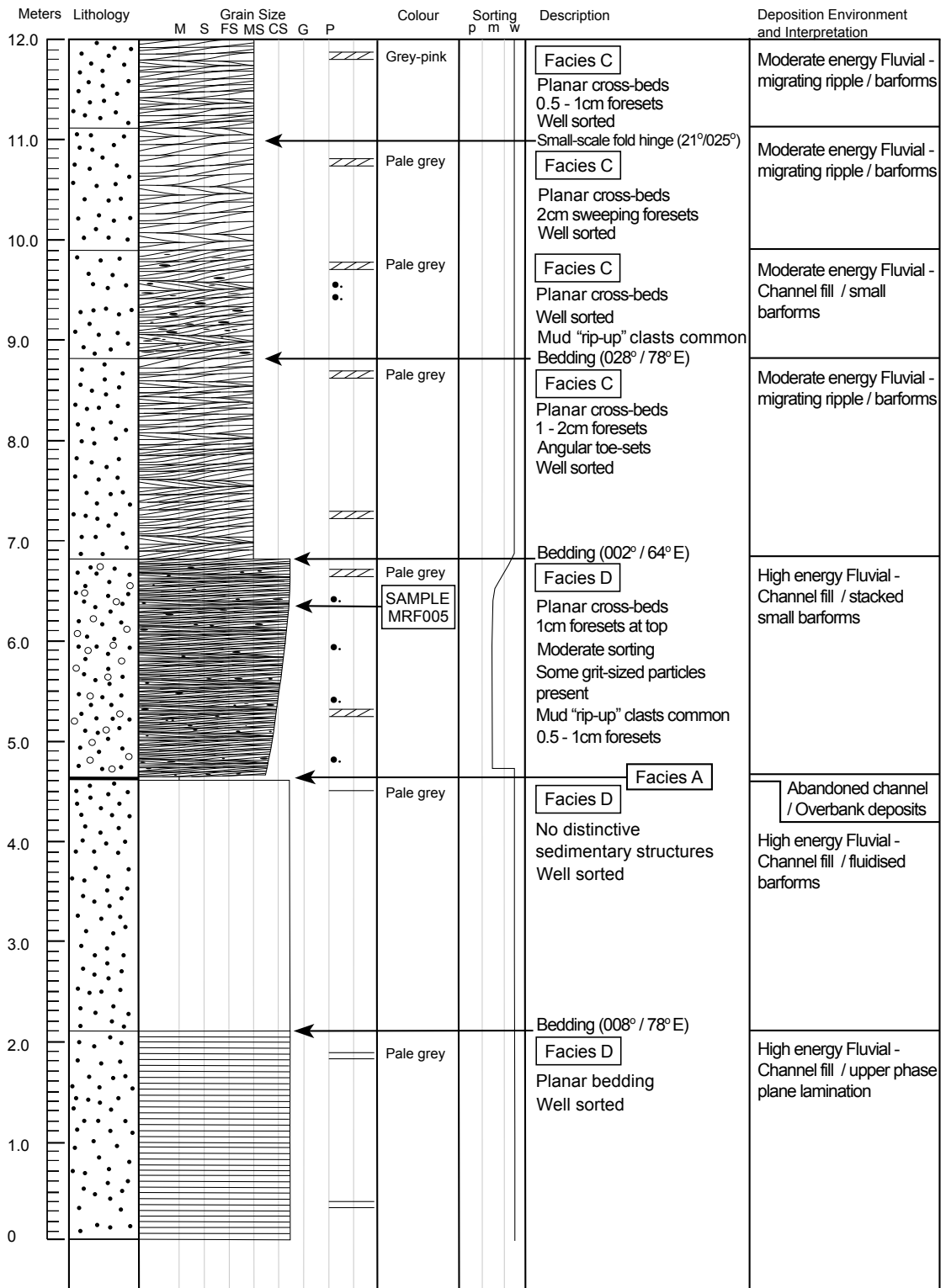


Figure 11. a) Mount Ragged Sedimentary Log 3; log sheet 1.

Mount Ragged Sedimentary Log 3 - Cliff section, south side of Tower Peak

Name: P. Waddell / N. Timms

Date: 21 October 2012

Location: 51H 0544109 6299230 WGS84 (~490 m/asl) Log Sheet: 2 (of 2)

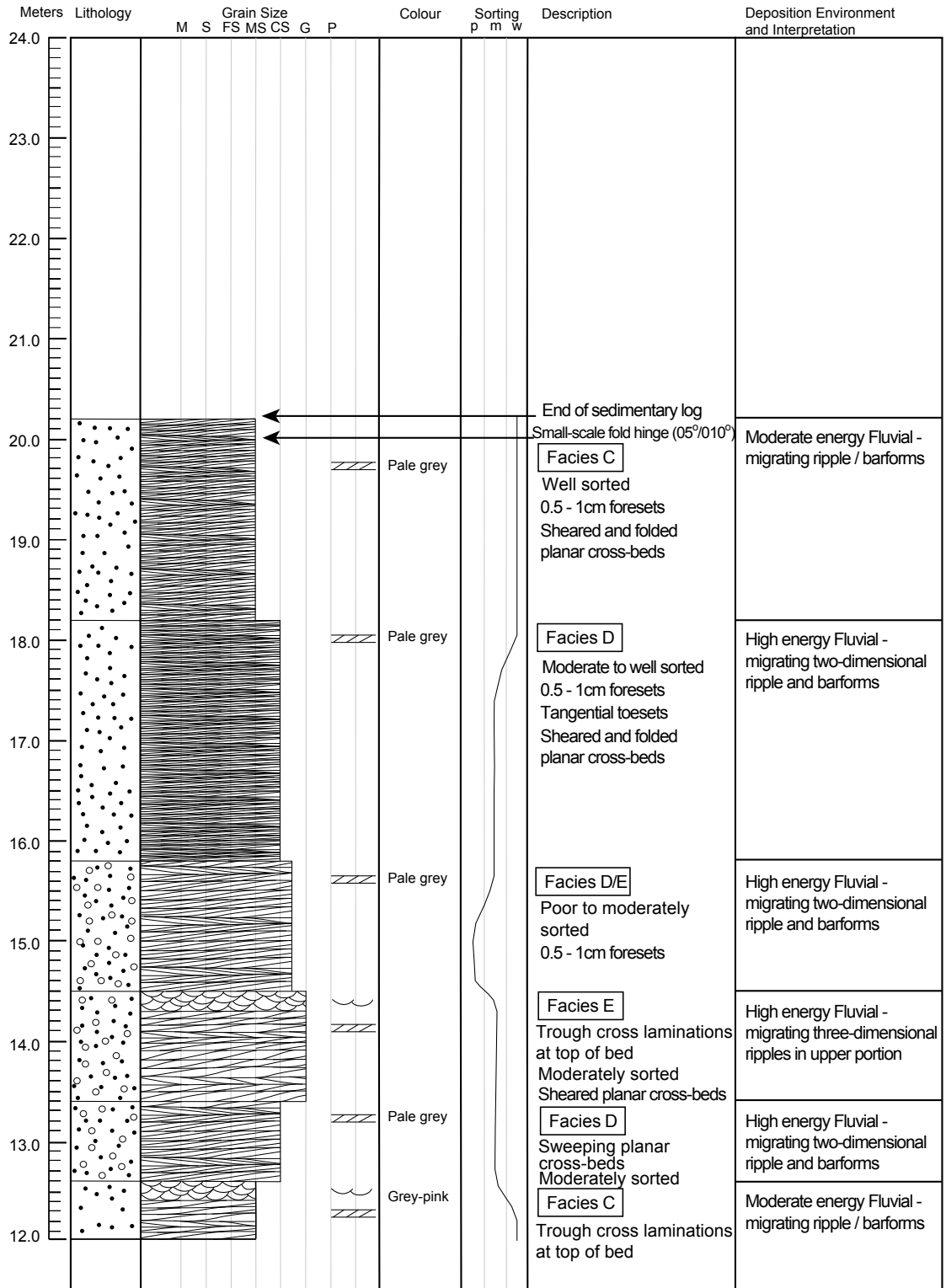


Figure 11. b) Mount Ragged Sedimentary Log 3; log sheet 2.

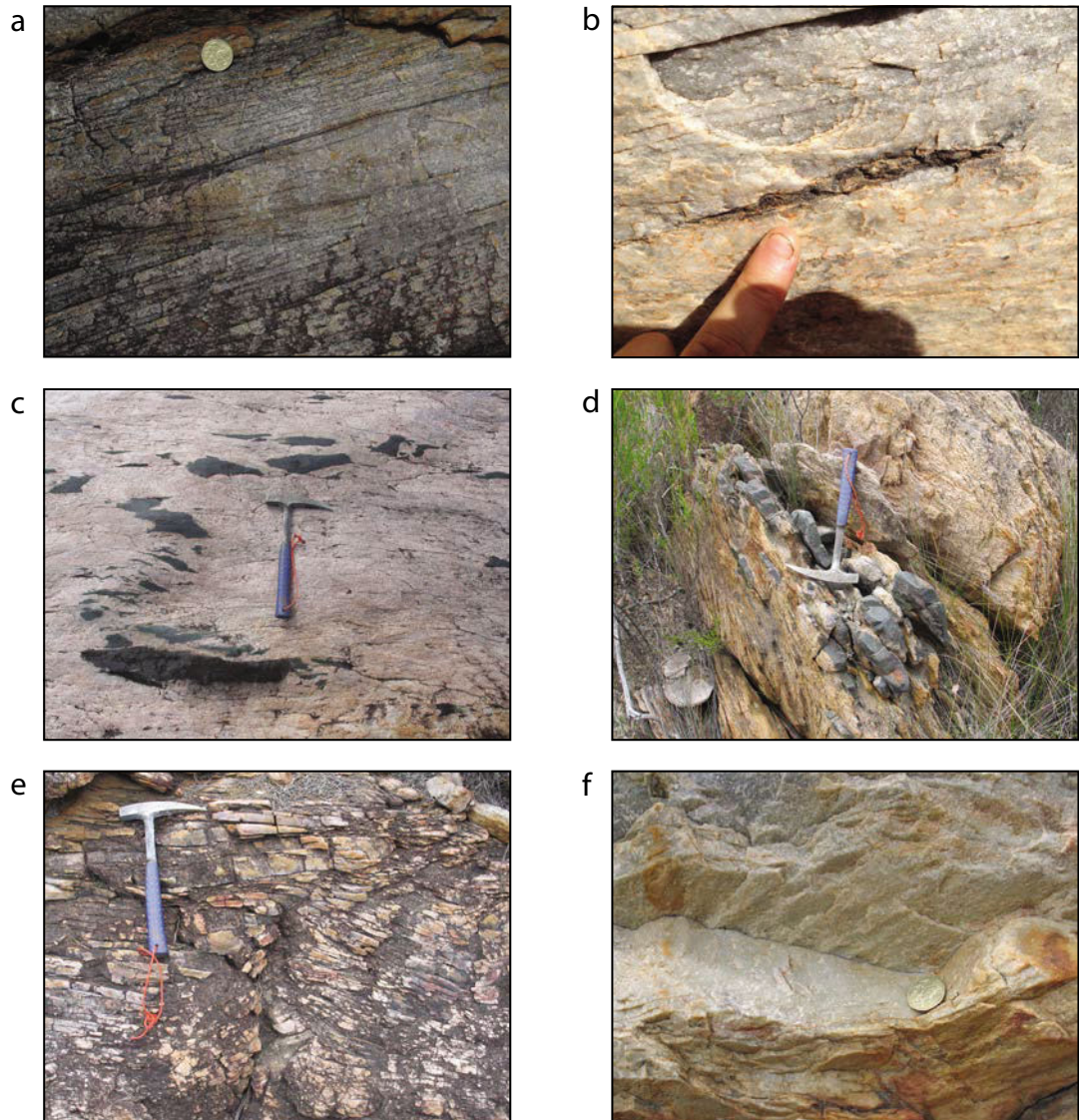


Figure 12. Sedimentary structures common to the Mount Ragged Formation. a) Truncated cross-beds with micaceous lined foresets in medium-grained quartzite, Mount Ragged (MGA 543122E, 6297081N); Australian one dollar coin for scale; b) Mud clast on foreset in medium-grained quartzite, Mount Ragged (MGA 543122E, 6297081N); c) Rip up clasts of metasiltstone within medium-grained quartzite, Mount Esmond (MGA 560215E, 6314262N); d) Rip up clasts of metasiltstone within fine-grained metasandstone beds, Mount Esmond (MGA 560206E, 6314258N); e) Truncated cross-beds by a scoured surface, medium-grained quartzite, Mount Ragged (MGA 545291E, 6300228N); f) Ripples above a medium-grained quartzite bed, Mount Ragged (MGA 543122E, 6297081N); Australian one dollar coin for scale.

#### 4.1.2 Lithofacies analysis of the Mount Ragged Formation

Across all the areas visited in this study (i.e. Mica Hill, Mt Esmond, Mt Ragged, and Russell Range) the sedimentary rocks had distinctive characteristics such that they could be divided into five sedimentary facies. A facies scheme was developed, which is summarised in Table 1 and described in detail below (Figure 13).

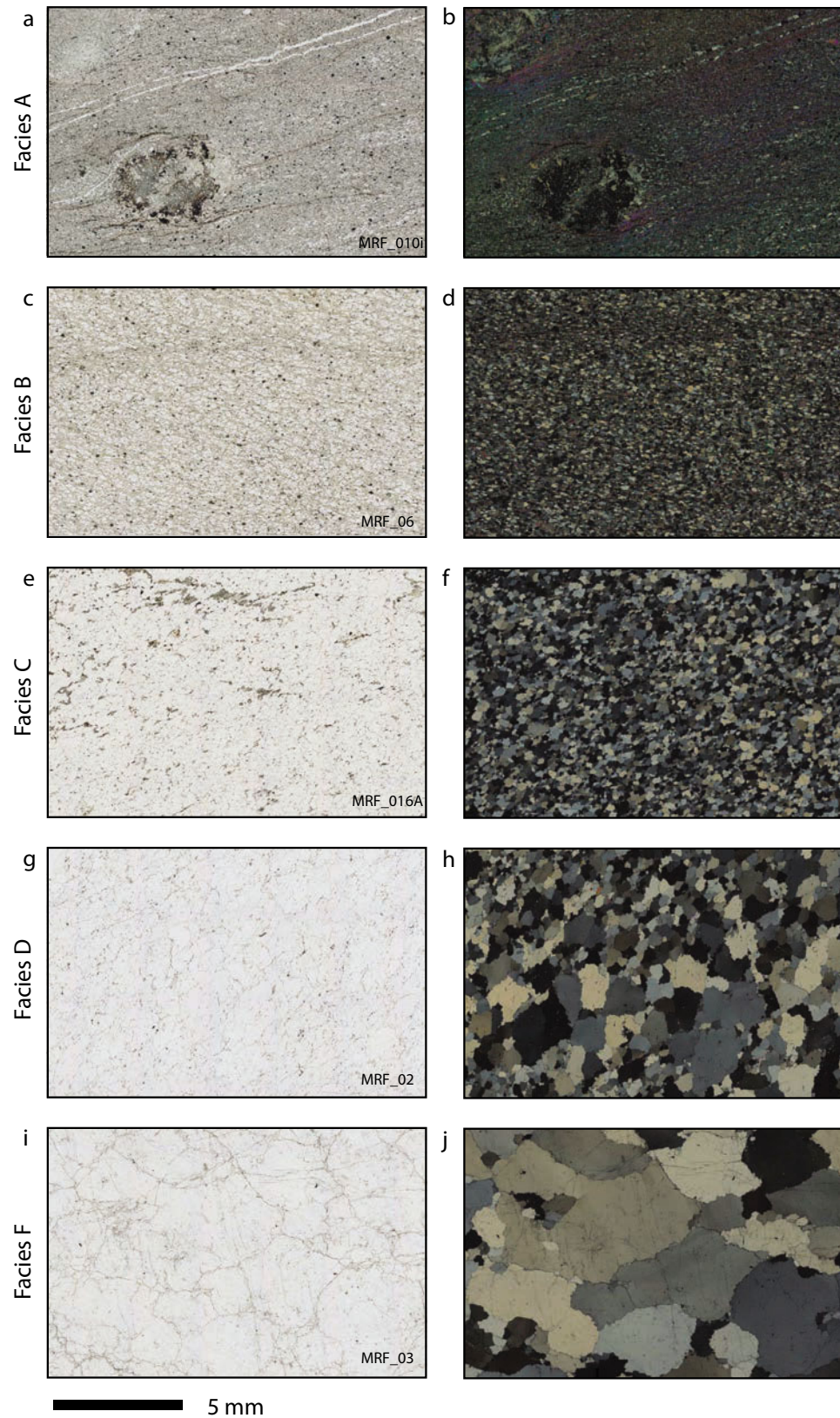
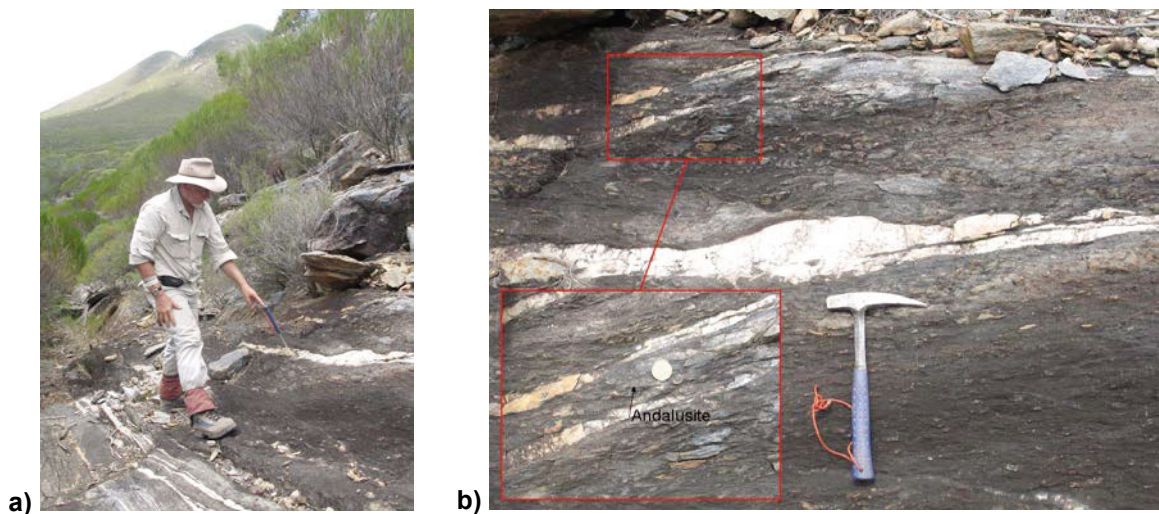


Figure 13. Plane-polarised light and cross-polarised light images of Mount Ragged Formation facies. a-b) Facies A: Metapelite (Andalusite-Chlorite-Muscovite schist); c-d) Facies B: Fine-grained metasandstone; e-f) Facies C: Medium-grained quartzite; g-h) Facies D: Coarse-grained quartzite; i-j) Facies E: Quartz gritstone.

#### 4.1.2.1 Facies A: Metapelite to laminated metasiltstone

These finely laminated layers consist of very fine to fine-grained sediments, ranging from muds to silts (Figures 13a & b). Lenses can range in width from a few millimetres to tens of centimetres. Layers can be up to a several metre wide and laterally continuous over tens of metres (Figures 14a). In the lowermost topographic units thin layers and lenses of metapelite and metasiltstone are infrequently interspersed between the more common fine- to medium-grained quartzites. Large outcrops of siltstone are poorly preserved and metapelite schists were only ever observed on the western flanks of Mount Ragged and Russell Range. However, access to the eastern slopes of Mount Ragged and Russell Range was extremely difficult due to vegetation and topography, and so the presence of laterally continuous, larger units of Facies A elsewhere cannot be precluded.

Infrequent rip-up clasts of mud and silt occurred amongst the beds of the larger grained units. Often such rip-up clasts tended to be located in proximal strata above more intact layers of mud and siltstone (Figures 12c & d).



**Figure 14. a) Metapelite schist and metasiltstone beds exposed in narrow gully, Russell Range (MGA 546468E, 6306648N); Upright geo-pick indicates the southeasterly angle of dip. b) Andalusite-bearing metasiltstone (same location); Australian one dollar coin for scale; Sample MRF\_010 (Figures 13a & b).**

#### 4.1.2.2 Facies B: Planar-laminated, fine-grained metasandstone

Generally, this fine-grained lithofacies occurs in thin beds around 50 cm thick, though rare beds were observed at thickness of around 1.5 metres. The internal structure of beds commonly consists of 5 mm thick planar, parallel laminations (Figure 15). Ripple marks were sometimes present on bed surfaces. This facies has a cream to orange colouration due to weathering.

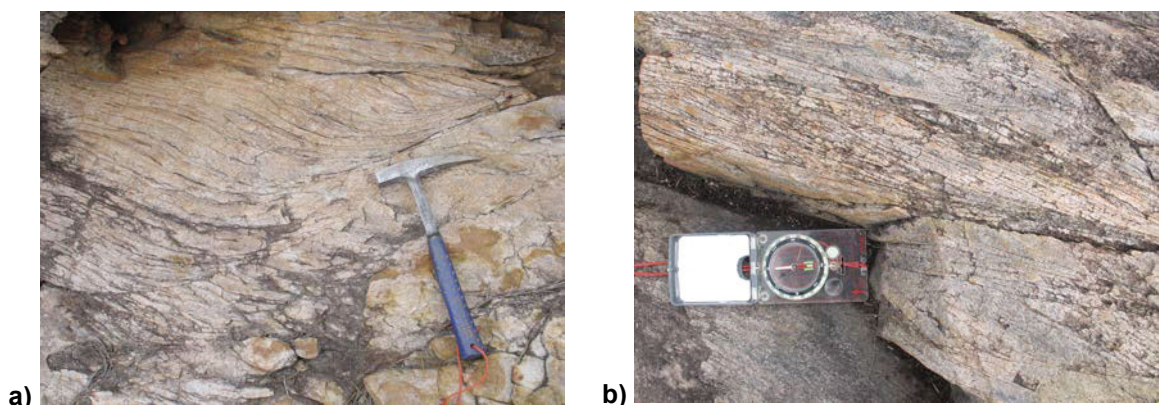
Rocks associated with this facies consist of a fine-grained, homogenous quartz matrix with interstitial opaques and small laths of muscovite. These beds consist of fine-grained, rounded, well-sorted metasandstone (Figures 13c & d) and are typically interspersed between the more common medium-grained quartzites or occurring immediately below and grading into mud and siltstone layers.



**Figure 15. Fine-grained, planar laminated metasandstone, Russell Range (MGA 545298E, 6305674N).**

#### 4.1.2.3 Facies C: Cross-bedded, medium-grained quartzite

The most dominant lithology across the Mount Ragged Formation are medium-grained, well-sorted quartzites with sub-rounded to rounded grains (Figures 13e & f). Typically, these quartzites are well bedded, with beds ranging from 30 to 160 cm. Cross-stratification is common within bedforms, with co-sets consisting of a variable number of sets which are commonly about 10 cm thick. Planar cross-bedding is most common, and tangential toesets are commonly preserved (Figure 16a). The thicknesses of individual foresets ranged from 0.5 to 2 cm. Infrequently, upper foreset surfaces were mud-draped, and some contain mud rip-up clasts. Foreset truncation was the most common sedimentary structure used to determine the way-up of beds (Figure 16b). Whilst cross-stratification generally was unidirectional multi-directional cross-stratification within sets was occasionally observed.



**Figure 16. a) Tangential toe-sets in planar cross-bedded, medium-grained quartzite, Mount Ragged (MGA 545237E, 6300182N). b) Truncated cross-beds in medium-grained quartzite, Mount Esmond (MGA 560798E, 6314242N).**

#### 4.1.2.4 Facies D: Coarse-grained quartzite

This facies consists of beds of medium- to coarse-grained quartzite with sub-angular to sub-rounded grains, poorly sorted matrix with occasional, angular coarse-grained or granular clasts (Figures 13g, 13h & 17). These quartzites tend to be dark grey in colour. Quartzites associated with this facies occur in thick beds ranging from 150 to 250 cm. Cross-stratification co-sets consist of a numerous sets which are commonly about 10 - 20 cm thick.

Individual foresets thicknesses ranged from 0.5 to 1 cm, though some foresets were up to 2 cm thick. Internal bedding structures typically consist of planar cross-bedding, though trough-cross bedding, massive and planar bedding are also present. This lithofacies can be subdivided into four sub-facies based on these sedimentary structures.



**Figure 17. Poorly-sorted, coarse-grained quartzite, Mount Ragged (MGA 543627E, 6297322N); Sample MRF\_02 (Figures 13g & h).**

1. Planar cross-bedded sub-facies
2. Trough cross-bedded sub-facies
3. Massive sub-facies
4. Planar laminated sub-facies.

This facies was most frequently observed on the uppermost ridges and amongst the boulders and scree slopes of Mount Ragged.

#### 4.1.2.5 Facies E: Quartz gritstone to pebble conglomerate

Within the strata dominated by poorly-sorted quartz-dominated gritstone and quartz-pebble conglomerates are thick beds ( $\leq 1.5$  m) consisting solely of a well-sorted, coarse grained matrix of granular ( $\leq 8$ mm), transparent, quartz clasts.

These pebble conglomerates or gritstones typically consist of angular grains of low sphericity (Figures 13i, 13j & 18). They are dark grey and weather to a rough surface. Like facies D this lithofacies can be subdivided into sub-facies based on three internal bedding structures: thick massive beds, planar cross-beds and trough cross-beds. Quartz-pebble conglomerate occurs sporadically on the uppermost ridges of Mount Ragged, and is commonly associated with Facies D: Coarse-grained quartzites.



**Figure 18. Well-sorted, pebble conglomerate quartzite, Mount Ragged (MGA 543627E, 6297322N); Sample MRF\_03 (Figure 13i & j).**

#### 4.1.2.6 Facies summary

The Mount Ragged Formation consists of stacked cross-bedded sandstones with a few mudstone and siltstone interbeds. Table 1. summarises the primary characteristics of each facies unit.

**Table 1.** Primary characteristics of the facies units of the Mount Ragged Formation

<b>Facies</b>	<b>A</b>	<b>B</b>	<b>C</b>	<b>D</b>	<b>E</b>
	Metapelite to laminated metasilstone	Planar-laminated, fine-grained metasandstone	Cross-bedded, medium-grained quartzite	Coarse-grained quartzite	Quartz gritstones to pebble conglomerate
<b>Grainsize*</b>	Clay - Silt	Fine sand	Medium sand	Coarse sand	Granules - Pebbles
<b>Roundness</b>	Well-rounded	Rounded	Rounded - Sub-rounded	Sub-rounded - Sub-angular	Angular
<b>Sphericity</b>	High	High	Medium	Low	Low
<b>Sorting</b>	Moderate	Well	Well	Poor	Well
<b>Primary Sedimentary structures</b>	Finely laminated	Planar laminations occasion ripples	Planar cross-beds	Planar cross-beds Trough-cross beds Massive beds Planar beds	Planar cross-beds Trough-cross beds Massive beds
<b>Deposition environment</b>	Channel abandonment or overbank deposits	High energy, channel fill or distal fluvial environment	Moderate energy, fluvial environment	High energy, proximal, braided fluvial environment	High energy, proximal, braided fluvial environment

\* Wentworth Grade Scale (Wentworth 1922)

## **4.2 Igneous rocks (Prominent local Nornalup Zone outcrop)**

As well as the metasedimentary hills and ridges of the Russell Range, the only other prominent geological features to outcrop at the surface are sparse low-lying hills and pavements of granitic rocks of the Nornalup Zone. These are interpreted as representing the unconformable basement rocks to the Mount Ragged Formation. The following descriptions and information has been summarised from GSWA Warox sites in the surrounding area of the Mount Ragged Formation (Location details are provided in Appendix 4 - Table A4.1), and are key to 'ground truthing' the interpretation of aeromagnetic presented in Section 4.3.

### **4.2.1 Gora Hill**

The following information is provided from Warox site CVSEAF000332 and is based on sample 194876. Gora Hill is a large hill of metamonzogranite and is considered similar to the pavement outcrop at Warox site CVSEAF000331. It is equigranular, fine- to medium-grained, quartz-rich and leucocratic. It is slightly banded with biotite defining a foliation that strikes 048°, with some alignment of quartz and feldspar. There are also thin layer and foliation parallel granitic veins that are slightly coarser than the host, as well as cross cutting pegmatite veins. The magnetic susceptibility readings are zero.

### **4.2.2 Junana Rock**

The following information is provided from Warox site CVSEAF000333 and is based on sample 194877. Junana Rock is a 600 metre long pavement section of medium-grained and homogeneous metamonzogranite. It has a strong foliation defined by elongate biotite aggregates that are evenly distributed throughout, plus a minor amount of hornblende. The foliation is stronger and more gneissic, and the rock more biotite-rich than Gora Hill to the southeast. The foliation is cut by granitic to coarse pegmatitic veins and minor quartz veins. The magnetic susceptibility readings range from 460 to 860 x 10<sup>-5</sup> SI.

### **4.2.3 Juranda Rockhole**

The following information is provided from Warox site CVSEAF000335 and is based on sample 194879. Juranda Rockhole is a large waterhole flanked by rock. On the southeastern side it is a fine-grained, equigranular, garnet-bearing metamonzogranite with

a weak fabric, locally. On the northwestern side it is similar but lacks garnet. There is a small west-northwest trending brittle fault between the two phases. The foliation strikes  $050^{\circ}$ . Magnetic susceptibility readings in garnet-bearing phase range from 100 to  $200 \times 10^{-5}$  SI, whereas in the non-garnet phase readings range from 700 to  $1100 \times 10^{-5}$  SI.

#### 4.2.4 Outcrop northeast of Gora Hill

The following information is provided from Warox site CVSEAF000331. Granitic gneiss pavement southeast of the Balladonia Track, northeast of Gora Hill. The pavement consists of banded, even-grained granitic gneiss with layer-parallel leucosomes. The magnetic susceptibility readings range from 910 to  $1150 \times 10^{-5}$  SI.

#### 4.2.5 Pine Hill

The following information is provided from Warox site CVSEAF000334 and is based on sample 194878. Pine Hill refers to a large section of pavement outcrop of fine- to medium-grained, homogeneous, equigranular metamonzogranite. It has a moderate to strong foliation defined by biotite. Numerous fine- to coarse-grained granitic veins are present. The magnetic susceptibility readings range from 80 to  $130 \times 10^{-5}$  SI.

#### 4.2.6 Scott Rock

The following information is provided from Warox site CVSEAF000384 and is based on samples 192584, 192586 and 192587. Scott Rock consists of isolated pavements and low rises of monzogranite surrounded by dense scrub. It is medium-grained (1-4 mm) with an average grain size of 3 mm and consists of an equigranular matrix of two feldspars, quartz, biotite and magnetite. Porphyritic 2-3 cm long K-feldspar phenocrysts are also present. This monzogranite also contains small mafic xenoliths (probably mafic to hybrid enclaves). These are mostly a few centimetres long and rectangular, though some are rounded. There are no signs of deformation. The magnetic susceptibility readings are moderate to high which matches the aeromagnetic data.

#### 4.2.7 She-oaks Hill

The following information is provided from Warox site CVSEAF000328 and is based on sample 194873. She-oaks Hill refers to a small pavement outcrop of porphyritic monzogranite that is medium to coarse-grained. Abundant, large (2-3 cm long) K-feldspar phenocrysts are weakly to moderately aligned, trending 045°, and is interpreted to be a magmatic foliation. Biotite and hornblende are common. Magnetic susceptibility readings show that rocks at this locality are non-magnetic.

#### 4.2.8 Wolgrah Hill

The following information is provided from Warox sites CVSEAF000390 and CVSEAF000391 and is based on sample 192588. Wolgrah Hill comprises homogeneous and medium-grained metagranite with an equigranular to seriate texture. The grainsize is 3-4 mm, though some K-feldspar phenocrysts are up to 5 cm. It is of monzogranite to granodiorite composition and plagioclase is common. There are locally abundant quartz veins up to 30 cm. There is a moderately developed foliation that is defined mostly by biotite and quartz, and that strikes northeast. This metagranite is considered to be different to the monzogranite of Scott Rock. The magnetic susceptibility readings average  $6 \times 10^{-3}$  SI, which is less than those at Scott Rock.

### 4.3 Geophysical interpretation

Several subsurface features and regions with different properties can be distinguished on the aeromagnetic images within the project area (Figure 19 and Appendix 5, Figures A5.1 & A5.2). These are indicated by colours that correspond to magnetic highs and lows. The outcropping ridges of the Mount Ragged Formation and several adjacent 'along strike' domains are areas of low magnetism (dark blue areas) (Figure 19). These are considered to indicate the subsurface extent of lithologies of the Mount Ragged Formation, i.e. the Ragged Basin sediments, whilst also corresponding with the lows in the magnetic imagery.

Whilst most of the blue shaded areas are interpreted as corresponding with Ragged Basin sediments, some blue areas are interpreted as indicating an area with a low magnetic signature rather than actual lithology. This is because they are adjacent to and between zones with a higher magnetic signature. These are typically linear bands immediately between two zones with a high magnetic signature.

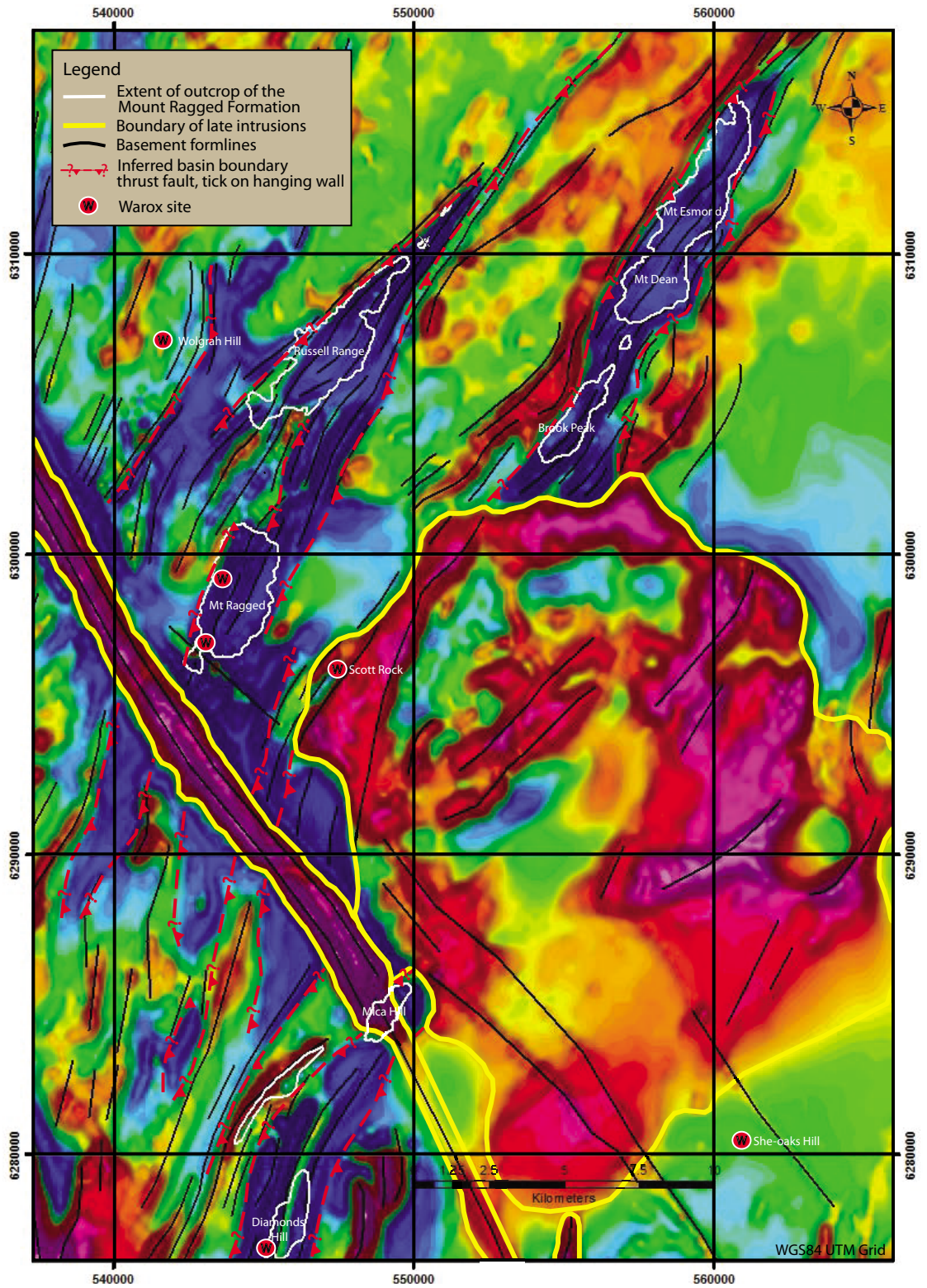


Figure 19: Aeromagnetic image of Mount Ragged Formation and surrounds (Reduction to pole; Sun angle directly overhead)

The RTP aeromagnetic image shows that the subsurface of the project area elsewhere is dominated by rocks with similar magnetic properties (Appendix 5, Figure A5.1). This is interpreted to represent typical basement (gneiss and granitoid) rocks of the Nornalup Zone, here predominantly from the Recherche Supersuite.

In the project area, two prominent subsurface features with different magnetic properties appear to cross-cut all other features (Figure 19). Both show a high magnetic signature. One is a long, northwest-southeast trending linear structure that is interpreted to be a dyke. It lies to the south of Mount Ragged and terminates below the surface expression of Mica Hill. Interestingly, this subsurface dyke is orientated in the same alignment as a northwest-southeast fault that truncates through the middle of Mica Hill (Appendix 6, Figure A6.1).

The other subsurface feature is a large sub-circular object that truncates the southeastern strike continuation of the Ragged Basin sediments of Mount Esmond and other basement rocks. The only outcrop of this prominent feature is the isolated monzogranite outcrop of Scott Rock (Section 4.2.6). This feature is considered to represent a late granite intrusion. No significant deformation structures are visible in the aeromagnetic image of this structure.

#### **4.4 Structural data**

Geological maps relevant to each of the four field sites are provided in Appendix 6. These maps display locations of structural measurements such as the strike and dip of bedding and cleavage, as well as fold information. A map with stereographic projections of all four field sites is provided at the rear of this report (Plate 1). Plate 1 includes stereographic projections of poles to bedding, poles to cleavage, fold hinges and axial surfaces and mean cleavage planes. Individual maps with stereographic projections relevant to all four field sites are provided in Appendix 7.

##### **4.4.1 Mica Hill**

Mica Hill is a low-lying, elongate hill orientated in a northeast-southwest direction (Appendix 1, Aerial photograph A1.1). The mid-section of Mica Hill is truncated by a deep, narrow gully that cuts down to the level of the surrounding calcareous plain. This gully is inferred to be coincident with a northwest-southeast trending fault.

Field structural measurements were predominantly taken from beds consisting of coarse-grained, well-sorted quartzite. Structural formlines shown on the geological map of Mica Hill correspond to bedding surfaces that define a gently, southwest plunging, moderately inclined, tight fold, with northwest vergence (Appendix 6, Figure A6.1). The quartzite beds typically dip to the southeast, with a mean strike of  $35^\circ$ , and are moderately inclined with dips ranging between  $40^\circ$  and  $76^\circ$ , with mean and median dip angle of  $50^\circ$ ;  $n=12$  (Appendix 7, Figure A7.1a). The strike of bedding planes is typically aligned closely with cleavage. The mean principal orientation of cleavage is with a strike of  $034^\circ$  and dip of  $84^\circ$  ( $n=15$ ) (Appendix 7, Figure A7.1b).

The most common fold structures observed in the field were small- to meso-scale parasitic, synform fold hinges (Figure 20). Only one meso-scale antiform fold hinge was observed. The mean principal orientation of fold hinges indicates a plunge of  $31^\circ$  with a plunge direction of  $209^\circ$  ( $n=16$ ). The mean principal orientation of the bedding-cleavage intersection indicates a plunge of  $9^\circ$  with a plunge direction of  $218^\circ$  ( $n=6$ ), which is nearly parallel with the measured meso-scale fold hinges (Appendix 7, Figure 7.1c). Mica Hill is interpreted as a series of gently southwest plunging, steeply inclined folds, with northwest vergence.



**Figure 20. Folded cross-beds in coarse-grained quartzite, Mica Hill (MGA 549384E, 6285449N); Australian one dollar coin for scale, photograph looking southwest.**

Whilst poorly defined across most of the strata at Mica Hill, the occasional truncation of cross-stratification in cosets within bedding facilitated the determination of a younging direction. Twenty-two observations of way-up structures were taken to determine younging direction. In the northeastern part of Mica Hill, beds on the western side young to the east whilst the beds on the eastern side predominantly indicated younging to the west, indicating that the main fold is a syncline. In the southeastern hill section, way-up structures predominantly indicated younging to the east though rare beds indicating younging to the west were very occasionally observed. Aligned linear domains in between beds with opposite younging directions commonly contain chaotic bedding in association

with numerous, parallel quartz veins, and/or are topographic lows (as viewed through a stereoscope). Thus, these domains are inferred to be hinge zones of synforms (Figure 21).



**Figure 21. Chaotic bedding in coarse-grained quartzite, inferred to be a synform hinge zone, Mica Hill (MGA 548990E, 6284470N).**

#### 4.4.2 Mount Esmond

During fieldwork for this project, only the northernmost flanks and ridge of Mount Esmond were traversed due to difficulties with access causing time constraints. Mount Esmond is laterally continuous with Mount Dean and together form a long, linear ridge that is orientated in a northeast-southwest direction (Appendix 1, Aerial photograph A1.2).

Structural measurements were predominantly taken from beds consisting of fine- to medium-grained, well-sorted metasandstones and quartzites (Facies B and C). Formlines shown on the geological map of Mount Esmond are based on prominent bedding surfaces identified from the aerial photograph (Appendix 6, Figure A6.2). The majority of beds dip to the southeast and are steeply inclined with dips ranging between  $48^{\circ}$  and  $89^{\circ}$ , with a mean strike of  $29^{\circ}$  and dip angle of  $74^{\circ}$  and a median dip angle of  $78^{\circ}$ ;  $n=18$  (Appendix 7, Figure A7.2a). Bedding and cleavage planes are typically closely aligned in strike, and cleavage is, on the whole, steeper dipping. The mean principal orientation of cleavage is with a strike of  $030^{\circ}$  and dip of  $87^{\circ}$  ( $n=21$ ) (Appendix 7, Figure A7.2b).

During traverses over Mount Esmond, only three fold structures were observed. These consisted of two small-scale, synform fold hinges and one tight meso-scale antiform fold hinge. The mean principal orientation of fold hinges from these three structures plunges  $11^\circ$  towards  $031^\circ$  ( $n=3$ ). When plotted together, the mean cleavage plane ( $030^\circ / 87^\circ$ ;  $n=21$ ) shows a good correlation with the mean axial plane of the three folds ( $11^\circ / 031^\circ$ ;  $n=3$ ) (Appendix 7, Figure 7.2d). Mount Esmond is interpreted as a series of gently northeast plunging, steeply inclined folds with northwest vergence.

Truncated cross-stratification in cosets provided the only effective means of determining younging direction at Mount Esmond, though it was typically poorly defined. Thirty observations of way-up structures taken across the traverse indicate that the stratigraphy predominantly youngs to the west, with rare beds indicating younging to the east. Chaotic bedding, in association with numerous, parallel quartz veins, was often observed aligned between beds with opposite younging directions. These beds are inferred to be the hinge zones of synforms, similar to those shown in Figure 21.

#### 4.4.3 Mount Ragged

Mount Ragged is a steep, elongate ridge orientated in a northeast-southwest direction (Appendix 1, Aerial photograph A1.3). Structural measurements were taken from beds consisting of all the lithological types listed in Section 4.1 (i.e. from metapelites to coarse-grained and granular quartzites). Formlines shown on the geological map of Mount Ragged are based on bedding surfaces (Appendix 6, Figure A6.3). Mount Ragged beds predominantly dip to the southeast, with mean strike of  $37^\circ$ , and are steeply inclined with a mean dip angle of  $64^\circ$  and a median dip angle of  $69^\circ$ ;  $n=175$  (Appendix 7, Figure A7.3a). However, a significant proportion ( $\approx 27\%$ ) of beds dipped to the northwest, whilst  $< 3\%$  of beds were considered to be vertical. Cleavage was hard to distinguish from other sedimentary structures (e.g. foresets of cross-beds) and only nine cleavage measurements were made with confidence. However, these measurements indicate that the strike of cleavage is aligned closely to bedding, but with steeper dips. The mean principal orientation of cleavage has a strike of  $029^\circ$  and dip of  $84^\circ$  ( $n=9$ ) (Appendix 7, Figure A7.3b).

The most common fold structures observed on Mount Ragged were small- to meso-scale, steeply inclined synform hinges in thinly bedded facies (Figure 22). Antiform fold hinges were much less commonly seen ( $n = 2$ ), and folded foresets were observed at two locations. Meso-scale folds are consistently orientated on Mount Ragged, with a mean hinge plunge of  $26^\circ$  towards  $027^\circ$  ( $n=30$ ). (Appendix 6, Figure A6.2c). Mount Ragged is interpreted as a series of gently, northeast plunging, steeply inclined folds with northwest vergence.



**Figure 22. Small-scale S-folds in medium-grained, quartzite, Mount Ragged (MGA 543678E, 6297324N); Australian dollar coin for scale.**

Seventy-one way-up structures were observed and used to determine younging directions across Mount Ragged. The stratigraphy predominantly youngs to the west, although less common observations of younging to the east coincide with the short limbs of west-verging folds.

#### 4.4.4 Russell Range

Due to accessibility issues, traverses on Russell Range were restricted to the southern half of the range. Russell Range proper is a long, linear ridge that is orientated in a northeast-southwest direction (Appendix 1, Aerial photograph A1.4).

Structural measurements were predominantly taken from beds consisting of medium-grained, well-sorted quartzites (i.e. Facies B and C). Formlines shown on the geological map of Russell Range are based on prominent bedding surfaces (Appendix 6, Figure A6.4). The majority of beds dip to the southeast and are steeply inclined with dips ranging between  $20^\circ$  and  $90^\circ$ , with mean strike of  $38^\circ$  and dip angle of  $65^\circ$  and a median dip angle of  $70^\circ$ ;  $n=31$  (Appendix 7, Figure A7.4a). Typically bedding and cleavage planes are closely aligned in strike, with a mean orientation  $037^\circ$  and dip of  $86^\circ$  ( $n=28$ ) (Appendix 7, Figure A7.4b).

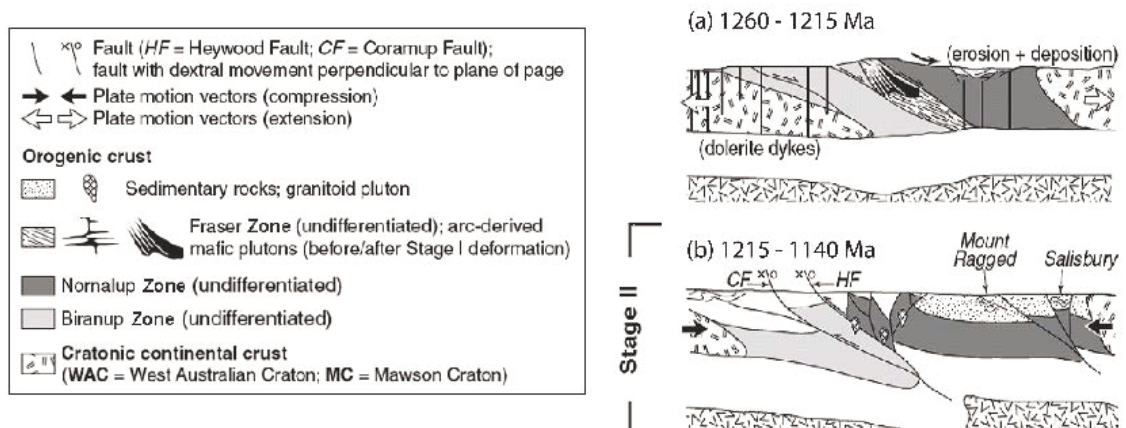
Only six folds were observed along the traverses over the southern areas of Russell Range. These consisted of four small-scale, synform fold hinges, one S-form fold and one M-form fold. The mean orientation of fold hinges from these six structures plunges of  $21^\circ$  towards

037° (n=6). When plotted together the mean cleavage plane (037° / 86°; n=28) and the mean principal orientation of the six folds (21° / 037°; n=6) shows a good correlation (Appendix 7, Figure A7.4d). The Russell Range proper is interpreted as a series of gently northeast plunging, steeply inclined folds, with northwest vergence.

Twenty-two observations of way-up structures were taken in confidence to determine younging direction. Across the area traversed way-up structures predominantly indicated younging to the east, though younging to the west was also observed but less frequently. Despite the lack of folded structures it appears that the western side of fold structures were younging to the east and the eastern sides were younging to the west.

#### 4.5 Metamorphism

Metamorphism of the metasediments of the Mount Ragged Formation is considered to have occurred during the repeated intracontinental reworking of the Albany-Fraser Orogen during Stage II (Clark *et al.* 2000). This occurred when the Nornalup Zone underwent simultaneous dextral shearing, northwest-southeast directed compression resulting in thrusting and crustal thickening, specifically over-thrusting of the Salisbury Gneiss along the Rodona Shear Zone (Clark *et al.* 2000) (Figure 23). This resulted in the burial and subsequent metamorphism of the Mount Ragged sedimentary rocks to amphibolite facies at conditions of 500-600°C and 4-5 kbar (Clark *et al.* 2000). Though not visited in this investigation, previous reports (Lowry & Doepel 1974; Clark 1999) state that in the most southerly outcrops, such as Diamonds Hill, veins bear sillimanite and biotite rather than andalusite, and muscovite is rare. The presence of sillimanite further supports recrystallisation in upper greenschist to lower amphibolite facies.



**Figure 23. Deposition and metamorphic setting of Mount Ragged Formation (Modified from Bodorkos & Clark 2004b, figures 10e & f, p.724)**

The majority of the rocks exposed in the Mount Ragged Formation are hard, pink or grey coloured quartzites interspersed with minor amounts of muscovite-bearing quartzite and metapelitic schists. With the exception of where recrystallisation has occurred, the quartz grain boundaries generally display little to no strain. Muscovite is the dominant mica present, though chlorite and, less frequently, biotite are also present. Primary bedding planes are most often defined by opaque grains, typically haematite, which are commonly anhedral. Opaque grains also locally define the former boundary of larger quartz clasts (coarse to pebble sized / 1 to 5 mm) now recrystallised to smaller grained aggregates or other minerals (Figures 24b & c). There are also sporadic components of quartz-pebble conglomerate which occurred most frequently on the upper ridges and scree slopes of Mount Ragged.

Clark (1999) identified four types of metasediments which fieldwork and sampling for this investigation concur with. Amongst other characteristics, the most notable difference was the oxidation state of iron-oxides. The most common and abundant quartzite present across the formation Clark (1999) refers to as Type 1 metasediments. These contain hematite as the dominant opaque phase. Clark (1999) considers Type 2 metasediments to be areally restricted to the southwest flank of the Russell Range proper. These differ from Type 1 metasediments due to the stability of magnetite, together with almandine garnet and biotite.

The other two types of metasediments are the metapelitic schists which Clark (1999) subdivided into two types based on petrographic analysis: Type 1 schists contain hematite as the dominant opaque phase and lack minerals containing ferrous iron as a constituent (i.e. biotite); and Type 2 schists consist of magnetite, almandine garnet and biotite. Using this scheme, Type 1 schists are most abundant along the southwest flank of Mount Ragged. These schists consist of unaligned andalusite and gahnitic spinel porphyroblasts which overprint a fine-grained fabric defined by quartz, muscovite and haematite (Figures 24d & e; 25a & b). Clark (1999) also noted that subsequent to folding and the development of a related cleavage a static overprinting assemblage including muscovite, margarite, chlorite and rare kyanite formed. Clark (1999) considers Type 2 schists to only occur in the vicinity of Type 2 metasediments on the southwest flank of the Russell Range proper (Figures 14a & b). Type 2 schists consist of almandine garnet, andalusite and biotite porphyroblasts, which overprint a fine-grained matrix of muscovite, quartz and magnetite. This assemblage is overprinted by late random chlorite aggregates.

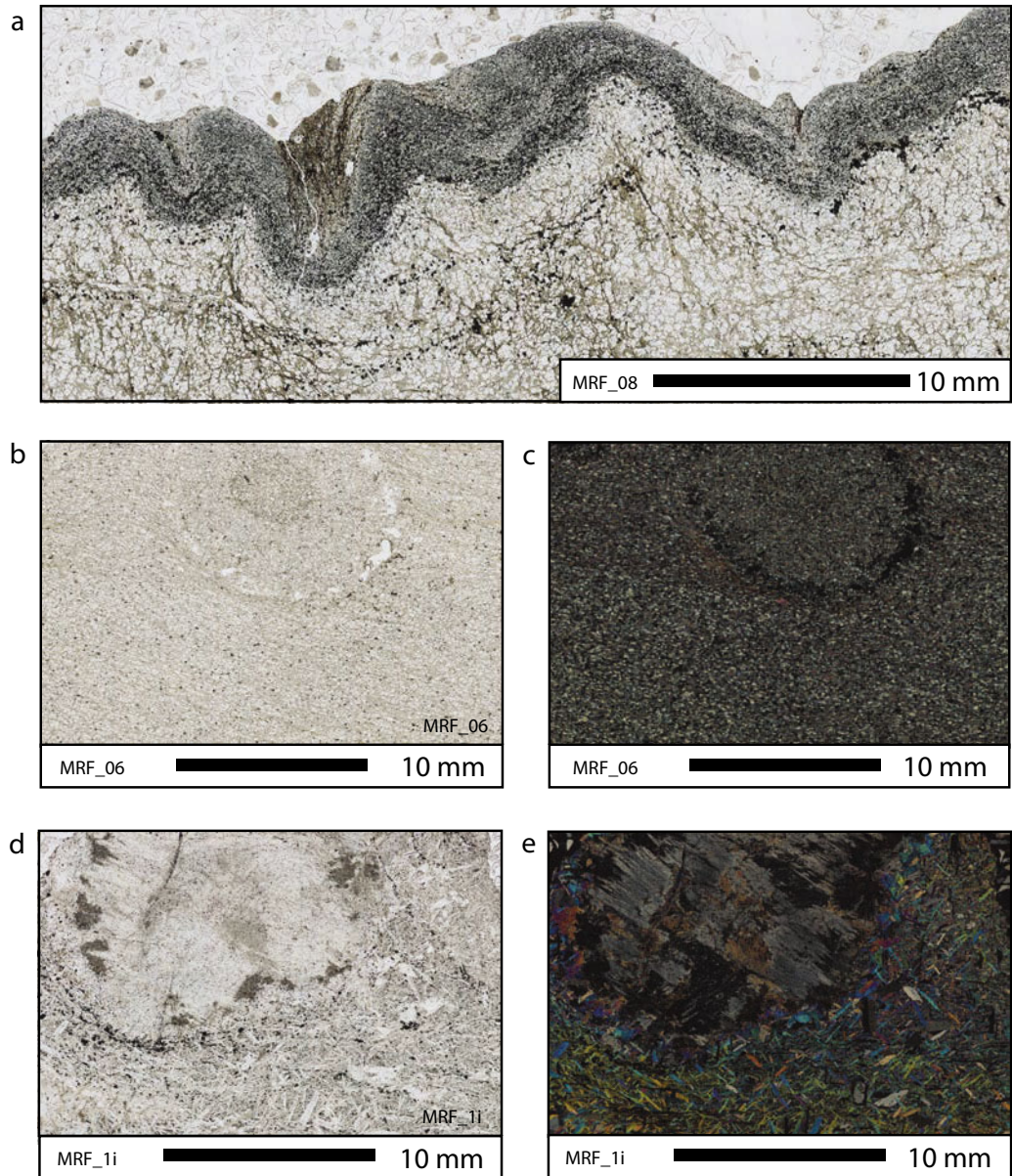
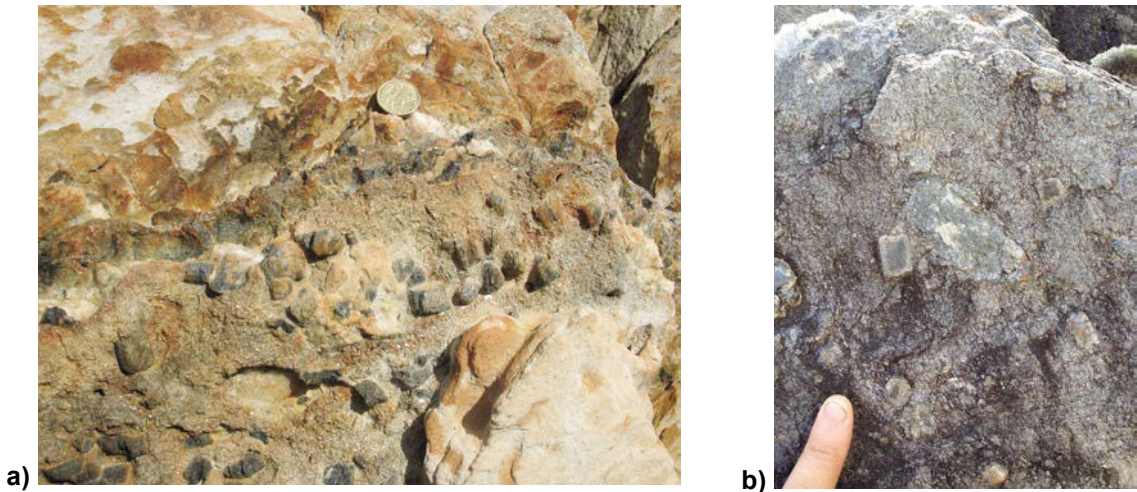
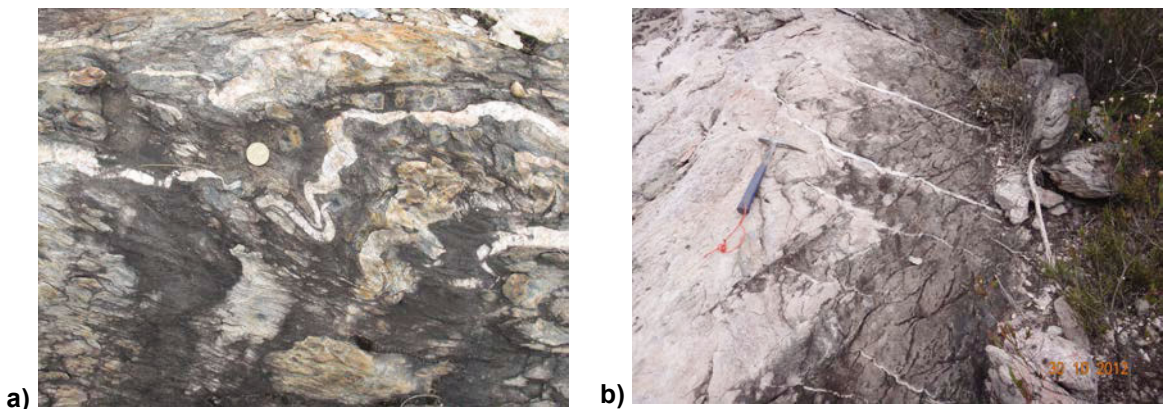


Figure 24. Photomicrographs of characteristic mineral assemblages and features in metasediments from the Mount Ragged Formation.  
 a) Metasandstone with metasiltstone foliation surface (Russell Range);  
 b [ppl] & c [xpl]) Opaques (hematite) define the outline of a larger clast or mineral, now recrystallised to an aggregate of smaller quartz grains (Mount Ragged);  
 d [ppl] & e [xpl]) Andalusite-Chlorite-Muscovite Schist (Mount Ragged).



**Figure 25. a) Andalusite-bearing metapelite schist (Type 1 schist) between fine-grained metasandstone, Mount Ragged (MGA 543205E, 6297088N); Australian one dollar coin for scale. b) Andalusite crystals with reaction rims in metapelite schist, Mount Ragged (MGA 543181E, 6297087N); Sample MRF\_01 (Figures 24d & e).**

Throughout the metasedimentary rocks of the Mount Ragged Formation quartz veins truncate the various lithologies. Whilst the majority of veining appears to be associated with deformation (Figure 26a), some veins are post-deformation and appear associated with later extensional events (Figure 26b).



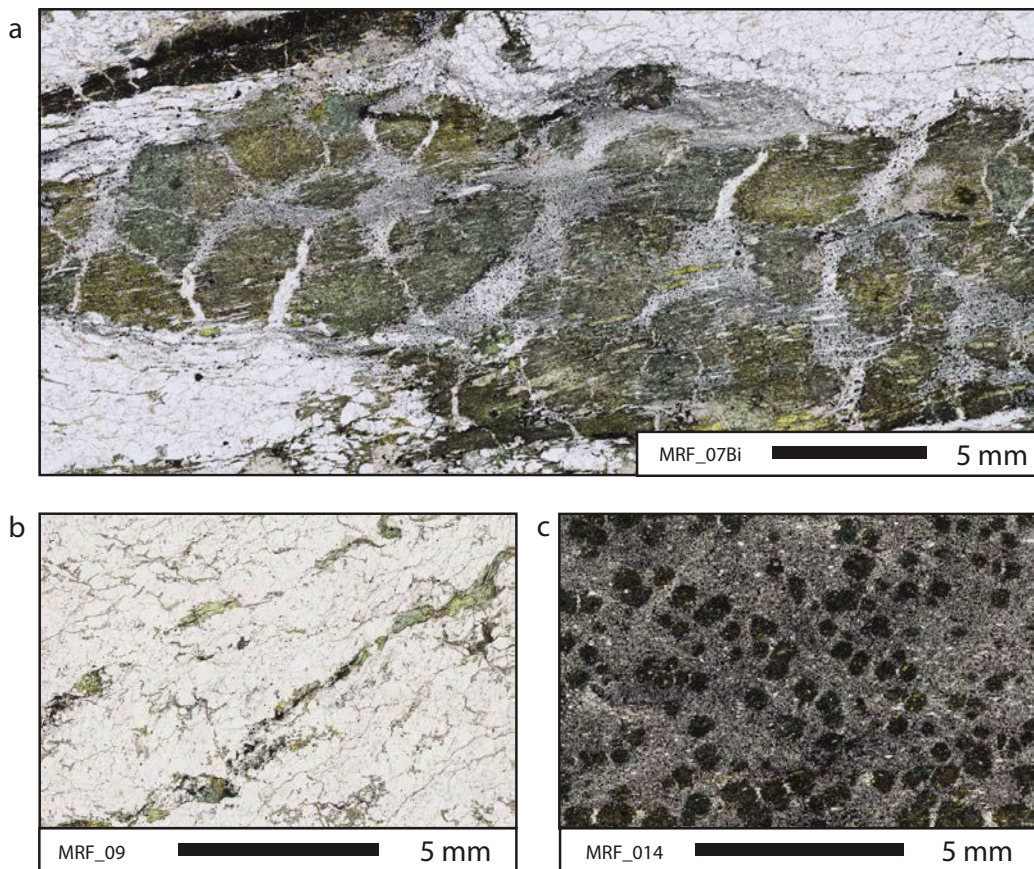
**Figure 26. a) Small-scale folded and sheared quartz veins in andalusite-bearing metapelite, Mount Ragged (MGA 543502E, 6296760N); Australian one dollar coin for scale. b) Post deformation, quartz vein tension-gash array in medium-grained quartzite, Mount Ragged (MGA 544079E, 6299045N); Geo-pick handle aligned due magnetic north (000°).**

Infrequently accompanying some quartz-veins or between bedding planes close to quartz veins is a bright green mineral (Figures 27 and 28a, b & c). Petrographic analysis by Prider (1960) and Clark (1999) has identified this as the aluminosilicate mineral viridine. In the north of the formation Clark (1999) also recognised that the aluminosilicate accompanying quartz-mica veins was exclusively viridine, whilst in the south the less stable aluminosilicate viridine-sillimanite occurs.

Based on Clark's (1999) petrographic analysis of quartzites close to these types of veins, that viridine forms anastomosing networks of anhedral grains interstitial to the quartz matrix, the presence of viridine-andalusite suggests precipitation from a fluid phase.



**Figure 27. Viridine-bearing quartz vein between beds of medium-grained quartzite, Mount Ragged (MGA 544044E, 6299239N); Australian one dollar coin for scale.**



**Figure 28. Photomicrographs of plane-polarised light images of various forms of viridine.**  
a) Boudinaged viridine: Viridine-enriched rip up clasts in medium-grained quartzite (Mount Ragged);  
b) Viridine veins growing with opaques within a medium-grained quartzite (Russell Range);  
c) Viridine overgrowths in a muscovite-opaque fabric: Rip up clast in medium-grained quartzite (Mount Esmond).

#### 4.6 Detrital zircon U-Pb geochronology

Synchronous to this project, five samples from the Mount Ragged Formation and outcrops in the surrounding area were selected for U-Pb zircon analysis by SHRIMP by the Geological Survey of Western Australia in order to constrain the ages of zircon-bearing rocks in the region. In the vicinity of the Mount Ragged Formation two granitic rocks were collected for U-Pb zircon analysis to ascertain the age of magmatic crystallisation: Sample 194876 from Gora Hill is a metamonzogranite; and sample 192586 from Scott Rock is a monzogranite. Three samples from the Mount Ragged Formation are from quartzites: sample 194866 from Diamonds Hill; and samples 194874 and 194875 are from Mount Ragged. Preliminary U-Pb SHRIMP zircon geochronology information was supplied courtesy of Kirkland and Wingate (2013), and are summarised with sample locations in Tables 2 and 3.

**Table 2.** Summary of SHRIMP sample locations, dataset sizes and age of magmatic crystallisation of igneous outcrop in the vicinity of the Mount Ragged Formation. Preliminary data supplied courtesy of GSWA (Kirkland and Wingate, 2013).

Location	Sample No.	MGA (Zone 51H)		Preliminary concordia age
		Easting	Northing	
Gora Hill	194876	533378	6287989	1327 ± 8 Ma
Scott Rock	192586	547537	6296127	1175 ± 12 Ma

**Table 3.** Summary of SHRIMP sample locations, dataset sizes and maximum deposition ages of Mount Ragged Formation metasedimentary rocks. Preliminary data supplied courtesy of GSWA (Kirkland and Wingate, 2013).

Location	Sample No.	MGA (Zone 51H)		Preliminary weighted mean <sup>207</sup> Pb*/ <sup>206</sup> Pb* age of youngest group
		Easting	Northing	
Diamonds Hill	194866	545094	6276797	1331 ± 19 Ma
Mt Ragged	194874	543567	6299223	1340 ± 16 Ma
Mt Ragged	194875	543042	6296990	1314 ± 19 Ma

## **5.0 Discussion**

### **5.1 Depositional environment of the Ragged Basin sediments**

The Mount Ragged Formation consists of stacked cross-bedded metasandstones with sparse interbedded metamudstone and metasilstone. Based on distinctive sedimentary characteristics the sedimentary rocks of the Mount Ragged Formation can be divided into five metasedimentary facies. As outlined below, facies analysis based on rock samples and sedimentary logs (Section 4.2) indicates that sedimentation occurred within a fluvial system, dominated by a shifting complex of sandy braided channels.

The metapelites and laminated metasilstones belonging to Facies A are considered to represent quiescent periods when sediments settled out after sheet or overbank flooding or as a result of fluvial channel abandonment. These fine-grained deposits may represent large pools within active channels, which accumulated fine sediment after flood abatement or after becoming isolated through channel abandonment, possibly later developing into overbank wetlands. Where rip-up clasts of mud and silt are present within the beds of the coarser-grained units, these are considered to represent a return to higher energy conditions or the reactivation of abandoned channels resulting in the erosion and redistribution of these finer deposits as larger clasts.

The planar-lamination that dominates the fine-grained metasandstones of Facies B is considered to indicate upper phase deposition which indicates high flow velocities suggestive of sedimentation in a high-energy environment. The fine grain size precludes lower phase deposition that typically occurs in coarser-grained, bed load sediments. Similarly, no gradational micro-scale layering, indicative of deposition from suspension currents, was observed in thin section. Cobble-sized siltstone rip-up clasts interspersed amongst some beds of this facies supports the likelihood of a high-energy fluvial system (Figure 12d). The fine grain size could be indicative of channel-fill deposits and/or that sedimentation occurred at a considerable distance from the sediment source area.

The cross-bedded, medium-grained quartzites of Facies C consist of rounded, medium-sphericity, well-sorted sediments. These are considered to have been deposited in a moderate-energy fluvial environment. The cross-stratification of bedding is considered to represent cross-bedded barforms. The planar cross-bedding was produced by migrating subaqueous bedforms and migrating two-dimensional ripple and channel bar and braid bar sands. At lower velocities, the basal contact of foresets with the previous set is angular. However, with increasing velocity and localised turbulence, generated on the lee slope of

foresets, the toe-set contacts become more tangential. The micaceous layering on some foresets may also indicate slack water after high flow or peak rainfall events. The presence of ripples, small scour channels with planar laminae, rip-up clasts and foreset mud draping also indicate fluctuating flow velocities synonymous with fluvial systems. Whilst cross-stratification is generally unidirectional, multi-directional cross-stratification within sets was observed locally. This is possibly the result of changes in current and flow direction caused by channel migration and switching.

The poorly sorted, coarse-grained quartzites of Facies D can be subdivided into four sub-facies, described below, based on internal structures:

- Migrating subaqueous dunes are considered responsible for producing planar cross-bedding in migrating two-dimensional ripple and barforms. Angular and tangential toe-sets are present.
- The occurrence of trough cross-beds is considered to indicate an increase in flow-energy regime resulting in the transition from straight rippled subaqueous dunes into more sinuous, undulating three-dimensional ripples. Very rarely, trough-cross beds are interspersed with isolated mud lenses, similar in appearance to flaser beds.
- Some beds display no distinctive sedimentary structures, but typically consisted of well-sorted coarse-grained sediments. These massive beds are likely to indicate periods of rapid sedimentation where there was insufficient time for bed forms to develop, possibly during periods of debris flows. The well-sorted character and uniformity of coarse grains may indicate a single, homogenous sediment source. Alternatively, these massive, well-sorted beds may represent periods of high-energy channel fill or the development of fluidised barforms. The obliteration of structures through considerable bioturbation is considered unlikely because of the paucity of fluvial biota during the Proterozoic.
- Planar beds may indicate high flow velocities in the upper flow regime within channels resulting in channel-fill consisting of horizontal laminae.

These typically poorly-sorted deposits of low sphericity are considered to represent sedimentation periods associated with high-energy flows, similar to those that occur in braided fluvial environments. The variety of sub-facies and resultant modification to bed forms is likely to be attributed to variations in fluvial flood phases.

The metaquartz gritstones and pebble conglomerates of Facies E are well-sorted. However, the angularity and low sphericity of the clasts indicate these are texturally immature sediments. The thick, coarse granular nature of the beds and absence of low energy material indicates relative proximity to the sediment source and/or rapid sedimentation in the form of migrating bar forms associated with high velocity flows. These features are characteristic of proximal, braided fluvial dominated systems.

## **5.2 Regional-scale structural architecture of the Mount Ragged Formation**

### **5.2.1 Aeromagnetic interpretation**

The basement rocks of the project area are dominated by a common magnetic fabric (Appendix 5, Figure A5.1 displays this well). This comprises predominantly granitic gneisses of the Nornalup Zone. Interspersed between the basement rocks of the eastern Nornalup Zone are long, linear units with significantly lower magnetic signature. These are inferred to represent the lateral continuation of exposed Mount Ragged Formation sedimentary rocks (Figure 19). At least three different sub-parallel elongate domains with low magnetic signature are evident. In the west of the project area, one domain of low magnetic signal encompasses Russell Range and Mount Ragged. In the northwest, another domain of low magnetic signal contains Brook Peak, Mount Dean and Mount Esmond. In the south, another domain of low magnetism corresponds to Mica Hill and the Diamonds. Based on the orientation of formlines derived from aeromagnetic images, the Russell Range and Mount Ragged domain can be further subdivided into two smaller domains that account for the angular difference in the trend of their surface expressions in the aerial photographs (Appendix 1) and as mapped as formlines on geological maps (Appendix 7).

The low magnetic signature of these domains contrasts starkly against the surrounding basement rocks (Figure 19 and Appendix 5, Figure A5.2). The linearity and sub-parallel alignment of these low magnetic domains between higher magnetic domains suggests that they are different rock types (Figure 29). The abrupt contacts of these domains, which appear to cut the basement fabric, could indicate zones of displacement by faulting. This scenario would therefore make the Ragged Basin sedimentary rocks fault-bound packages, which based on structural observations (Section 4.4) dip to the southeast (Figure 29 - diagrammatic section).

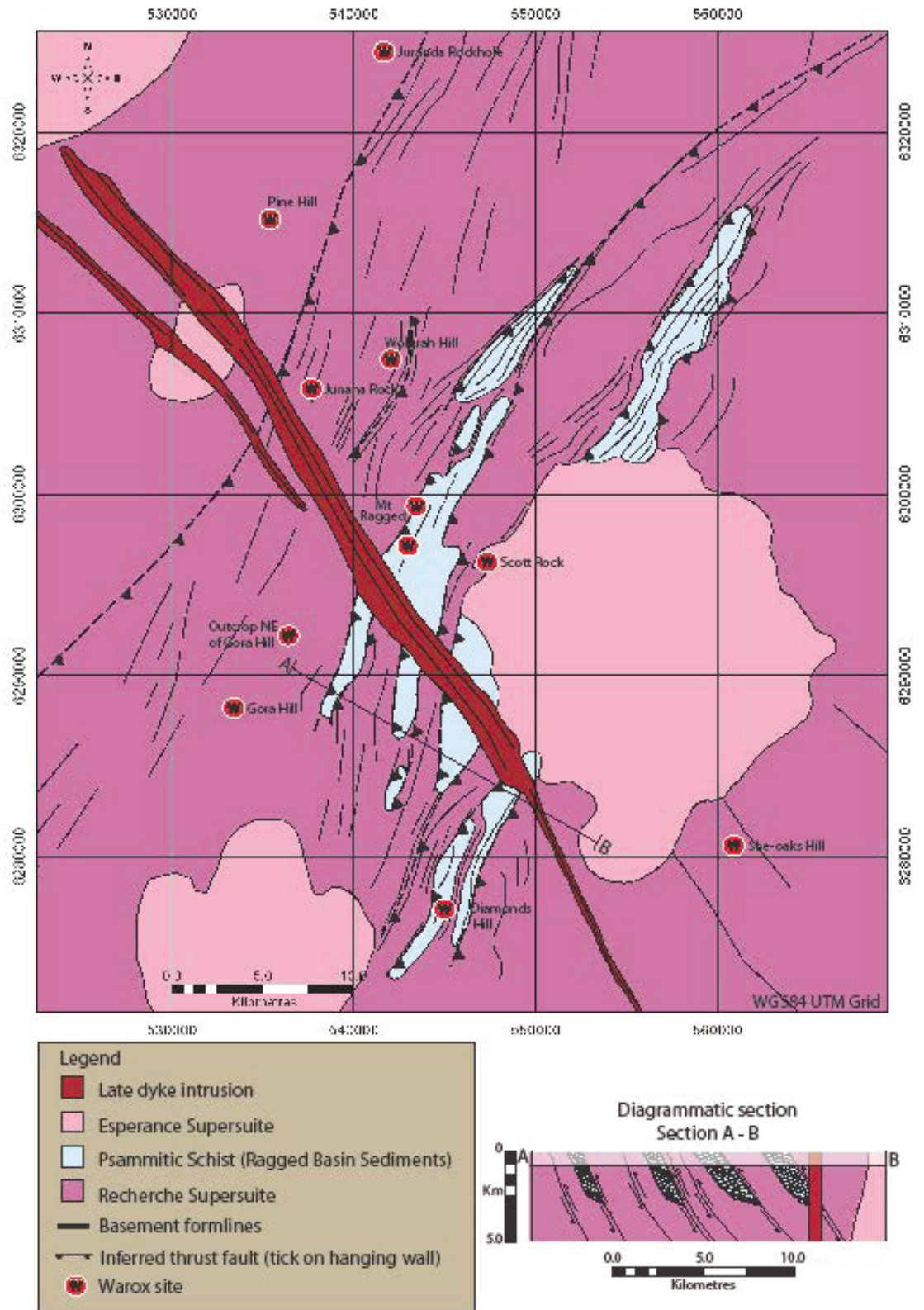


Figure 29. Basement map of the Mount Ragged Formation project area.

The only surface expression of the large circular, magnetic high anomaly to the southeast of the northern ridges of the Mount Ragged Formation is an isolated outcrop of undeformed monzogranite, known as Scott Rock (Section 4.2.6). This anomaly truncates the magnetic-low domains of the Mount Ragged Formation and other, moderately magnetic, basement gneisses and is, therefore, considered to represent a late granite intrusion. The lack of deformation in the aeromagnetic image of the subsurface Scott Rock monzogranite, compared to the deformation fabric of the surrounding eastern Nornalup Zone rocks, further substantiates its presence as a late intrusion. Preliminary geochronology yielded a concordia age of  $1175 \pm 12$  Ma (sample 192586, preliminary data supplied courtesy of GSWA), which is interpreted as the magmatic crystallisation age and indicates that this monzogranite is part of the Esperance Supersuite.

The long, northwest-southeast trending linear-shaped magnetic anomaly is interpreted to represent a mafic dyke belonging to the Beenong Dyke Suite (Spaggiari & Pawley 2012). This dyke terminates beneath the surface expression of Mica Hill to the south of Mount Ragged, and is in the same orientation as a fault that cuts across the middle of Mica Hill. This fault appears to have offset the northeastern half of the Mica Hill section by approximately 250 metres from the southwestern section (Appendix 6, Figure A6.1).

### **5.3 Structural history of the Mount Ragged Formation**

Within the metapelitic layers of the Mount Ragged Formation Clark (1999) suggested pervasive bedding parallel schistosity existed, defined by segregations, sheets of opaque minerals and orientated micas. Clark (1999) considered this schistosity to be representative of an  $S_1$  fabric and related it to strain partitioning into the more micaceous rocks in preference to the interbedded massive quartzites during the early stages of the burial of Ragged Basin sediments. However, it is possible that this  $S_1$  fabric of Clark (1999) is really syn- or post-deformational axial planar cleavage and relates to strain partitioning into micaceous layers, tight folding, chaotic bedding and shear zones.

Across the northern exposures of the Mount Ragged Formation (i.e. Mount Esmond, Mount Ragged and Russell Range) structural observations and compiled datasets display similarities in all structural aspects (i.e. bedding and cleavage strike and angle of dip, fold hinge and axial plane orientation, interlimb angles and fold shape) (Plate 1; rear attachment). The majority of bedding planes in these three ridges have a northeasterly strike and dip steeply to the southeast. Whilst distinguishing cleavage from other

sedimentary structures was difficult, cleavage measurements show that the cleavage planes are closely aligned to the bedding planes. Cleavage planes trend northeast and dip to the southeast, though dips are generally steeper than bedding.

The similarity in steepness of dip and close alignment of strike in the axial planar cleavage and bedding planes suggests they are related to the same deformation event. These findings correlate with the  $S_2$  fabric of Clark (1999); planes trend northeasterly and dip steeply to the southeast. However based on the view that: a) bedding parallel segregations and mineral alignment can occur through burial alone without differential stress; and b) the  $S_1$  fabric of Clark (1999) is really syn- or post-deformational; for the purpose of this study this fabric is considered to represent  $S_1$ , which is equivalent to  $S_2$  of Clark (1999). Henceforth, all references to  $S_1$  in this report relate to the fabric characterised by cleavage planes that trend northeast and dip steeply to the southeast.

Whilst large-scale folds are visible in the aerial photographs they remained cryptic in the outcrop and, like cleavage, folds were sometimes difficult to distinguish from deformed foresets within cross-stratification. The most common fold structures observed are small- to meso-scale synform hinges. Antiform fold hinges are less common. The scarcity of observed antiform folds may be due to brittle failure within antiform hinge zones in response to ongoing horizontal shortening. Other variations in folding observed included S-form and M-form folds, and folded foresets. The northern ridges of the Mount Ragged Formation consist of a series of gently northeast plunging, steeply inclined folds. Folds range from open to isoclinal. Mica Hill, which is located south of Mount Ragged and Scott Rock, is similar in all respects structurally with the one exception; fold axes gently plunge to the southwest.

The generation of northwest-verging folds in the Mount Ragged Formation is considered to correlate with the development of the northeast trending axial planar cleavage  $S_1$  fabric. The development of folding and the  $S_1$  fabric are considered to coincide with horizontal shortening due to northwest-southeast tectonic compression.

A range of fold styles is present throughout the Mount Ragged Formation. Whilst open folds are the most commonly observed amongst the quartzite beds, tight to isoclinal folds are present in beds proximal to- or within chaotic bedding. The variation in interlimb angles of the folds is possibly due to the variable competency of different sedimentary facies. For example, planar laminar beds containing metapelites would be considerably more ductile and conducive to folding than thick beds of medium- to coarse-grained

quartzite. Similarly, well-bedded quartzite units, with an abundance of foresets and cross-stratification, may also be more conducive to accommodating strain via shearing along foresets than the thick, massive quartzite beds.

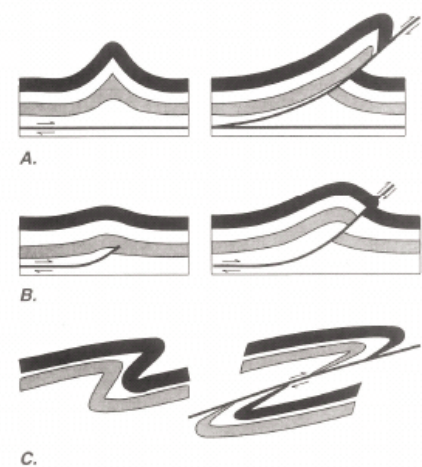
Folds were also inferred from switches in younging interpreted from various sedimentary way-up or younging features. Whilst cross-bedding is common throughout much of the formation, the truncation of cross-stratification in cosets within bedding is typically poorly defined. The truncation of cross-stratification within bedding planes, where recognisable, along with other sedimentary structures aided in the interpretation of younging. Another feature used to assist in the identification of fold structures is the presence of numerous, parallel quartz veins, occasionally within metapelites, in association with zones of chaotic bedding, where bedding and cleavage appeared parallel. Isoclinal, fold hinges were inferred where these aligned in linear domains between beds with opposite younging directions. Chaotic bedding zones with interleaved metapelites layers or slivers are often surrounded by well-bedded quartzites. This is consistent with isoclinal hinge zones of less competent rock between competent quartzite limbs.

On Mount Ragged and Mount Esmond the stratigraphy predominantly indicated younging to the east on the western side of fold structures and younging to the west on the eastern sides. Similarly on Russell Range, whilst way-up structures predominantly indicated younging to the east, the western side of fold structures displayed younging to the east and the eastern sides showed younging to the west. The northwestern part of Mica Hill also displayed similar features; the western beds showed younging to the east whilst eastern beds predominantly indicated younging to the west. Stratigraphy in all four of the study sites shows a similarity in younging within the bedding; in bedding planes on the western side of fold structures younging is to the east, whilst in bedding planes on the eastern side of fold structures younging is to the west. This indicates that the majority of bedding planes occur within a synform structure with a northwest vergence.

The consistency of younging across the strata within the formation is suggestive of overturned limbs. The tight, overturned nature of the folds has either been responsible for obscuring the limb with the opposed younging direction or it is obliterated in the chaotic bedding associated with the hinge zones. On Mount Esmond the regularity of chaotic bedding was indicative of close folding. The frequency with which indicators of hinge zones occur throughout the formation is suggestive of the presence of pervasive higher-order folding, (i.e. parasitic folding), superimposed on a regional-scale fold.

Across the Mount Ragged Formation bedding characteristics may be a controlling factor in the evolution of folds, shear zones and possible faults. Units conducive to accommodating strain correlate with areas exhibiting tight to isoclinal folding, chaotic bedding or shear zones. The more competent and resistant units, such as the thick, massive beds of medium- to coarse-grained quartzite, tend to exhibit open folds or, as is more usual, appear structureless. The apparent resistance to fold tightening by some units within the formation may be responsible for the nucleation and propagation of faults within the stratigraphic layers. In particular, faulting may occur along bedding planes and/or through cross-stratification.

Folding and thrust faulting are often related and their occurrence together commonly takes place in four ways (Twiss & Moores 2007). First, during the fold development a stage may be reached when the fold limbs can no longer accommodate any further shortening. This results in the development of a thrust fault through the steepest or overturned limb of the fold (Figure 30a). Second, where thrusting has developed to accommodate deformation, folds may develop above the tip line of the thrust fault resulting in “fault-propagation folds”. With increasing fault displacement the tip line cuts the steep line of the fold (Figure 30b). Third, a ductile thrust fault may develop in folds that become so steep or inverted that the limb becomes increasingly thinned and eventually shears (Figure 30c). Fourth, where alternating ramp-flat geometry develops in a thrust fault, movement along the fault results in fault-bend folds forming in the hanging-wall block. Drag folds are especially common along many thrust faults.



**Figure 30. Diagrammatic cross-sections demonstrating the relationship between fold and thrust faults (Twiss & Moores 2007).**

**(a) Thrust fault cuts up from a decollement fault through the forelimb of a fold when the fold becomes too tight to accommodate further shortening, (b) Fold forms in association with the propagation of a thrust fault, (c) Formation of a fold by ductile flow can result in the shearing out of limb to form a ductile thrust fault.**

If fault propagation was controlled by the axial planes of folds, then high-angle thrust or reverse faults are the likely types. Given that the fold vergence of the formation is to the northwest, it can be reasonably inferred that the upward direction of displacement of the

hanging-wall block along fault structures, relative to the footwall block, will also be to the northwest. However, given the scarcity of well-exposed, quality fault structures with measurable displacement, the significance and prevalence of fold-associated thrust faulting within the formation remains uncertain. The very few structures observed within the formation indicating possible displacement range from small-scale decollement faults in outcrop to large-scale structures observed within cliffs and ridges inferred from afar (Figure 31). Fault-propagation folding or drag folding between some of the more massive bedded units may be responsible for obscuring any evidence of actual fault propagation surfaces. The scarcity of observed antiformal folds may also be due to such structures, as displacement was accommodated through brittle failure in antiformal hinges.

Other evidence for possible displacement surfaces is suggested by the presence of viridine-bearing quartz veins, which were commonly observed in the vicinity of or accompanying such structures. These veins are considered to be indicative of fluid flow between and within bedding planes (Figure 31e).

The progression from parallel bedding ( $S_0$ ) to near upright cleavage and bedding planes ( $S_1$ ) could occur during a single progressive deformation event. With the commencement of horizontal shortening bedding would begin to buckle, fold and shallow angles of cleavage would develop. With time early fold hinges and cleavage would gradually steepen as axial trace is modified and compressed by new, younger fold structures. In this scenario, the angle of the cleavage would steepen with time in the zones that were compressed and folded first.

Similarly, if during fold development certain stratigraphic units remain resistant to fold tightening then there is the likelihood that the strain generated by compression will be accommodated through the development of decollement faults, fault-propagation folding or drag folds along bedding planes. If so, then early, low-angle thrust faults that propagated through resistant stratigraphy would then steepen over time into high-angle reverse faults, possibly cutting up through stratigraphy. Therefore, it is also likely that such structures have developed in association within the same, progressive deformation event.

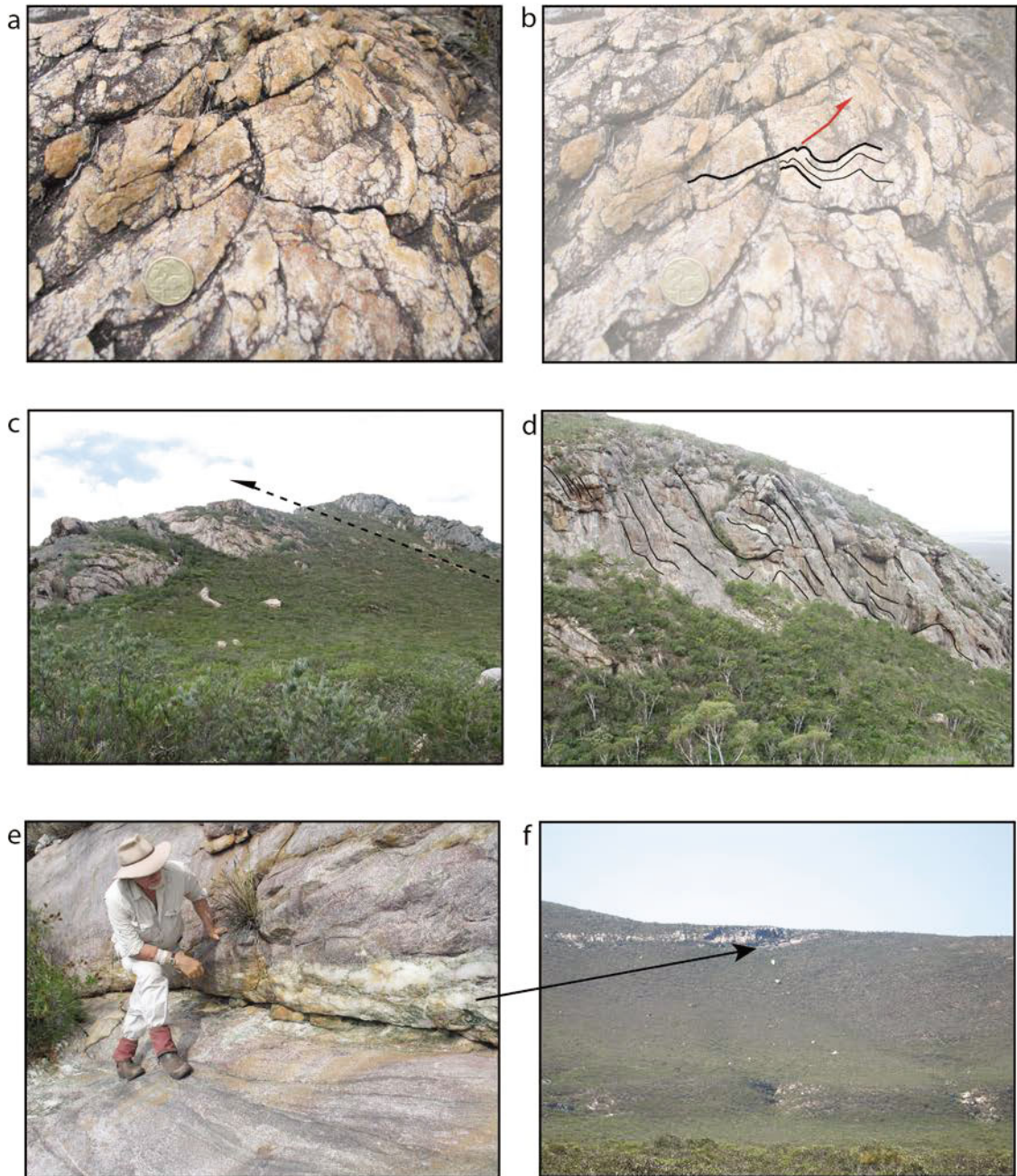


Figure 31. Photographs of suspected displacement features in the Mount Ragged Formation. a/b) Small-scale decollement fault in coarse-grained quartzite, Mica Hill (MGA 549385E, 6285449N); c) Interpreted area of displacement due to propagation of a thrust fault, deformed well-bedded, medium-grained pink quartzites overlain by massive coarse-grained grey quartzites, Mount Ragged (MGA 543700E, 6297155N); d) Interpreted area of displacement due to fault-bend folding in massive, structureless coarse-grained grey quartzites, Mount Ragged (MGA 544404E, 6298814N); e/f) Large viridine-bearing quartz vein between suspected footwall of viridine-rich, medium-grained pink quartzites and hanging-wall of consists of massive, structureless coarse-grained grey quartzites, Russell Range (MGA 546117E, 6305811N).

The development of reverse faults within the metamorphosed sediments of the Ragged Basin is likely to correspond with the larger scale thrust structures that probably were also active during the same deformation event, such as the Tagon and Wininup thrust faults and the Rodona Shear Zone (Clark 1999; Spaggiari et al. 2011). The accommodation of strain in the region may also have resulted in minor thrust faults which developed in the basement proximal to the Mount Ragged Formation. The subsequent development of decollement faults between the eastern Nornalup Zone basement rocks and the metasedimentary rocks of the formation may have resulted in basal detachment. This would facilitate the thrusting of linear domains of basement rocks over and/or between the linear domains of younger Ragged Basin metasedimentary rocks. If so each linear domain of metasedimentary rocks would be considered to represent the hanging-wall of a thrust sequence. Therefore, the Mount Ragged Formation possibly represents a zone where regional strain was accommodated, in part, through their emplacement as fault-bound metasedimentary packages.

#### **5.4 Timing constraints for the development of the Mount Ragged Formation**

On the basis of the preliminary zircon dates, a maximum age range for deposition of the Mount Ragged Formation is provided by the Mount Ragged detrital samples 194874 and 194875 of between  $1340 \pm 16$  Ma and  $1314 \pm 19$  Ma (preliminary data supplied courtesy of GSWA; Section 4.6). The detrital sample 194866 from Diamonds Hill yields a maximum depositional age within this range ( $1331 \pm 19$  Ma, preliminary data supplied courtesy of GSWA). The conservative maximum deposition age of  $1314 \pm 19$  Ma, (sample 194875, preliminary data supplied courtesy of GSWA) is also the youngest recorded maximum depositional age for detrital sediments from both the Arid and Ragged Basins.

Previously, the protolith sediments of the Mount Ragged Formation were considered to have been deposited during a period of extension and erosion following Stage I (1260-1215 Ma) of the Albany-Fraser Orogeny (Clark 1999; Clark *et al.* 2000; Bodorkos & Clark 2004b). Clark *et al.* (2000) provided constraints for the maximum deposition age for the Mount Ragged Formation of  $1321 \pm 24$  Ma from SHRIMP U-Pb analysis of detrital zircon from a Mount Ragged quartzite. In view of the new geochronological age data from GSWA presented herein, the maximum deposition age for the Mount Ragged Formation of  $1314 \pm 19$  Ma does not preclude the possibility that deposition may have commenced during Stage I (c. 1345-1260 Ma) of the Albany-Fraser Orogeny, albeit after  $1314 \pm 19$  Ma.

Both ages of magmatic crystallisation yielded from the granitic rocks nearby correlate well with other previously dated Mesoproterozoic granitic intrusions within the Albany-Fraser Orogen. The magmatic age of crystallisation from sample 194876, the metamonzogranite from Gora Hill, of  $1327 \pm 8$  Ma (preliminary data supplied courtesy of GSWA), coincides well with older granites of the Recherche Supersuite. Other granites from the Recherche Supersuite have been dated between c. 1330-1280 Ma (Spaggiari *et al.* 2011 and references cited therein). The foliated fabric within this metamonzogranite, predominantly defined by biotite, and the presence of foliation parallel granitic veins are indicative of metamorphism. These features are similar to other rocks from the Recherche Supersuite from within the eastern Nornalup Zone, in particular the biotite-hornblende monzogranitic gneisses identified by Clarke (1999).

Given that the Scott Rock granitic intrusion truncates the Ragged Basin belts that include Brook Peak, Mount Dean and Mount Esmond, Mica Hill and Diamonds Hill, the zircon U-Pb age of the Scott Rock monzogranite must represent a minimum age for the deposition of the Mount Ragged Formation of  $1175 \pm 12$  Ma (sample 192586, preliminary data supplied courtesy of GSWA; Section 4.6). This magmatic crystallisation age coincides well with the Stage II granites of the Esperance Supersuite. Other granites from the Esperance Supersuite have been dated at c. 1200-1140 Ma (Spaggiari *et al.* 2011). The lack of deformation in the Scott Rock monzogranite (Sections 4.3 & 5.1) also correlates well with the other granites of the Esperance Supersuite, which typically display less deformation than rocks of the Recherche Supersuite (Myers 1995b; Nelson *et al.* 1995).

The absolute timing constraints for the deposition of the Mount Ragged Formation show that (a) deposition of the Mount Ragged Formation could possibly be contemporaneous with that of the Arid Basin sediments; and (b) are insufficient to link the timing of deposition of the Mount Ragged Formation to a particular tectonic event between  $1314 \pm 19$  Ma and  $1175 \pm 12$  Ma, and thus the likely tectonic setting of the sedimentary basin. Therefore, other lines of evidence, such as sedimentary fill, depositional environment, geometry and nature of subsequent deformation must be considered to elucidate the tectonic setting and style of the Ragged Basin.

## 5.5 Controls on sedimentary basin style

Stacked cross-bedded sandstones dominate the Mount Ragged Formation, along with localised mudstone and siltstone interbeds in the lower sequences and rare occurrences of quartz-pebble conglomerate in the upper sequences. The sediments of the formation's protolith are considered to have been deposited within a shallow intracratonic basin by a large fluvial system dominated by a shifting complex of sandy braided channels.

In intraplate settings, intracratonic basins are the dominant basin type. These basins are characterised by prolonged, gradual subsidence. Intracratonic basins are commonly supplied by endoreic drainage systems delivering terrestrial sediments to centrally located, shallow lakes or seas. Generally there are two variations of basin-fill: siliclastic fluvial, lacustrine and aeolian deposits or shallow marine carbonates and evaporites (Allen & Allen 2005). The lack of marine carbonates and evaporites indicates that the sediments of the Mount Ragged Formation protolith were not deposited in a shallow sea. Furthermore, distinctive sedimentary characteristics common to fluvial settings are exhibited throughout the stratigraphy of the formation.

The base of the Mount Ragged Formation is characterised by finely laminated pelitic and siltstone layers intercalated with fine to medium-grained rounded to sub-rounded sandstones. The association of these facies is consistent with traction currents, two and three-dimensional subaqueous dune migration, barform modification resulting in channel migration, channel abandonment and/or in-filling, re-distribution of overbank deposits and rip-up clasts in a distal fluvial-braided river environment. Grading upwards the formation is characterised and dominated by medium-grained, well-sorted, cross-bedded sandstones. Mud and silt rip-up clasts become increasingly less common up the sequence. The uppermost units are dominated by poorly-sorted, quartz-pebble conglomerates interspersed with thick beds of well-sorted, granular gritstones. The coarsening upwards from medium-grained sandstones to pebble conglomerates suggests either a shallowing of the basin and/or an increased sediment supply. The deposition of massive, sandstone units are indicative of very rapid deposition. The angular nature of the sediments further supports a proximal fluvial setting.

The textural and chemical maturity of the Mount Ragged Formation quartzites indicates that sediment transportation was a significant process during sedimentation. The detrital mineralogy of predominantly quartz, zircons and heavy minerals (i.e. opaques such as hematite, magnetite and ilmenite) throughout the quartzites indicates a moderate to high

level of chemical maturity. Weathering and transportation were the likely processes responsible for removing the more unstable mineral components. Similarly, the sediments display moderate to high textural maturity. Aside from the coarse-grained facies the majority of the quartz-dominated metasediments exhibit rounded to sub-rounded grains. Also most of the quartz-dominated facies are moderately to well-sorted. The result of such well-sorted, increasingly spherical and winnowed sediments supports transportation in a high-energy environment and/or over considerable distances. The evidence for such chemically and texturally mature sediments being deposited in a fluvial environment is largely based on the paucity of mud or siltstone interbeds; rip-up clasts of similar composition; scour channels; the presence of greater than 1 mm sized, angular clasts; and sporadic components of poorly sorted, coarse-grained deposits. Based on textural maturity the sediments of the Mount Ragged Formation protolith can be considered as quartz arenites.

The maturity of these quartz arenites also support an intracratonic depositional setting rather than a foreland basin setting. In a foreland basin setting the typical development of the basin is at the front of an active thrust belt that is moving towards the evolving basin. This inevitably results in basin-fill adjacent to thrusting becoming involved in deformation. However, the detrital mineralogy and sphericity of the sediments indicates that there has been considerable time for weathering, erosion, transportation and sorting. The period of tectonic quiescence between 1260 and 1215 Ma would allow for such processes to produce sediments with the textural characteristics observed in the Mount Ragged Formation.

These findings support the interpretation by Clark *et al.* (2000) that the sediments of the Mount Ragged Formation are transported, detrital grains, which through zircon analysis identified rounded, fractured and abraded surfaces. Clark *et al.* (2000) concluded the clean, quartzitic nature of the Mount Ragged Formation quartzites precluded a volcanic or volcanoclastic origin and instead suggested erosion from a granitic source. Furthermore, SHRIMP U-Pb analyses of rocks from the formation also yielded an older detrital zircon component with a weighted mean age of  $1783 \pm 12$  Ma and a maximum depositional age of  $1321 \pm 24$  Ma (Clark *et al.* 2000). Spaggiari *et al.* (2011) consider this age to be consistent with a source of origin from the granitic rocks of the Recherche Supersuite. This salient evidence largely eliminates the likelihood for sedimentation having occurred within a retroarc foreland basin, which typically contains significant quantities of volcanic sediments derived from the orogenic belt.

Based on the high oxidation state and stability of haematite in the Mount Ragged metasedimentary rocks, Clark (1999) suggests that deposition took place in shallow, oxygenated environment. The findings from the facies analysis in this study support this conclusion. Facies sequences indicate that periods of high-energy flow were likely to be a common occurrence and in present day fluvial settings these environments are well oxygenated.

## **5.6 Summary of the tectonic evolution of the Mount Ragged Formation**

A period of tectonic quiescence is considered to have occurred between Stages I and II of the Albany-Fraser Orogeny between 1260-1215 Ma (Clark *et al.* 2000; Bodorkos & Clark 2004a). During this time erosion of the uplifted eastern Nornalup Zone, including the granitic rocks of the Recherche Supersuite, commenced (Clark *et al.* 2000). SHRIMP U-Pb analyses of detrital zircon from the Mount Ragged Formation are consistent with the Recherche Supersuite as a likely source of origin for the sediments that make up part of the basin fill of the Ragged Basin (Clark *et al.* 2000; Spaggiari *et al.* 2011).

The sediments of the Ragged Basin are considered to have been deposited within a shallow intracratonic basin by a large fluvial system dominated by a shifting complex of sandy braided channels. The gradual coarsening upwards sequence of lithofacies suggests the depositional setting was a distal fluvial environment characterised by channel migration and abandonment changing to a proximal fluvial environment characterised by rapid periods of sedimentation and coarser deposits.

Based on the new geochronological age data presented herein the maximum deposition age of the Ragged Basin sediments is  $1314 \pm 19$  Ma, which indicates deposition may have started during Stage I (c. 1345-1260 Ma) of the Albany-Fraser Orogeny. Truncation of the Mount Ragged Formation by the Scott Rock monzogranite constrains the minimum age for the deposition of Ragged Basin sediments to  $1175 \pm 12$  Ma.

Simultaneous dextral shearing, northwest-southeast directed compression in the eastern Nornalup Zone resulted in thrusting and crustal thickening (Clark *et al.* 2000). At around c.  $1182 \pm 13$  Ma (Clark *et al.* 2000) consider that westwards over-thrusting of the Salisbury Gneiss, along the Rodona Shear Zone, resulted in the burial and subsequent metamorphism of the Ragged Basin sediments to amphibolite facies at conditions of 500-600°C and 4-5 kbar (Clark 1999).

The development of upright of cleavage and inclined bedding planes is considered to represent an  $S_1$  fabric and correlates with the generation of northwest-verging folds in the Ragged Basin sediments. The close alignment in strike of the bedding and cleavage planes, as well as fold axes, suggests they are all related to the same deformation event resulting from horizontal shortening due to northwest-southeast tectonic compression. The presence of stratigraphic units resistant to fold tightening is likely to have resulted in the development of decollement faults, fault-propagation folding or drag folds along bedding planes to accommodate strain. The ongoing partitioning of strain resulted in the development of fault-bound packages consisting of metamorphosed Ragged Basin sediments between faulted domains of basement rocks. These structures are therefore also likely to have developed in association with the development of upright cleavage, inclined bedding and northwest-verging folds.

Through the eastern part of the Nornalup Zone, strain was accommodated by the Tagon and Wininup Thrust Faults and the Rodona Shear Zone (Clark 1999). The emplacement of fault-bound Ragged Basin metasedimentary packages is likely to correspond with simultaneous movement that occurred in conjunction to movement in these larger scale thrust faults and shear zones.

Based on the petrographic analysis Clark (1999) concluded that the main phase of crustal thickening, which coincided with the development of the  $S_1$  fabric and northwest-verging folds, occurred predominantly while the terrane was in the andalusite stability field. Clark (1999) considered a heating path under conditions of increasing pressure, in response to the combination of burial and juxtaposition of hot rocks (such as the Salisbury Gneiss), the most likely scenario for temperature increase. Metamorphism occurred in upper greenschist - lower amphibolite facies, which Clark (1999) considered to post-date the deformation by over-thrusting and burial. Clark's (1999) petrographic analysis concluded that aluminosilicate-bearing quartz-mica veins postdate the formation of the  $S_1$  fabric and whilst some occupy the plane of small shears, most are post-kinematic. Clark (1999) considered the presence of viridine-andalusite to indicate precipitation from a fluid phase and its presence in veins represented the stable form of an aluminosilicate polymorph. Peak assemblages were subsequently regressed under hydrous conditions (Clark 1999).

However, contrary evidence was observed during this investigation that may indicate other complexities in chronology. If the timing of viridine-andalusite postdates deformation and is associated with regression then it would be expected to be present in all rocks of the

formation. This is not the case. More specifically, on Russell Range a large viridine-bearing quartz-rich vein, which is considered to indicate a shear zone, truncates viridine-rich pink quartzite in the footwall and massive grey quartzite in the hanging wall (Figure 31e). The absence of viridine in the hanging wall suggests viridine was present before the displacement and/or is locally related to fluid flow associated with the thrust plane. If it had been present syn- or post-displacement then it would also be expected in the hanging wall. An explanation to support Clark's (1999) retrogression P-T path is that perhaps in the fluid phase viridine can only penetrate rocks along permeable zones such as fractures, shear zones, bedding planes, cross-stratification and foresets. In relatively impermeable units, such as the massive grey quartzites, hydrous fluids are unable to penetrate as readily.

Other contrary evidence includes the presence of boudinaged viridine-bearing veins (Figure 28a). These suggest a) deformation postdates the occurrence of viridine or b) deformation occurred during the regression under hydrous conditions. These remain unresolved scenarios. However, similar evidence for fluid flow in association with shear zone development has been recorded at Point Malcolm, approximately 30 kilometres southeast of Mica Hill. Monazite geochronology recorded monazite growth with a mean  $^{207}\text{U}/^{235}\text{Pb}$  age of c.  $1180 \pm 5$  Ma (Adams 2012). This age is linked to the formation of conjugate shear zones, recorded by fluid-aided alteration of monazite. Adams (2012) considers this c.  $1180 \pm 5$  Ma age to represent fluid-rock interaction due to shear zone formation during Stage II. This linkage between shear zone development and fluid flow associated with a high strain event, of possible similar age to deformation in the Mount Ragged Formation (Clark *et al.* 2000; Adams 2012), in rocks proximal to the Mount Ragged Formation supports the possibility that hydrous fluids were present during the deformation of the formation.

Clark (1999) considered granitic intrusions in the vicinity of the Mount Ragged Formation to be too small and insufficiently abundant to have contributed substantially to the upper-crustal heat budget, and therefore retrogression most likely occurred on the retrograde path of the peak event. However, Clark (1999) did not discount that retrogression could possibly reflect a discrete thermal event. With the benefit of the aeromagnetic imagery present herein (Section 4.3), the Scott Rock monzogranite intrusion, which is up to 15 kilometres in diameter, is very likely to be large and close enough to have influenced thermal properties in the Mount Ragged Formation. The cross-cutting relationship with the formation indicates the Scott Rock intrusion to be younger than the Ragged Basin sediments. The presence of sillimanite in veins in the most southerly outcrops, such as

Diamonds Hill (Lowry & Doepel 1974; Clark 1999), indicates that fluid flow in some parts of the formation did occur during peak temperature conditions. Given the proximity of the Scott Rock intrusion to the southern units of the Mount Ragged Formation, peak temperature conditions in the south of the formation may have occurred due to increased thermal conditions if the monzogranite intruded as a hot mass.

The magmatic age of crystallisation ( $1175 \pm 12$  Ma) and lack of deformation in the Scott Rock monzogranite coincides well with other granites from the Esperance Supersuite which have been dated between 1200 and 1140 Ma (Spaggiari *et al.* 2011 and references cited therein), and which typically display less deformation than granites from the Recherche Supersuite (Myers 1995b; Nelson *et al.* 1995). The magmatic crystallisation age of Scott Rock coincides with the timing of peak metamorphism throughout the eastern Nornalup Zone (Spaggiari *et al.* 2011 and references cited therein). Stage II of the Albany-Fraser Orogeny is considered to have concluded with the intrusion of high level felsic plutons throughout the eastern Nornalup Zone at around 1140 Ma (Clark *et al.* 2000).

## **5.7 Future investigations**

Due to accessibility issues much of the eastern extent of the Mount Ragged Formation was not visited (i.e. Mount Dean and Brook Peak). To continue to validate the basin setting and correlate the stratigraphy across the formation sedimentary logs in these areas would be useful. Similarly, despite the difficulty in finding good sedimentary features in such ancient quartzites, an analysis of paleocurrent direction preserved in cross-stratification within bedding would assist in diagnosis of depositional processes, perhaps indicating transverse or longitudinal (axial) drainage patterns. Also geochronology of the different topographic localities of the Mount Ragged Formation to try and constrain ages of zircon-bearing rocks would be beneficial to determine ages of strata.

Whilst Clark (1999) has evidence of fine-grained muscovite schists no rocks fitting this description were observed during traverses across Mica Hill, despite it being one of the more accessible areas. Future investigations could undertake a more detailed investigation of the southern hills of the Mount Ragged Formation to locate sillimanite-bearing rocks for further investigation of peak temperature conditions of the formation.

However, any future geological investigations into the Mount Ragged Formation would best be planned shortly after a bush fire to eliminate the difficulties associated with traversing such steep terrain in the presence of such dense, sclerophyllous vegetation.

## 6.0 Conclusion

Based on the new geochronological age data obtained from U-Pb zircon analysis the maximum deposition age of the Ragged Basin sediments is  $1314 \pm 19$  Ma, which indicates deposition may have started during Stage I (c. 1345-1260 Ma) of the Albany-Fraser Orogeny. New geochronological age data constrains the magmatic age of crystallisation of the Scott Rock monzogranite to  $1175 \pm 12$  Ma. The truncation of the Mount Ragged Formation by the Scott Rock monzogranite constrains the minimum age for the deposition of Ragged Basin sediments to  $1175 \pm 12$  Ma.

The sediments of the Ragged Basin are considered to have been deposited within a shallow intracratonic basin by a large fluvial system dominated by a shifting complex of sandy braided channels. The gradual coarsening upwards sequence of lithofacies suggests the depositional setting was a distal fluvial environment characterised by channel migration and abandonment changing to a proximal fluvial environment characterised by rapid periods of sedimentation and coarser deposits.

The steep inclination of the bedding and cleavage planes, as well as their close alignment in strike with fold axes, suggests they are all related to the same deformation event resulting from horizontal shortening due to northwest-southeast tectonic compression. The development of an  $S_1$  fabric is considered likely to have developed during or soon after deformation and relates to strain partitioning into micaceous layers, tight folding, chaotic bedding and shear zones. The presence of stratigraphic units resistant to fold tightening is likely to have resulted in the development of fault-propagation folding or drag folds along bedding planes to accommodate strain.

The ongoing partitioning of strain is likely to have resulted in the development of decollement faults between basement rocks of the eastern Nornalup Zone and the metasedimentary rocks of the formation. Basal detachment would result in thrusting of linear domains of basement rock over and/or between the linear domains of younger Ragged Basin metasedimentary rocks. The development of southeasterly dipping thrust faults and steep reverse faults within the metamorphosed sediments of the Ragged Basin is likely to correspond with the larger scale thrust structures, such as the Tagon and Wininup thrust faults and the Rodona Shear Zone, that were most likely also active during the same deformation event.

Across the northern domains of the Mount Ragged Formation evidence of fluid flow was observed in areas associated with strain partitioning (i.e. shear zones, suspected thrust planes, hinge zones) or proximal to them in stratigraphic units consisting of permeable sedimentary structures (i.e. bedding planes, cross-stratification, foresets). Hydrous conditions are considered to be associated with deformation; the presence of viridine-andalusite possibly indicating that deformation occurred under hydrous conditions associated with regression. The likelihood that hydrous fluids were present during the deformation of the formation is supported by the linkage between shear zone development and fluid flow associated with a Stage II high strain event in rocks proximal to the Mount Ragged Formation.

The lack of deformation in the Scott Rock monzogranite in conjunction with the new geochronological age data indicating the magmatic age of crystallisation of  $1175 \pm 12$  Ma coincides with the characteristics of other granites from the Esperance Supersuite which have been dated between 1200 and 1140 Ma. The intrusion of high level felsic plutons throughout the eastern Nornalup Zone at around 1140 Ma is considered to indicate the conclusion of Stage II of the Albany-Fraser Orogeny.

Lowry and Doepel (1974) interpreted the exposures of the Mount Ragged Formation as belonging to an echelon pair of northeast-trending synclines (Figure 1). Based on the gently northeasterly plunge direction of meso-scaled folds in the north of the formation, the absence of surface outcrop in the vicinity of where one would expect to find surface exposures around the hinge zone of this proposed syncline makes it hard to substantiate the existence of a large-scale fold structure. Furthermore, the cross-cutting relationship by the Scott Rock monzogranite with the metasediments of the Mount Ragged Formation complicates the theory of a large-scale synform.

In view of the structural data and field observations presented herein, in conjunction with the interpretation of aeromagnetic imagery, the Mount Ragged Formation, rather than representing an echelon pair of northeast-trending synclines, represents a zone where regional strain was partially accommodated through the deformation and subsequent emplacement of fault-bound metasedimentary packages.

## 7.0 References

- Allen, PA and Allen, JR 2005, Basin Analysis: Principles and Applications, 2<sup>nd</sup> Edition, Blackwell Scientific Publications, Cambridge, 549 p.
- Adams, M 2012, Structural and geochronological evolution of the Malcolm Gneiss, Nornalup Zone, Albany-Fraser Orogen, Western Australia: Geological Survey of Western Australia, Record 2012/4, 132p.
- Beard, J.S. (1975). Vegetation survey of Western Australia: Nullarbor: 1:1,000,000 Vegetation Series, Explanatory notes to sheet 4. University of Western Australia Press, Perth.
- Beeson, J, Delor, CP and Harris, LB 1988, A structural and metamorphic traverse across the Albany Mobile Belt, Western Australia. *Precambrian Research*, v. **40/41**, pp. 117–136.
- Bodorkos, S and Clark, DJ 2004a, Evolution of a crustal-scale transpressive shear zone in the Albany–Fraser Orogen, SW Australia: 1. P–T conditions of Mesoproterozoic metamorphism in the Coramup Gneiss. *Journal of Metamorphic Geology*, v. **22**, no. 8, pp. 691–711.
- Bodorkos, S and Clark, DJ 2004b, Evolution of a crustal-scale transpressive shear zone in the Albany–Fraser Orogen, SW Australia: 2. Tectonic history of the Coramup Gneiss and a kinematic framework for Mesoproterozoic collision of the West Australian and Mawson cratons. *Journal of Metamorphic Geology*, v. **22**, no. 8, pp. 713–731.
- Clark, DJ 1999, Thermo-tectonic evolution of the Albany–Fraser Orogen, Western Australia. University of New South Wales, PhD thesis (unpublished).
- Clark, DJ, Hensen, BJ and Kinny, PD 2000, Geochronological constraints for a two-stage history of the Albany–Fraser Orogen, Western Australia. *Precambrian Research*, v. **102**, pp. 155–183.
- Clarke, EdeC, Phillipps, HT and Prider, RT 1954, The Precambrian geology of part of the south coast of Western Australia. *Journal of the Royal Society Western Australia*, v. **38**, pp. 1–64.
- Condie, KC and Myers, JS 1999, Mesoproterozoic Fraser Complex: geochemical evidence for multiple subduction-related sources of lower crustal rocks in the Albany-Fraser Orogen, Western Australia, *Australian Journal of Earth Sciences*, v. **46**, pp. 875–882.
- Cruse, T 1991, The sedimentary, depositional environment and Ediacaran fauna of Mondurup and Barnett Peaks, Stirling Range Formation, Western Australia. University of Western Australia, Perth, Western Australia, BSc Honours thesis (unpublished).
- Cruse, T and Harris, LB 1994, Ediacaran fossils from the Stirling Range Formation, Western Australia. *Precambrian Research*, v. **67**, pp. 1–10.
- Dawson, GC, Krapež, B, Fletcher, IR, McNaughton, NJ and Rasmussen, B 2002, Did late Palaeoproterozoic assembly of proto-Australia involve collision between the Pilbara, Yilgarn and Gawler Cratons? Geochronological evidence from the Mount Barren Group in the Albany-Fraser Orogen of Western Australia. *Precambrian Research*, v. **118**, pp. 195–220.
- Dawson, GC, Krapež, B, Fletcher, IR, McNaughton, N and Rasmussen, B 2003, 1.2 Ga thermal metamorphism in the Albany-Fraser Orogen of Western Australia: consequence of collision or regional heating by dyke swarms? *Journal of the Geological Society*, London, v. **160**, pp. 29–37.
- Doepel, JJG 1973, Explanatory notes on the Norseman 1:250 000 Geological Sheet, Western Australia, Geological Survey of Western Australia, Record 1970/9, 57 p.
- Fitzsimons, ICW 2003, Proterozoic basement provinces of southern and southwestern Australia, and their correlation with Antarctica. *Geological Society of London Special Publication*, v. **206**, pp. 93–130.
- Fitzsimons, ICW and Buchan, C 2005, Geology of the western Albany-Fraser Orogen, Western Australia – a field guide. Geological Survey of Western Australia, Record 2005/11, 32 p.

- Hall, CE, Jones, SA and Bodorkos, S 2008, Sedimentology, structure and SHRIMP zircon provenance of the Woodline Formation, Western Australia: implications for the tectonic setting of the West Australian Craton during the Paleoproterozoic. *Precambrian Research*, v. **162**, pp. 577–598.
- Harris, LB 1995, Correlation between the Albany, Fraser and Darling Mobile Belts of Western Australia and Mirnyy to Windmill Islands in the East Antarctica Shield: implications for Proterozoic Gondwanaland reconstructions. In: *India and Antarctica during the Precambrian* (Editors: Yoshida, M and Santosh, M), *Geological Society of India Memoirs*, v. **34**, pp. 47-71
- Jones, SA 2006, Mesoproterozoic Albany-Fraser Orogen-related deformation along the southeastern margin of the Yilgarn Craton. *Australian Journal of Earth Sciences*, v. **53**: 213-234.
- Krapež, B and Martin, DM 1999, Sequence stratigraphy of the Palaeoproterozoic Nabbyer Province of Western Australia. *Australian Journal of Earth Sciences*, v. **48**: 89-103.
- Kirkland, CL, Spaggiari, CV, Pawley, MJ, Wingate, MTD, Smithies, RH, Howard, HM, Tyler, IM, Belousova, EA and Poujol, M 2011a, On the edge: U-Pb, Lu-Hf, and Sm-Nd data suggests reworking of the Yilgarn Craton margin during the formation of the Albany–Fraser Orogen. *Precambrian Research*, v. **187**, pp. 223–247.
- Kirkland, CL, Spaggiari, CV, Wingate, MTD, Smithies, RH, Belousova, EA, Murphy, R and Pawley, MJ 2011b, Inferences on crust-mantle interaction from Lu-Hf isotopes: a case study from the Albany–Fraser Orogen. Geological Survey of Western Australia, Record 2011/12, 25 p.
- Kirkland, CL and Wingate MTD 2013, (unpublished) Preliminary reports on U-Pb Geochronology Samples. Geochronology Record Series.
- Lowry, DC 1970, Geology of the Western Australian part of the Eucla Basin, Geological Survey of Western Australia, Bulletin 122.
- Lowry, DC and Doepel, JJG (compilers) 1974, Malcolm-Cape Arid, Western Australia. Geological Survey of Western Australia, 1:250 000 Geological Series Explanatory Notes, 16 p.
- McClay, KR 1987, Mapping of Geological Structures. Geological Society of London, Handbook Series, John Wiley and Sons Ltd.
- Muhling, PC and Brakel, AT (compilers) 1985, Mount Barker – Albany, Western Australia. Geological Survey of Western Australia, 1:250 000 Geological Series Explanatory Notes, 21 p.
- Myers, JS 1985, The Fraser Complex – a major layered intrusion in Western Australia. Western Australia Geological Survey, pp. 57–66.
- Myers, JS 1990, Albany–Fraser Orogen. In: *Geology and Mineral Resources of Western Australia: Western Australia Geological Survey, Memoir 3*, pp. 255–263.
- Myers, JS 1993, Precambrian history of the Western Australian Craton and adjacent orogens. *Annual review of earth and planetary sciences*, v. **21**, pp. 453–485.
- Myers, JS 1995a, Geology of the Albany 1:1 000 000 sheet. Western Australia Geological Survey, 1:1 000 000 Geological Series Explanatory Notes, 10 p.
- Myers, JS 1995b, Geology of the Esperance 1:1 000 000 sheet. Western Australia Geological Survey, 1:1 000 000 Geological Series Explanatory Notes, 10 p.
- Myers, JS, Shaw, RD and Tyler, IM 1996, Tectonic evolution of Proterozoic Australia. *Tectonics*, v. **15**, pp. 1431–1446.
- Nelson, DR, Myers, JS and Nutman, AP 1995, Timing of events in the mid-Proterozoic Albany-Fraser Orogen, Western Australia, and implications for Gondwana correlations, *Australian Journal of Earth Sciences*, v. **42**: 481-495.
- Pridier, RT 1960, Viridine from Mount Ragged, Western Australia. *Indian Mineralogist*, v **1**, pp. 42-47.

- Rasmussen, B, Bengtson, S, Fletcher, IR and McNaughton, N 2002, Discoidal impressions and trace-like fossils more than 1200 million years old. *Science*, v. **296**, pp. 1112-1115.
- Rasmussen, B, Fletcher, IR, Bengtson, S and McNaughton, N 2004, SHRIMP U-Pb dating of diagenetic xenotime in the Stirling Range Formation, Western Australia: 1.8 billion year minimum age for the Stirling biota. *Precambrian Research*, v. **133**, pp. 329–337.
- Spaggiari, CV 2008, Making interpreted bedrock geology maps with the aid of geophysical data. Geological Survey of Western Australia, Unpublished presentation, June 2008.
- Spaggiari, CV, Bodorkos, S, Barquero-Molina, M, Tyler, IM and Wingate, MTD 2009, Interpreted bedrock geology of the South Yilgarn and central Albany–Fraser Orogen, Western Australia. Geological Survey of Western Australia, Record 2009/10, 84 p.
- Spaggiari, CV, Kirkland, CL, Pawley, MJ, Smithies, RH, Wingate, MTD, Doyle, MG, Blenkinsop, TG, Clarke, C, Oorschot, CW, Fox, LJ and Savage, J 2011, The geology of the East Albany–Fraser Orogen – a field guide. Geological Survey of Western Australia, Record 2011/23, 98 p.
- Spaggiari, CV and Pawley, MJ 2012, Interpreted pre-Mesozoic bedrock geology of the east Albany-Fraser Orogen and southeast Yilgarn Craton (1:500,000), in Spaggiari, CV, Kirkland, CL, Pawley, MJ, Smithies, RH, Wingate, MTD, Doyle, MG, Blenkinsop, TG, Clarke, C, Oorschot, CW, Fox, LJ and Savage, J 2011, The geology of the East Albany–Fraser Orogen – a field guide. Geological Survey of Western Australia, Record 2011/23, Plate 1.
- Thom, R and Chin, RJ (compilers) 1984, Bremer Bay, Western Australia. Geological Survey of Western Australia, 1:250 000 Geological Series Explanatory Notes, 20p.
- Thom, R, Chin, RJ and Hickman, AH (compilers) 1984, Newdegate, Western Australia. Geological Survey of Western Australia, 1:250 000 Geological Series Explanatory Notes, 24 p.
- Turek, A and Stephenson NCN 1966, The radiometric age of the Albany granite and Stirling Range Beds, southwest Australia. *Journal of the Geological Society of Australia*, v. **13**(2): 449-456.
- Twiss, RJ and Moores, EM 2007, Structural Geology (2nd Edition), W.H. Freeman and Company. New York, 736 p.
- Tyler, IM and Hocking RM (compilers) 2001, Tectonic units of Western Australia. 1:2,500,000, Geological Survey of Western Australia
- Vallini, D, Rasmussen, B, Krapež, B, Fletcher, IR, McNaughton, NJ 2002, Obtaining diagenetic ages from metamorphosed sedimentary rocks: U-Pb dating of unusually coarse xenotime cement in phosphatic sandstone. *Geology*, v. **30**, pp. 1083-1086.
- Vallini, DA, Rasmussen, B, Krapež, B, Fletcher, IR, McNaughton, N 2005, Microtextures, geochemistry and geochronology of authigenic xenotime constraining the cementation history of a Paleoproterozoic metasedimentary sequence. *Sedimentology*, v. **52**, pp. 101-122.
- Weatherly, S, Harris, LB and Ridley, J 1994, The tectonic setting of the Mount Barren Group, Albany-Fraser Orogen, WA,: implications for basin formation and subsequent deformation during a compressional orogen in eastern Gondwana. *Geological Society of Australia Abstracts*, **37**, pp 458-459.
- Wentworth, CK 1922, A scale of grade class terms for clastic sediments. *Journal of Geology*, v. **30**, pp. 377-392.
- Wingate, MTD and Kirkland, CL 2013, Introduction to geochronology information released in 2013: Geological Survey of Western Australia, 5p.
- Witt, WK 1997, Geology of the Ravensthorpe and Cocanarup 1:100 000 sheets. Geological Survey of Western Australia, 1:100 000 Geological Series Explanatory Notes, 26 p.
- Witt, WK 1998, Geology and mineral resources of the Ravensthorpe and Cocanarup 1:100 000 sheets. Geological Survey of Western Australia, Report 54, 152 p.

# APPENDICES LIST

## **Appendix 1: Mount Ragged Formation aerial photographs**

Figure A1.1: Aerial photograph of Mica Hill

Figure A1.2: Aerial photograph of Mount Esmond, Mount Dean and Brook Peak

Figure A1.3: Aerial photograph of Mount Ragged

Figure A1.4: Aerial photograph of Russell Range

## **Appendix 2: Mount Ragged Formation sample catalogue**

Table A2.1: Mount Ragged Formation sample catalogue

## **Appendix 3: Russell Range sedimentary log**

Figure A3.1: Russell Range sedimentary log

## **Appendix 4: GSWA Warox sites in the vicinity of the Mount Ragged Formation**

Map of GSWA Warox sites in the vicinity of the Mount Ragged Formation

Table A4.1: GSWA Warox sites in the vicinity of the Mount Ragged Formation

## **Appendix 5: Aeromagnetic images**

Figure A5.1: Aeromagnetic image of Mount Ragged Formation  
(reduction to pole; normal)

Figure A5.2: Aeromagnetic image of Mount Ragged Formation  
(reduction to pole, first vertical derivative; sun angle northwest)

## **Appendix 6: Geological maps**

Figure A6.1: Geological map of Mica Hill

Figure A6.2: Geological map of Mount Esmond

Figure A6.3: Geological map of Mount Ragged

Figure A6.4: Geological map of Russell Range

## **Appendix 7: Stereographic projections**

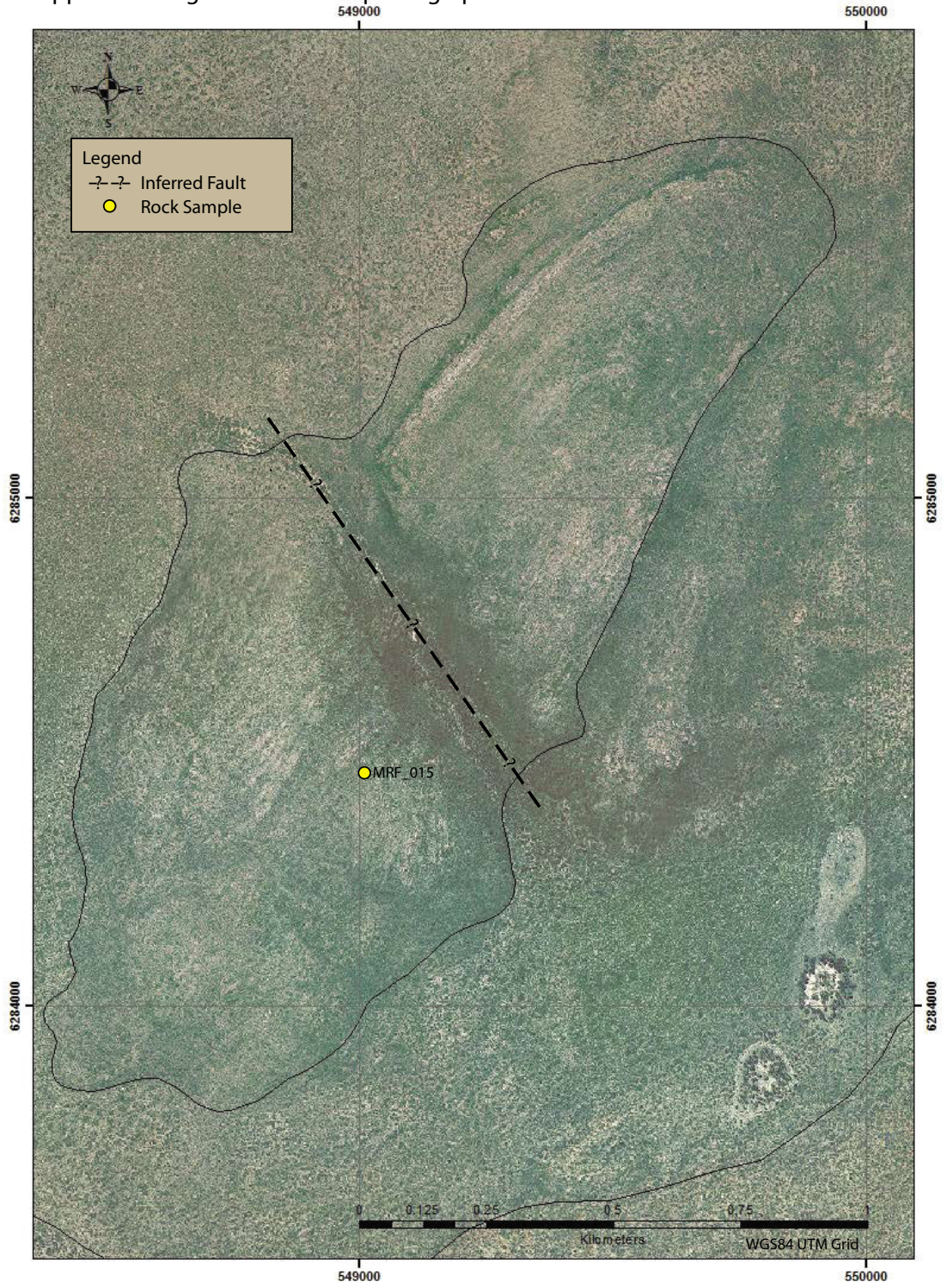
Figure A7.1: Mica Hill structural data

Figure A7.2: Mount Esmond structural data

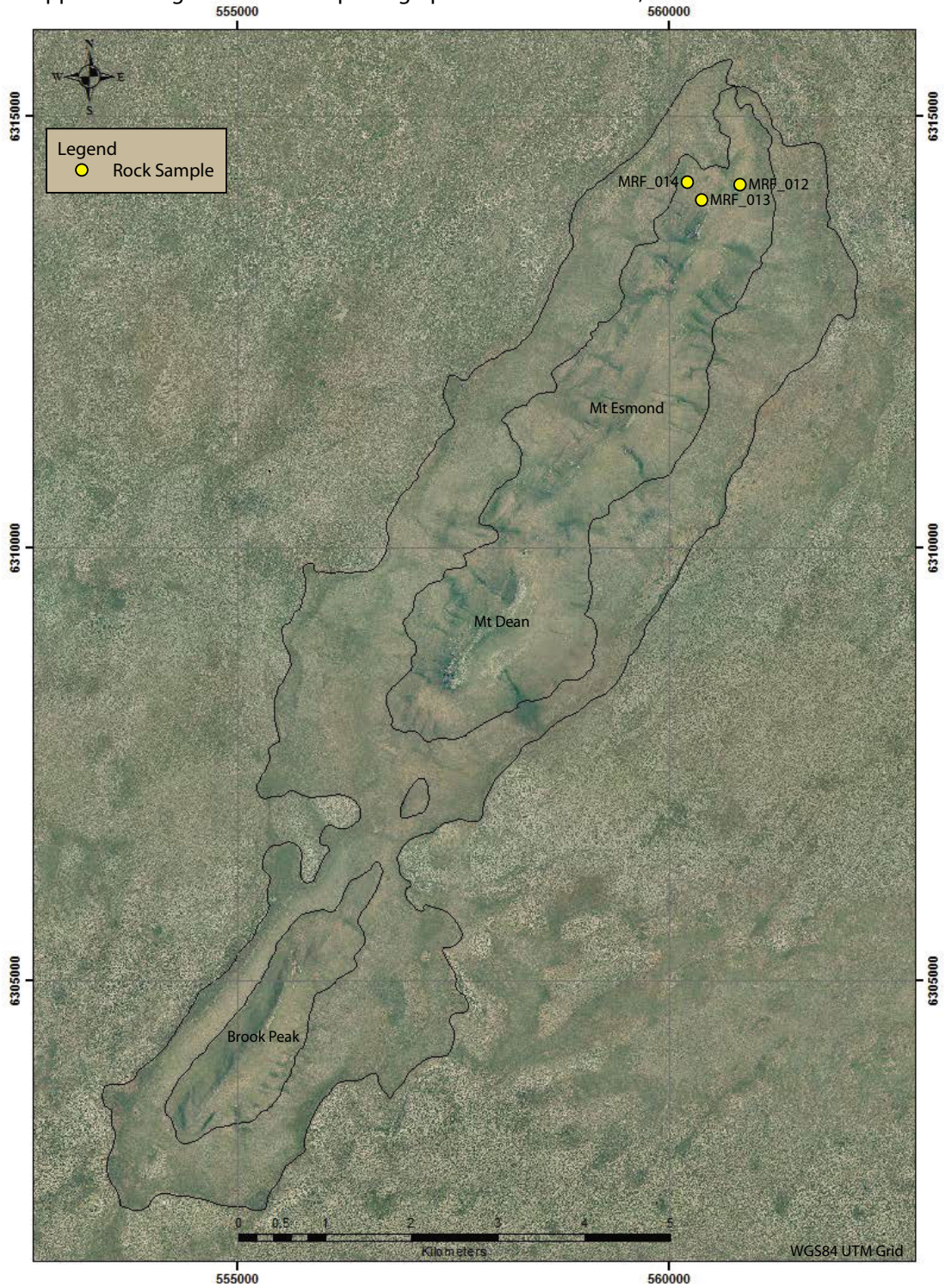
Figure A7.3: Mount Ragged structural data

Figure A7.4: Russell Range structural data

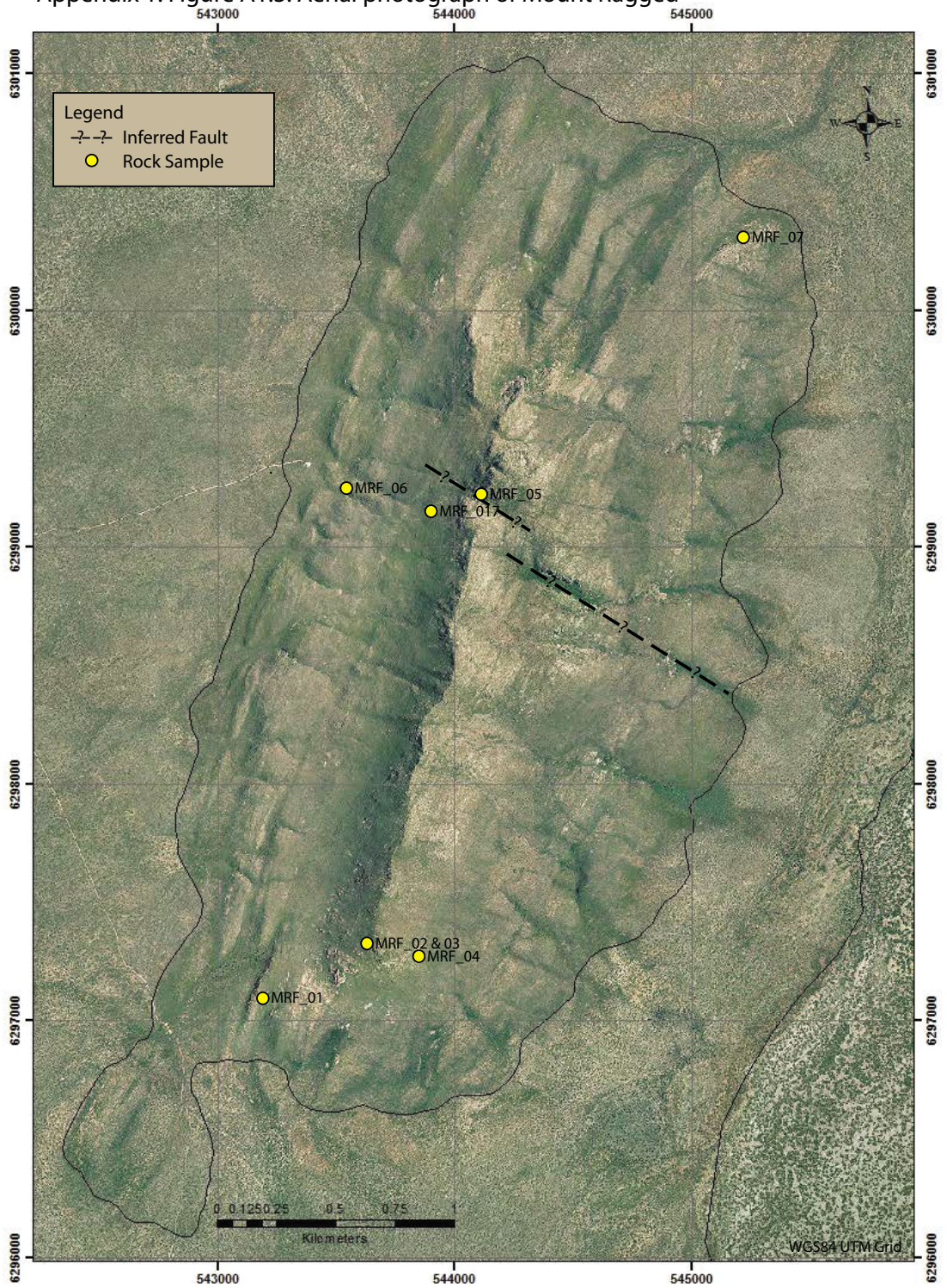
Appendix 1. Figure A1.1: Aerial photograph of Mica Hill



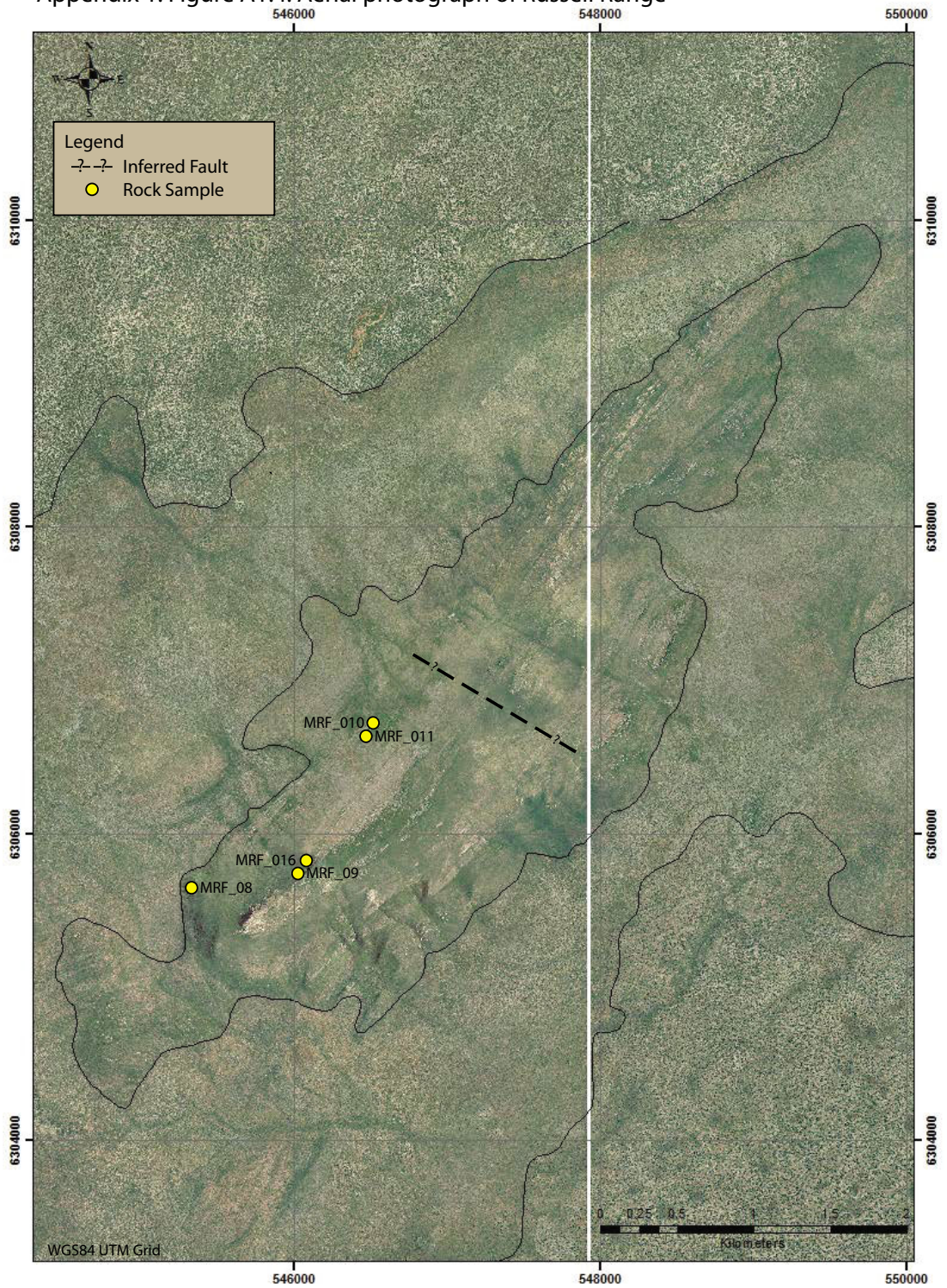
Appendix 1. Figure A1.2: Aerial photograph of Mount Esmond, Mount Dean and Brook Peak



Appendix 1. Figure A1.3: Aerial photograph of Mount Ragged



Appendix 1. Figure A1.4: Aerial photograph of Russell Range



## Appendix 2

**Table A2.1: Mount Ragged Formation sample catalogue**

All samples referred to in this catalogue are stored at the Department of Applied Geology, Curtin University, Perth, Western Australia

Sample ID	Collection ID	Locality	Easting*	Northing*	Collector	Lithology	Facies	Comments	Slide
MRF_01	PJW_01	Mt. Ragged	543181	6297087	P.Waddell	Metapelite schist	A	Quartz- Andalusite-Muscovite Schist	X
MRF_02	PJW_02	Mt. Ragged	543627	6297322	P.Waddell	Quartzite - Coarse-grained	D	Grey quartzite; Coarse grains in medium grained matrix; Poorly sorted	X
MRF_03	PJW_03	Mt. Ragged	543627	6297322	P.Waddell	Quartzite - Gritstone	E	Float; Well sorted	X
MRF_04	PJW_04	Mt. Ragged	543846	6297280	P.Waddell	Quartzite - Gritstone	E	Grey quartzite; Grit in coarse grained matrix; Poorly sorted	X
MRF_05	PJW_05	Mt. Ragged	544109	6299230	P.Waddell	Quartzite - Medium-grained	C/D	Pink/grey quartzite; medium grains with occasional coarse grains; Sedimentary Log 2	X
MRF_06	PJW_06	Mt. Ragged	543540	6299258	P.Waddell	Metasandstone - Fine-grained	B	Float; Well sorted	X
MRF_07	PJW_07	Mt. Ragged	545216	6300323	P.Waddell	Quartzite - Medium-grained	C	Well sorted; Viridine enriched mud drape	X
MRF_08	PJW_08	Russell Range	545298	6305674	P.Waddell	Metasandstone - Fine-grained	C	Siliceous (metasiltstone) tectonic foliation surface	X
MRF_09	PJW_09	Russell Range	546098	6305792	P.Waddell	Quartzite - Medium-grained	C	Well-sorted; Viridine veins	X
MRF_10	PJW_10	Russell Range	546468	6306648	P.Waddell	Metasiltstone	A	Andalusite-bearing metasiltstone	X
MRF_11	PJW_11	Russell Range	546468	6306648	P.Waddell	Quartzite - Metasiltstone	A/B	Andalusite-bearing metasiltstone surface	X
MRF_12	PJW_12	Mt. Esmond	560798	6314242	P.Waddell	Quartzite - Medium-grained	C	Well-bedded, pink quartzite	N/A
MRF_13	PJW_13	Mt. Esmond	560364	6314103	P.Waddell	Metasiltstone rip-up clasts in medium-grained quartzite matrix	C		N/A
MRF_14	PJW_14	Mt. Esmond	560206	6314258	P.Waddell	Metasiltstone rip-up clasts in medium-grained quartzite matrix	C		X
MRF_15	PJW_15	Mica Hill	548991	6284473	P.Waddell	Quartzite - Coarse-grained	D		X
MRF_16A	PJW_16A	Russell Range	546100	6305800	P.Waddell	Quartzite - Medium-grained	C	Grey quartzite; Massive	X
MRF_16B	PJW_16B	Russell Range	546100	6305800	P.Waddell	Quartzite - Medium-grained	C	Pink quartzite; Well bedded	X
MRF_17	PJW_17	Mt. Ragged	543898	6299164	P.Waddell	Quartzite - Medium-grained	C	Float; Weathered; Tower Peak Path	X

\* Using MGA Datum: WGS84; Field area within Zone 51H

### Appendix 3. Figure A3.1

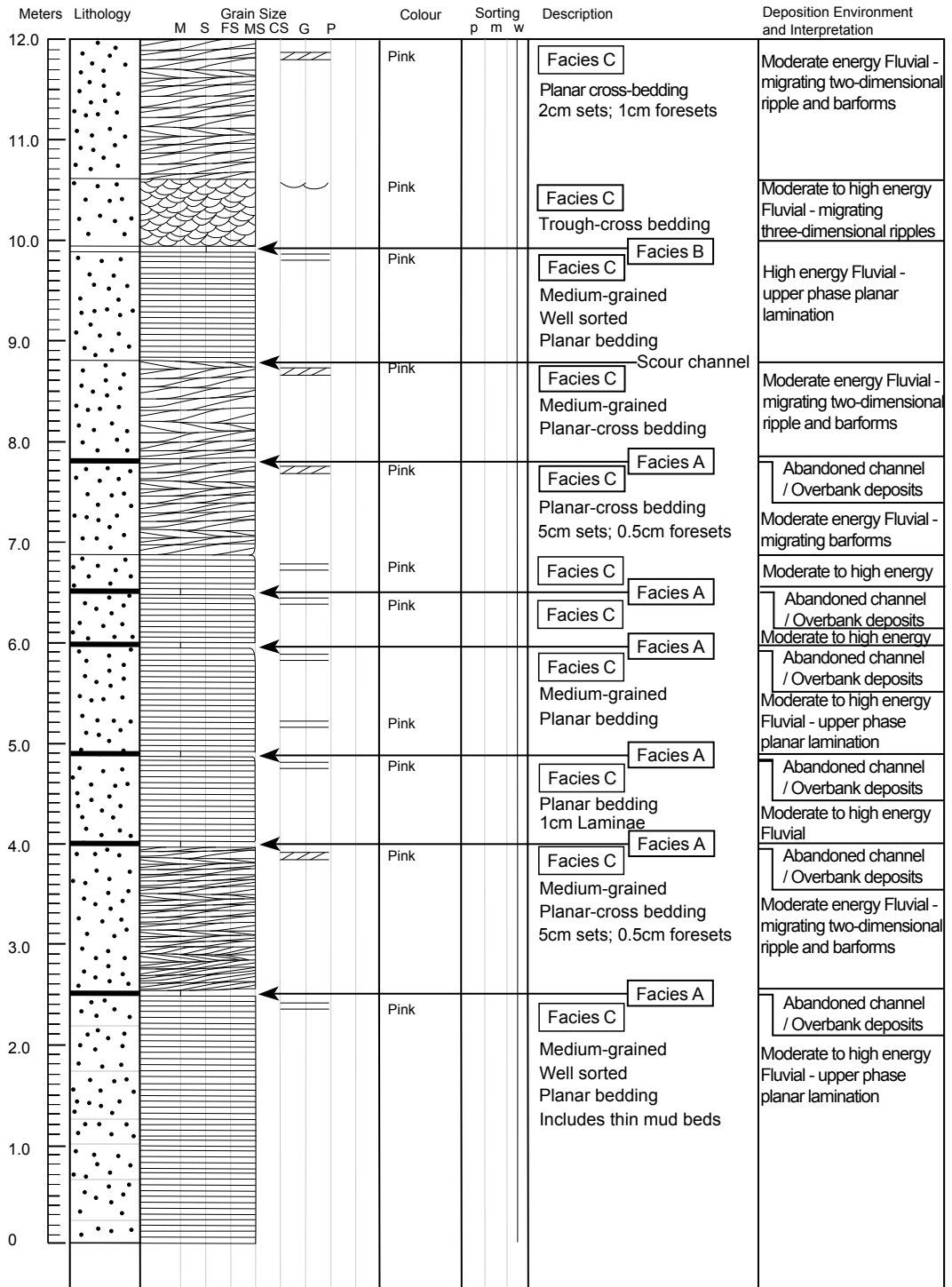
Russell Range Sedimentary Log 1 - Cliff section, southwest Russell Range

Name: P. Waddell / P. Russell

Date: 1 November 2012

Location: 51H 0545717 6305538 WGS84

Log Sheet: 1 (of 2)



### Appendix 3. Figure A3.1 (continued)

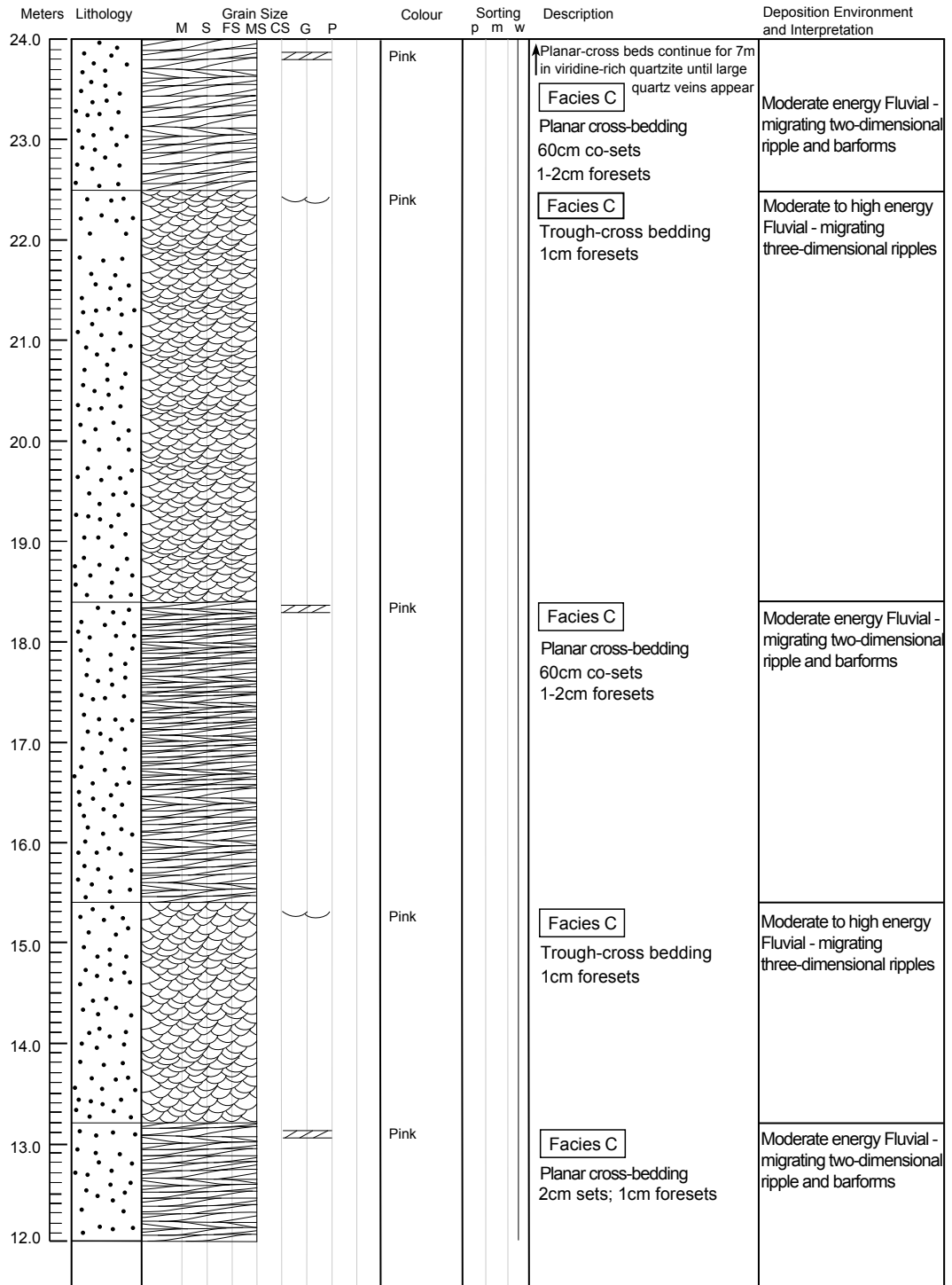
Russell Range Sedimentary Log 1 - Cliff section, southwest Russell Range

Name: P. Waddell / P. Russell

Date: 1 November 2012

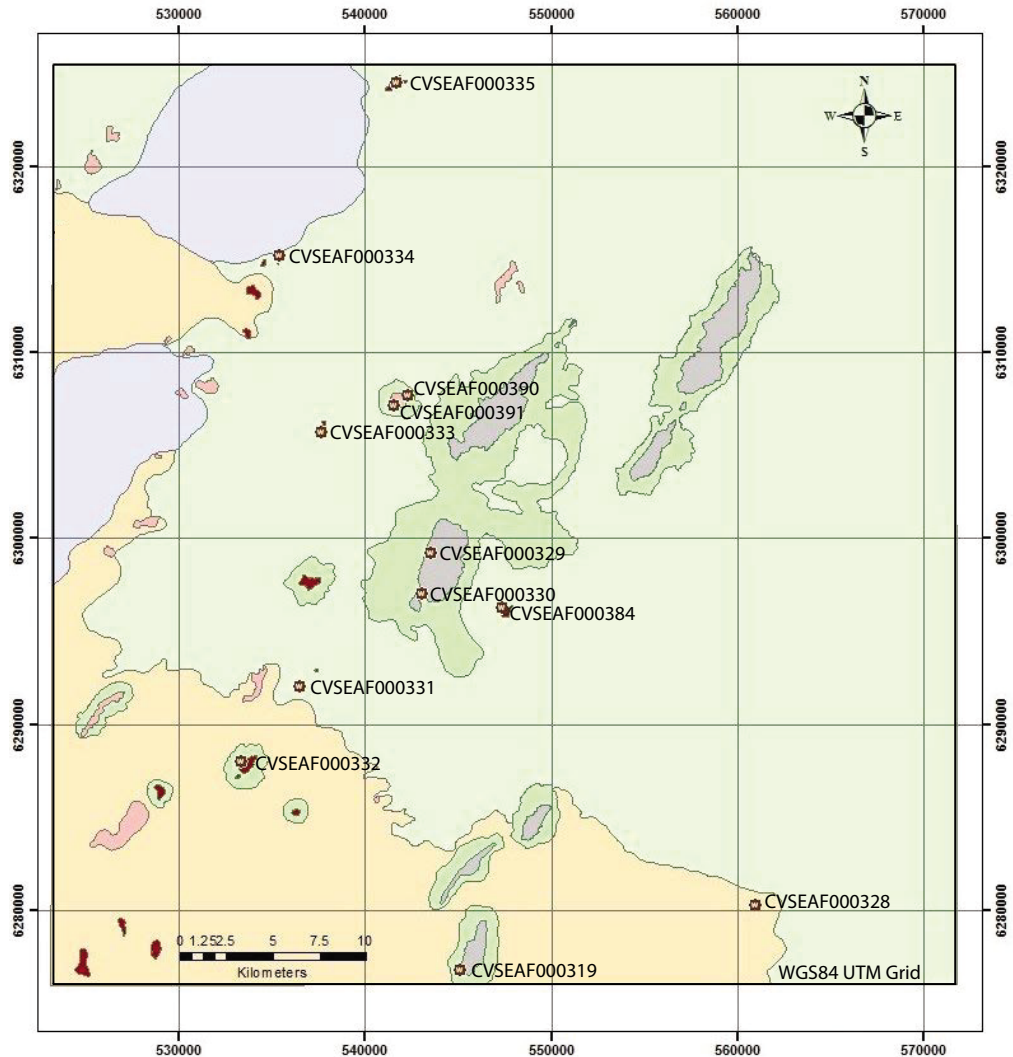
Location: 51H 0545717 6305538 WGS84

Log Sheet: 2 (of 2)



## Appendix 4

### GSWA Warox sites in the vicinity of the Mount Ragged Formation



Site ID	Lithology	Location
CVSEAF000319	Psammitic Schist	Diamond Hill
CVSEAF000328	Monzogranite	Sheoaks Hill
CVSEAF000329	Psammitic Schist	Mt. Ragged
CVSEAF000330	Psammitic Schist	Mt. Ragged
CVSEAF000331	Granitic Gneiss	Outcrop northeast of Gora Hill
CVSEAF000332	Metamonzogranite	Gora Hill
CVSEAF000333	Metamonzogranite	Junana Rock
CVSEAF000334	Metamonzogranite	Pine Hill
CVSEAF000335	Metamonzogranite	Juranda Rockhole
CVSEAF000384	Monzogranite	Scott Rock
CVSEAF000390	Foliated Metagranite	Wolgrah Hill
CVSEAF000391	Foliated Metagranite	Wolgrah Hill

## Appendix 4

**Table A4.1: Geological Survey of Western Australia Warox sites in the vicinity of the Mount Ragged Formation**

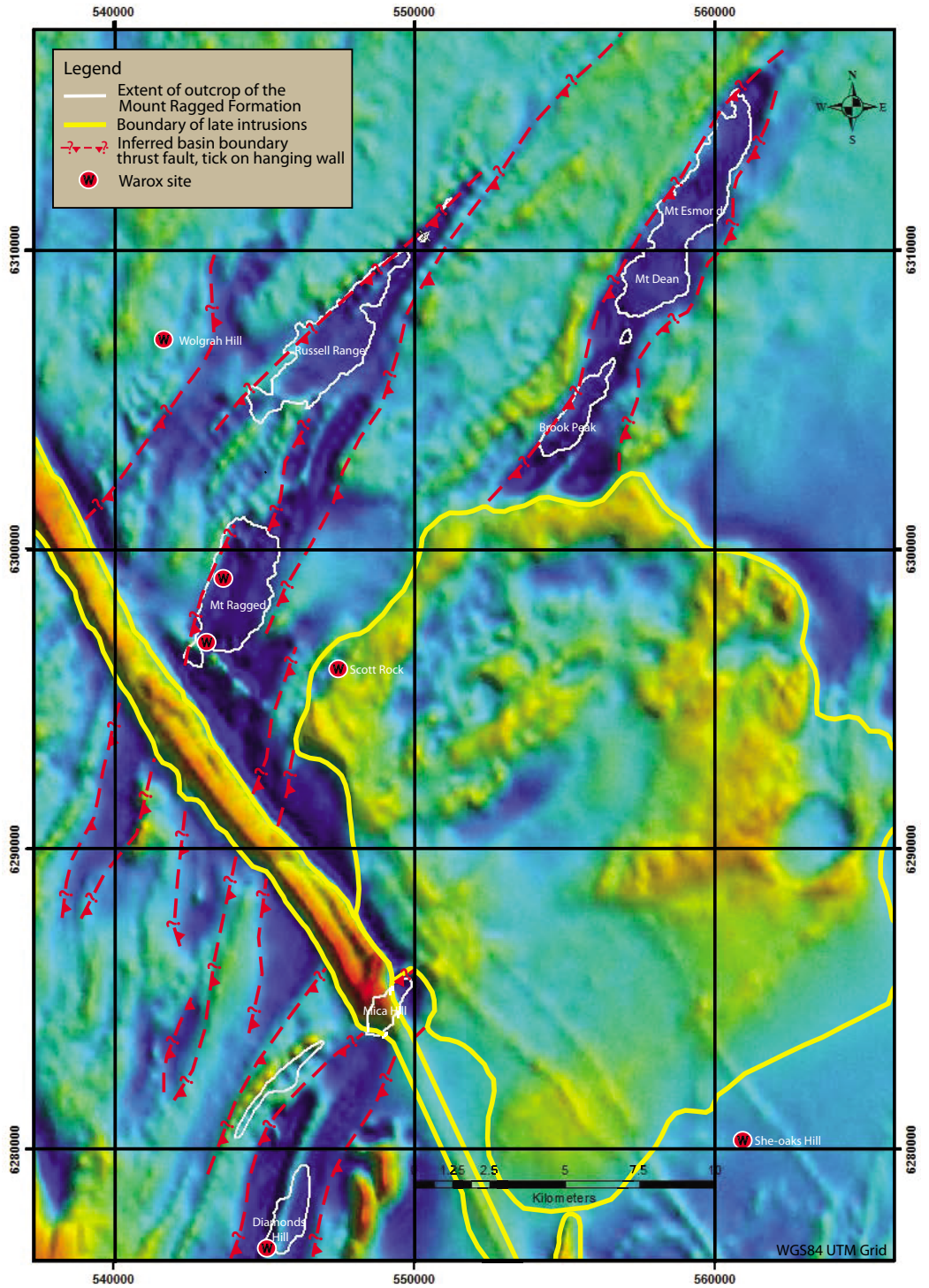
Information supplied by the Geological Survey of Western Australia through Warox summary reports and Kirkland & Wingate (2013 – unpublished preliminary reports on U-Pb Geochronology Samples); MSWD: Mean Standard Weighted Deviation.

Site ID	Sample ID	Location	Easting	Northing	Lithology	Rock Type	Lithology Description	Geochronology (U-Pb)
CVSEAF000319	194866	Diamonds Hill	545094	6276797	Psammitic Schist	Metasedimentary siliciclastic	Fine- to medium-grained, well foliated. Contains quartz, muscovite and biotite. Magnetic susceptibility readings are zero.	A conservative estimate of the maximum age of deposition is provided by the weighted mean $^{207}\text{Pb}^*/^{206}\text{Pb}^*$ date of <b>1331 ± 19 Ma</b> (MSWD = 0.91).
CVSEAF000328	194873	Sheoaks Hill	560930	6280270	Monzogranite	Igneous felsic intrusive	Medium- to coarse-grained. Abundant K-feldspar phenocrysts 2-3cm long. Moderate amounts of biotite and hornblende. Weak to moderate alignment of K-feldspar phenocrysts but not the matrix, which suggests a magmatic fabric. Non-magnetic susceptibility readings.	
CVSEAF000329	194874	Mt. Ragged	543567	6299223	Psammitic Schist	Metasedimentary siliciclastic	Medium-grained. Grades from quartzite to psammitic schist, with thin pelitic beds. Well developed cross-trough beds.	A conservative estimate of the maximum age of deposition is provided by a weighted mean $^{207}\text{Pb}^*/^{206}\text{Pb}^*$ date of <b>1340 ± 16 Ma</b> (MSWD = 2.0).
CVSEAF000330	194875	Mt. Ragged	543042	6296990	Psammitic Schist	Metasedimentary siliciclastic	Medium-grained. Grades from quartzite to psammitic schist.	A conservative estimate of the maximum age of deposition is provided by a weighted mean $^{207}\text{Pb}^*/^{206}\text{Pb}^*$ date of <b>1314 ± 19 Ma</b> (MSWD = 2.0).
CVSEAF000331	-	Northeast of Gora Hill	536485	6292005	Granitic Gneiss	Meta-igneous felsic intrusive	Banded, even-grained granitic gneiss with layer-parallel leucosomes. Magnetic susceptibility readings range from 910 to 1150 x 10 <sup>-5</sup> SI.	

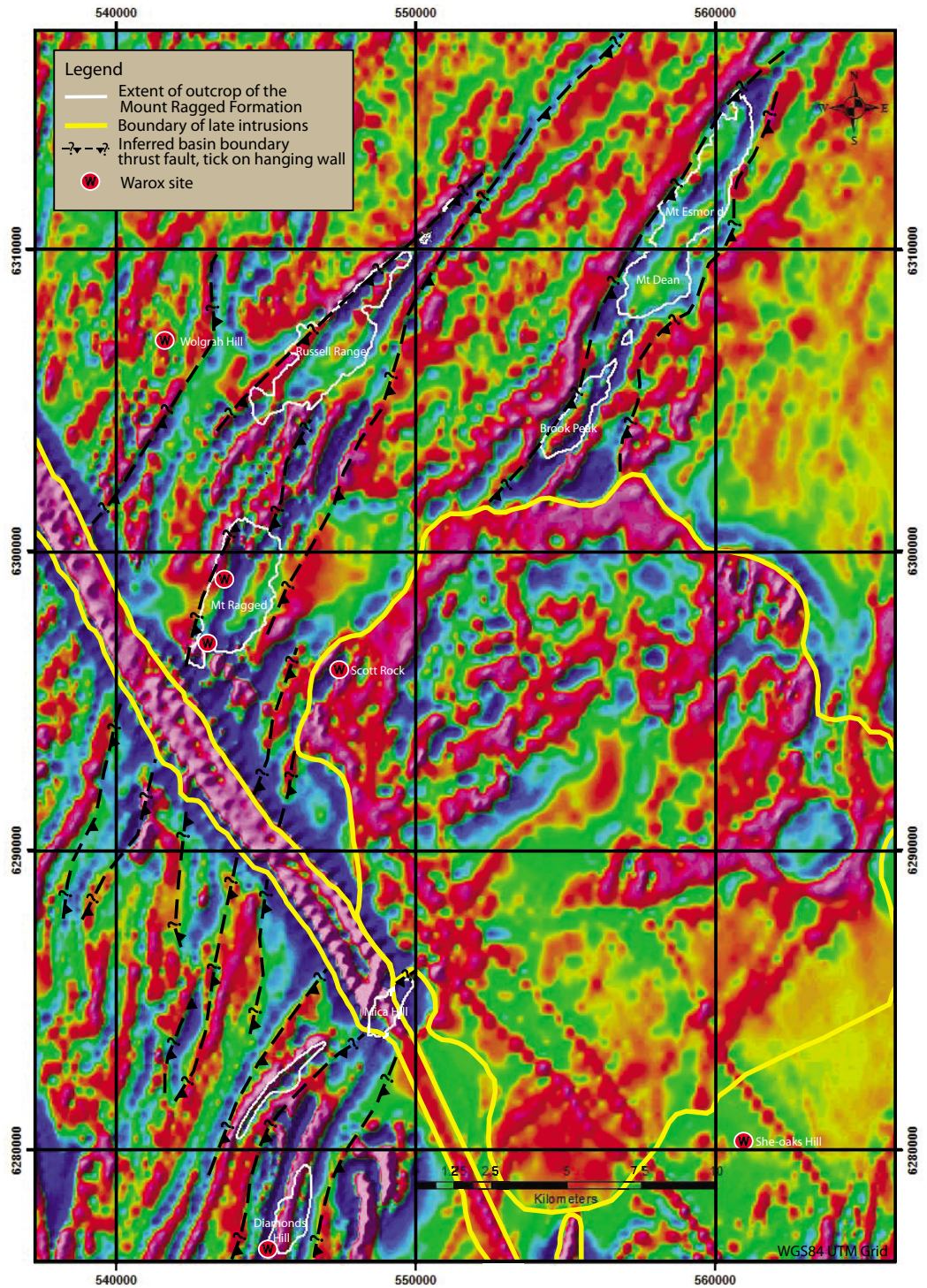
Site ID	Sample ID	Location	Easting	Northing	Lithology	Rock Type	Lithology Description	Geochronology (U-Pb)
CVSEAF000332	194876	Gora Hill	533378	6287989	Metamonzogranite	Meta-igneous felsic intrusive	Fine- to medium-grained, equigranular, slightly banded. Fairly quartz-rich and leucocratic. Magnetic susceptibility readings are zero.	Concordia age of <b>1327 ± 8 Ma (MSWD = 1.8)</b> , interpreted as the age of magmatic crystallization.
CVSEAF000333	194877	Junana Rock	537674	6305705	Metamonzogranite	Meta-igneous felsic intrusive	Medium-grained, slightly porphyritic with biotite aggregates. Minor hornblende. Homogeneous. Foliation is cut by granitic to coarser pegmatitic veins and minor quartz veins. Foliation is stronger, more gneissic, and the rock more biotite-rich than Gora Hill to the SE. Magnetic susceptibility readings range from 460 to 860 x 10 <sup>-5</sup> SI.	
CVSEAF000334	194878	Pine Hill	535399	6315167	Metamonzogranite	Meta-igneous felsic intrusive	Fine- to medium-grained, homogeneous, equigranular, moderate to strong foliation. Magnetic susceptibility readings range from 80 to 130 x 10 <sup>-5</sup> SI.	
CVSEAF000335	194879	Juranda Rockhole	541725	6324451	Metamonzogranite	Meta-igneous felsic intrusive	Fine-grained, equigranular. SE side garnet-bearing / NW side lacks garnet. Magnetic susceptibility readings in garnet-bearing phase range from 100 to 200 x 10 <sup>-5</sup> SI, whereas in the non-garnet phase readings range from 700 to 1100 x 10 <sup>-5</sup> SI.	
CVSEAF000384	192584 <b>192586</b> 192587	Scott Rock	547537	6296127	Monzogranite	Igneous felsic intrusive	Medium-grained, porphyritic with 2-3cm long K-feldspar phenocrysts. Equigranular matrix of two feldspars, quartz and biotite, average grainsize 3mm. Also has magnetite. Contains small mafic xenoliths, mostly a few cm long and rectangular or rounded. No signs of deformation. Moderate to high magnetic susceptibility.	Concordia age of <b>1175 ± 12 Ma (MSWD = 1.5)</b> , interpreted as the magmatic crystallization age.

Site ID	Sample ID	Location	Easting	Northing	Lithology	Rock Type	Lithology Description	Geochronology (U-Pb)
CVSEAF000385	192585	Scott Rock	547449	6295994	Xenolith in Monzogranite	Mafic intrusive	Here is a long xenolith ~ 3m long x 20 cm wide, finely layered on the mm-cm scale. Thinly layered mafic to granitic compositions in matrix of feldspar, quartz and biotite, with an average grainsize 3mm. Same magnetic susceptibility as host monzogranite.	
CVSEAF000390	-	Wolgrah Hill	542147	6307391	Foliated Metagranite	Meta-igneous felsic intrusive	Medium-grained, equigranular to seriate textured. Grainsize 3-4 mm; some K-feldspar phenocrysts ≤5cm. Plagioclase common; Monzogranite to granodiorite composition. Homogeneous with a moderately developed foliation trending NE. Metagranite is not the same as Scott Rock Monzogranite. Magnetic susceptibility readings less than Scott Rock; averaging $6 \times 10^{-3}$ SI.	
CVSEAF000391	192588	Wolgrah Hill	541722	6307231	Foliated Metagranite	Meta-igneous felsic intrusive	Medium-grained, equigranular to seriate textured. Grainsize 3-4 mm; some K-feldspar phenocrysts ≤5cm. Plagioclase common; Monzogranite to granodiorite composition. Homogeneous with a moderately developed foliation trending NE. Metagranite is not the same as Scott Rock Monzogranite.	

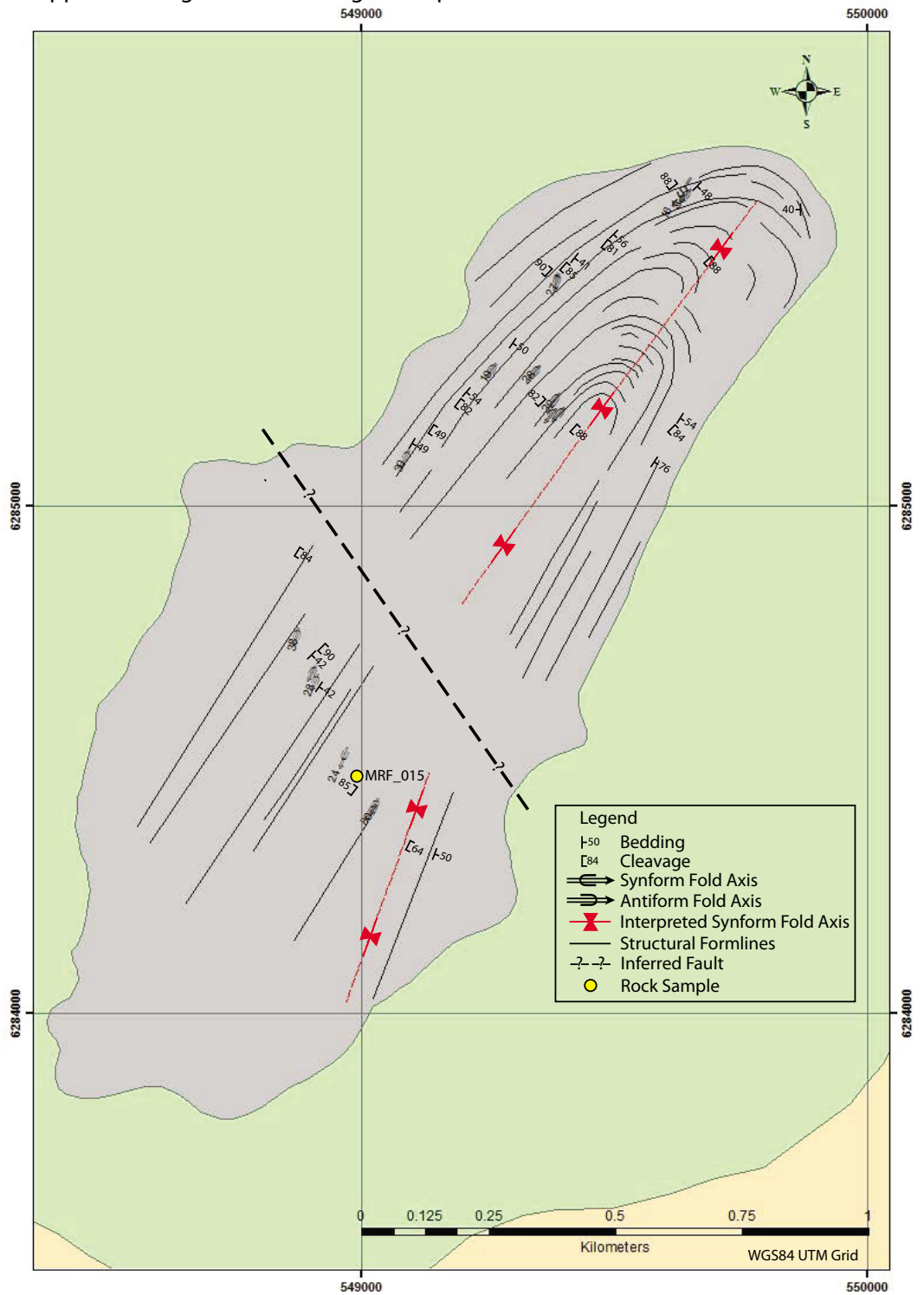
Appendix 5. Figure A5.1: Aeromagnetic image of Mount Ragged Formation  
(Reduction to pole; normal)



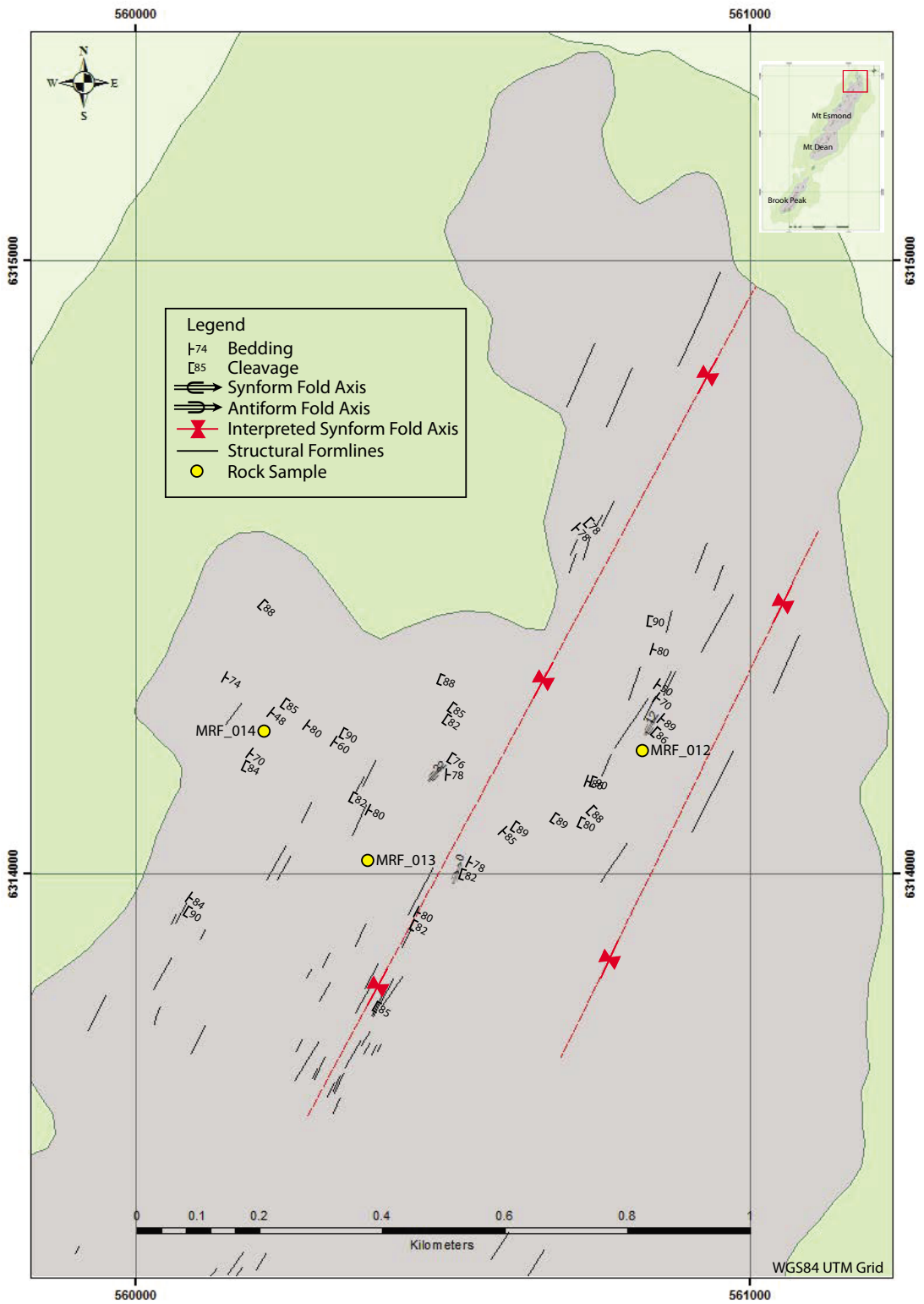
Appendix 5. Figure A5.2: Aeromagnetic image of Mount Ragged Formation  
(Reduction to pole, first vertical derivative; Sun angle northwest)



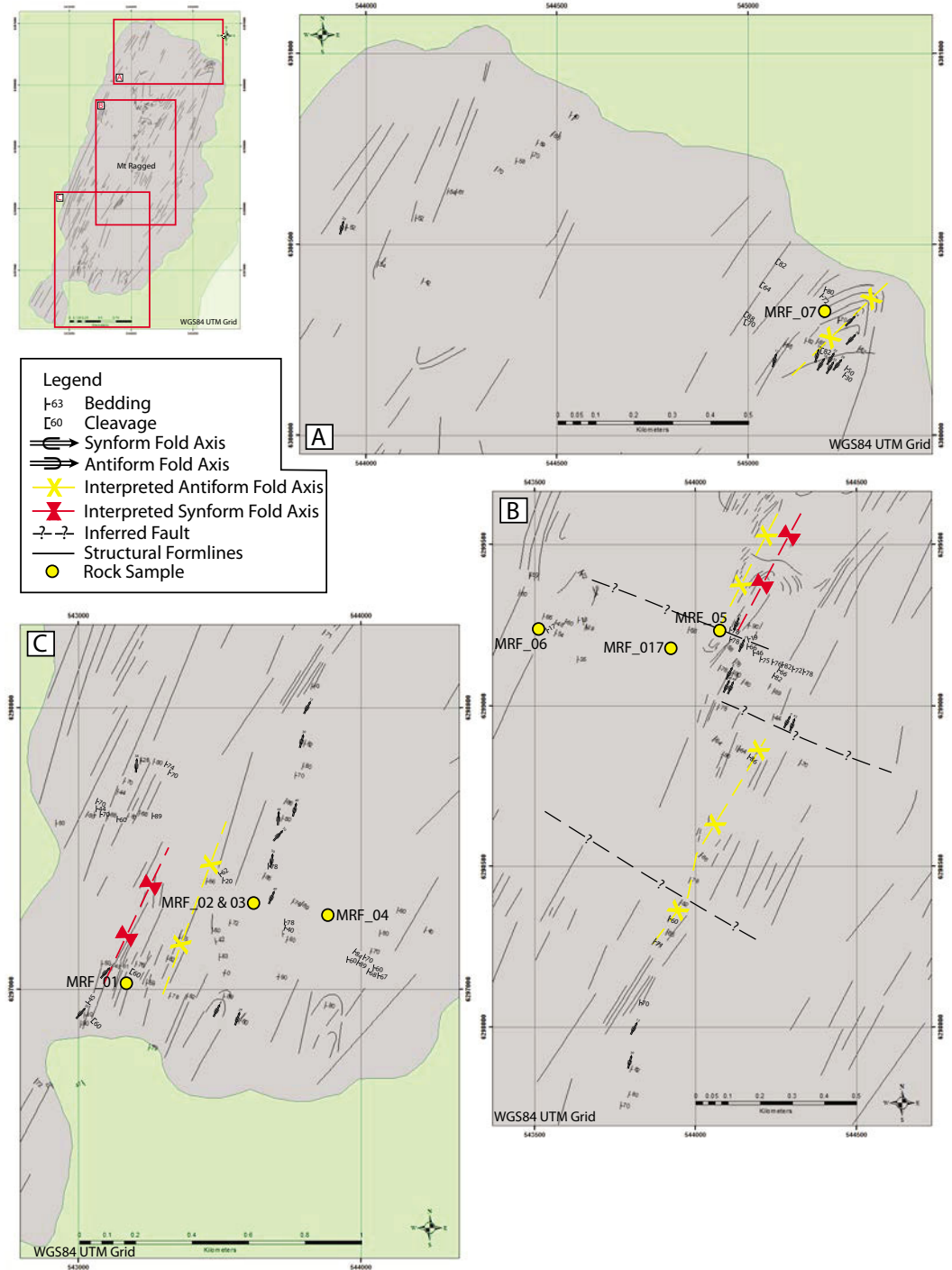
Appendix 6. Figure A6.1: Geological map of Mica Hill



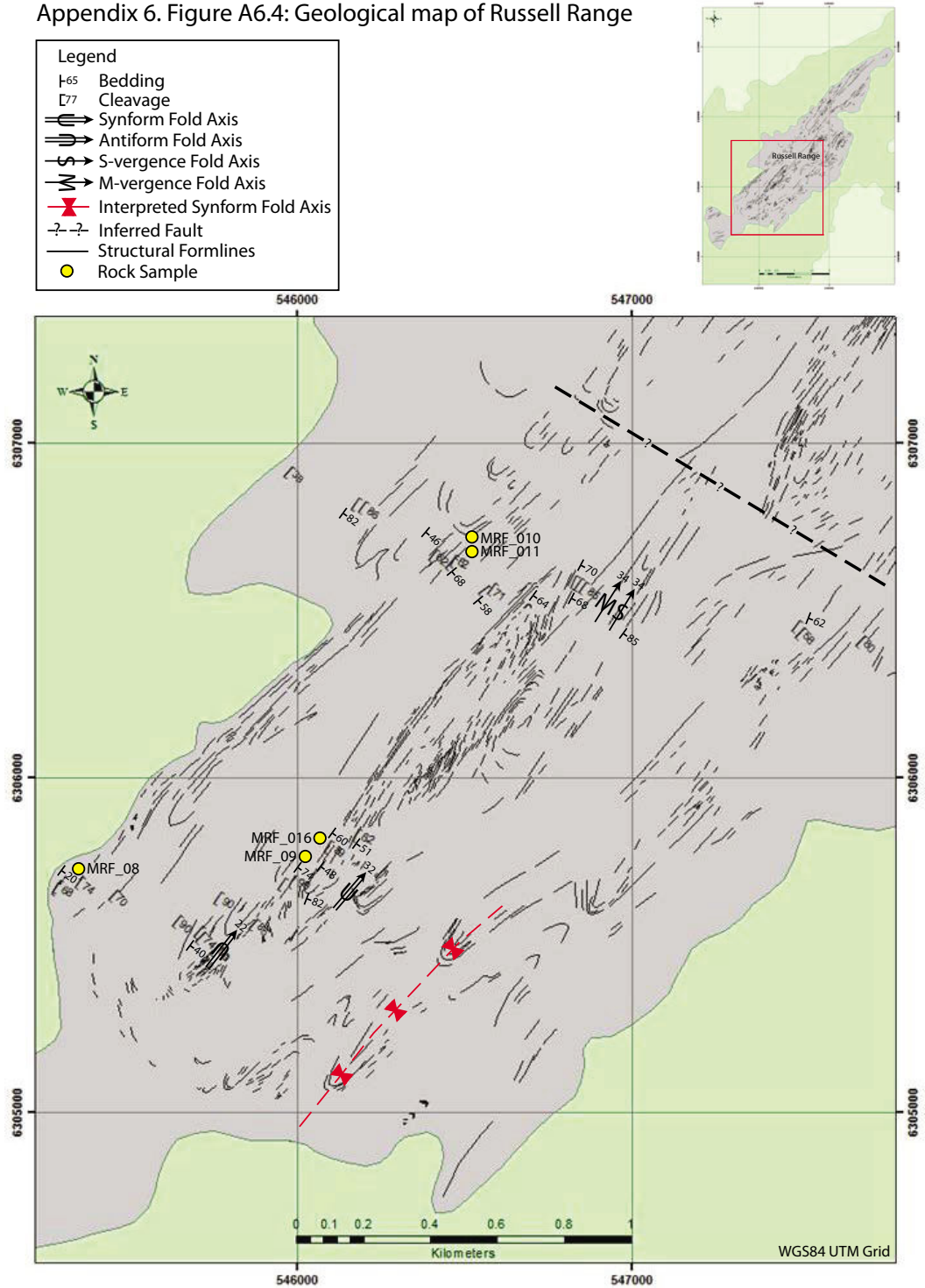
Appendix 6. Figure A6.2: Geological map of Mount Esmond



Appendix 6. Figure A6.3: Geological map of Mount Ragged



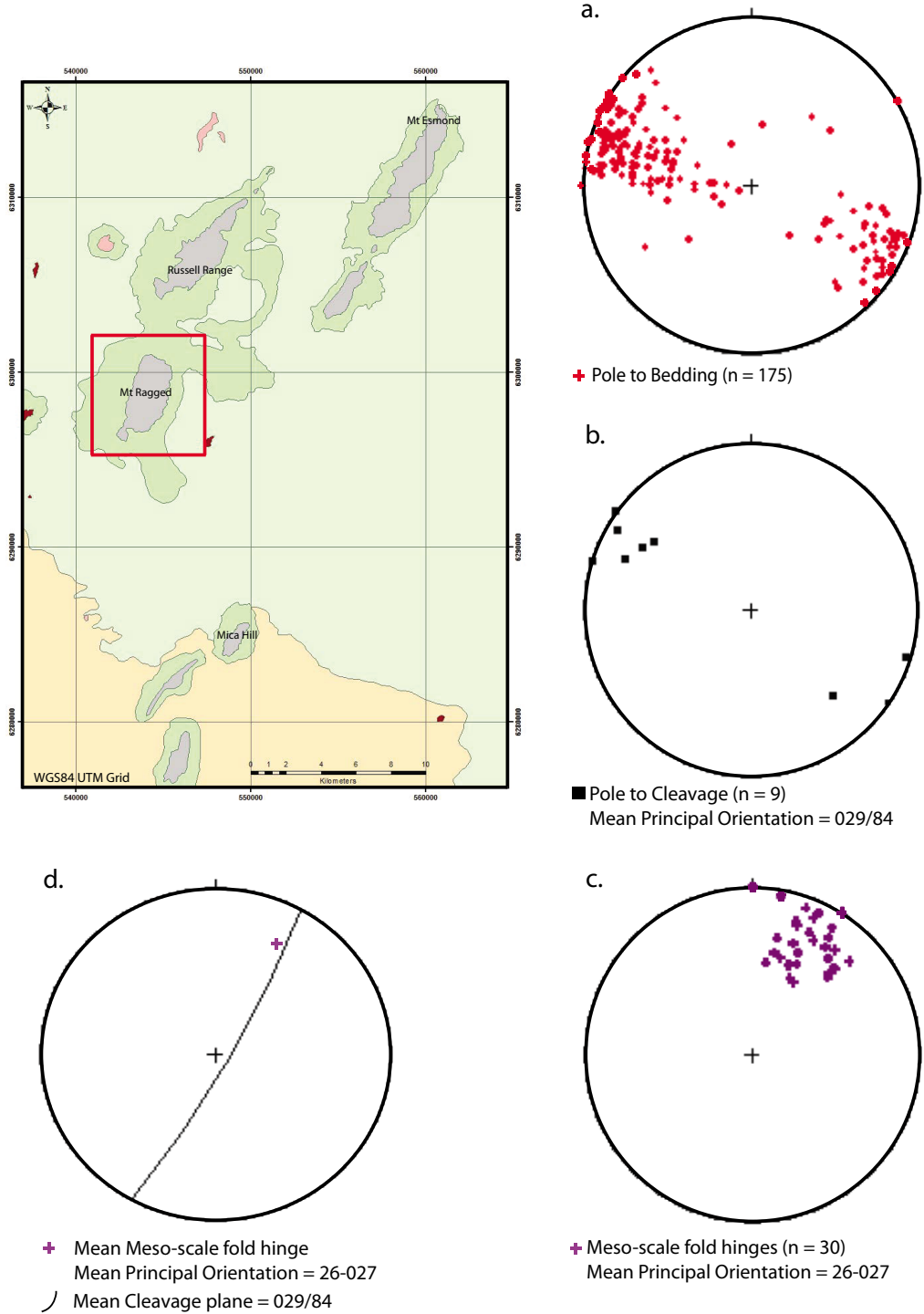
Appendix 6. Figure A6.4: Geological map of Russell Range



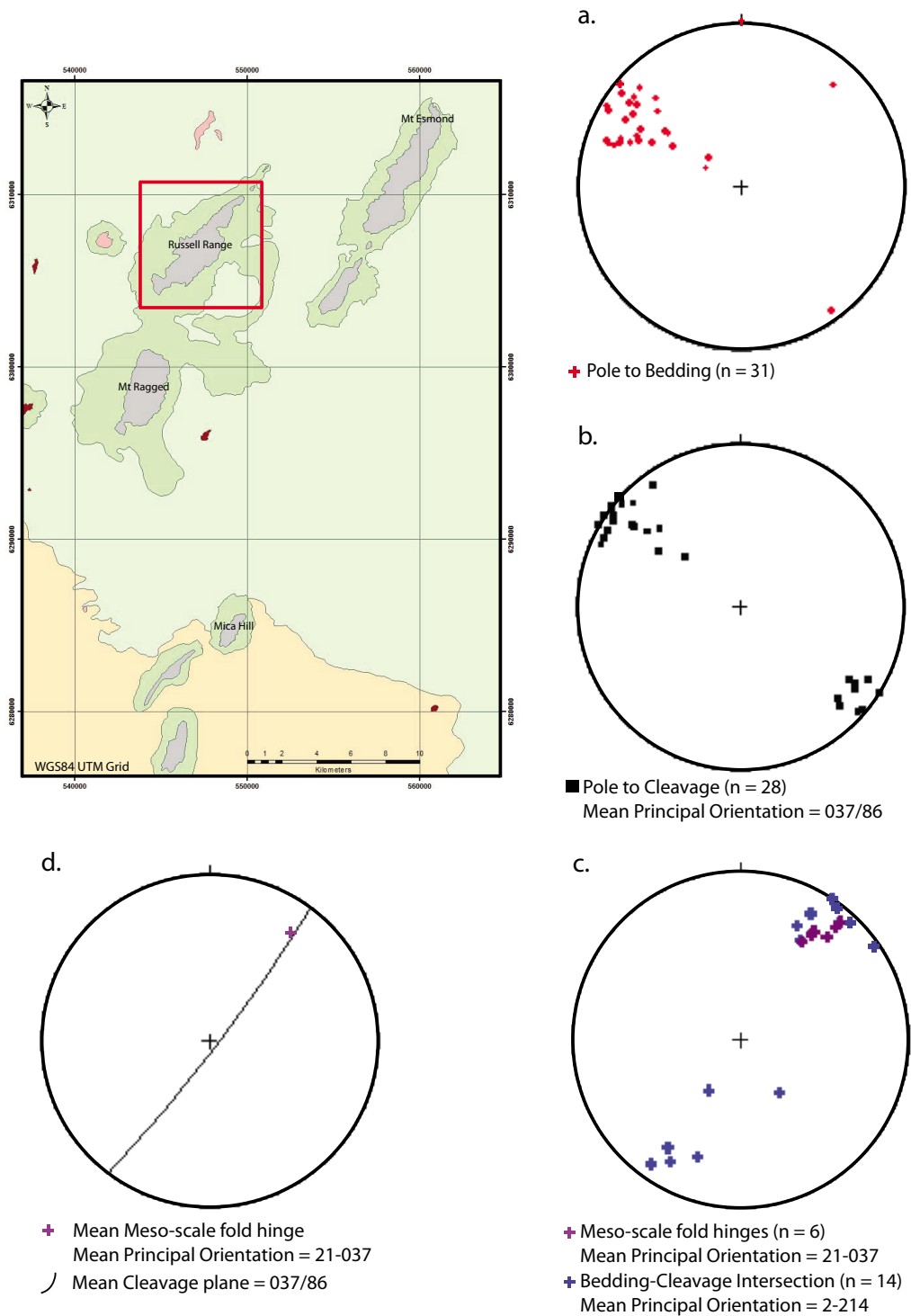




Appendix 7. Figure A7.3: Mount Ragged Structural Data



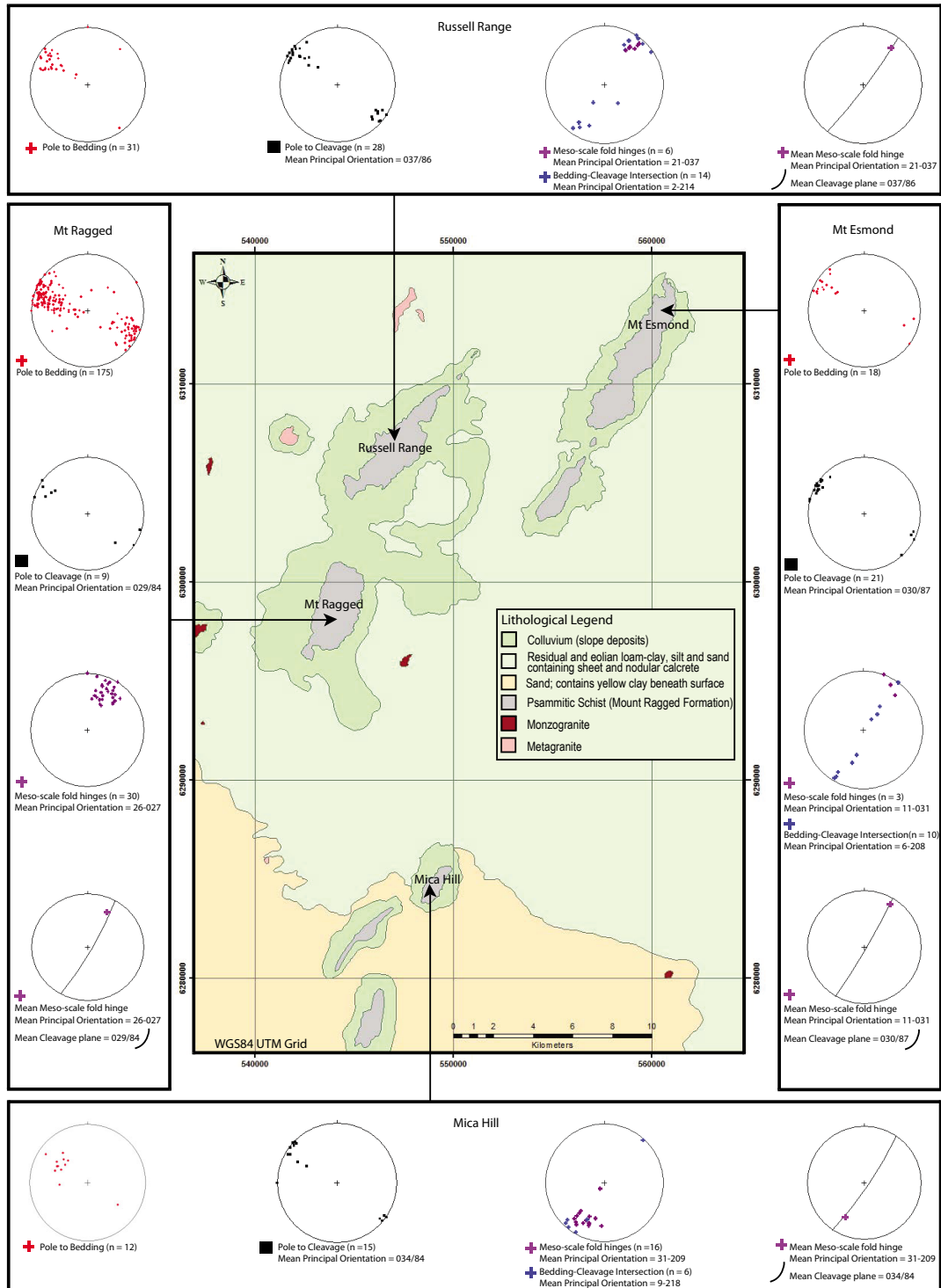
Appendix 7. Figure A7.4: Russell Range Structural Data



# PLATES

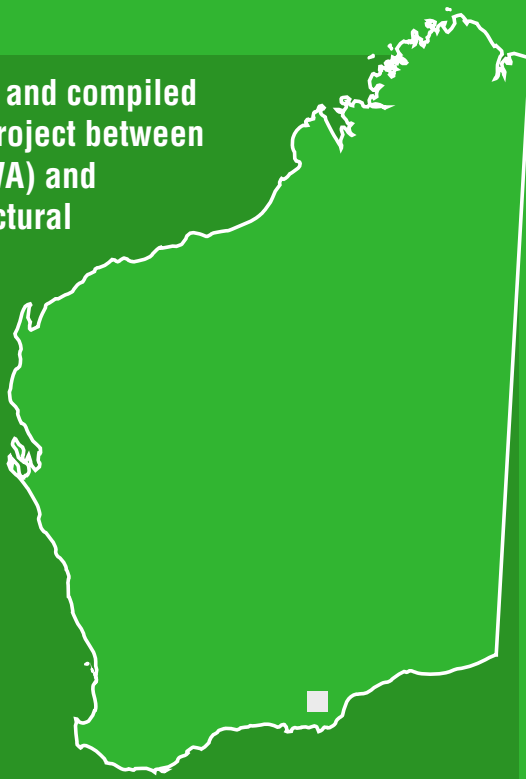
Plate 1: Compilation of structural data for the Mount Ragged Formation

Plate 1: Compilation of structural data for the Mount Ragged Formation



This Report is an MSc thesis researched, written and compiled by the author through an ongoing collaborative project between the Geological Survey of Western Australia (GSWA) and Curtin University. The sedimentological and structural development of the Mesoproterozoic Mount Ragged Formation is characterized based on detailed field mapping, interpretation of aerial photography and aeromagnetic datasets, facies and sedimentary petrography analysis, and structural analysis of field data.

The sediments are interpreted to have been deposited within a shallow intracratonic basin by a large fluvial system dominated by a shifting complex of sandy braided channels. The gradual coarsening upwards sequence of lithofacies suggests the depositional setting was a distal fluvial environment characterized by channel migration and abandonment changing to a proximal fluvial environment. This environment, in turn, was characterized by rapid periods of sedimentation and coarser deposits. The structural data, field observations, and interpretation of aeromagnetic imagery suggest the Mount Ragged Formation occurs in a zone where regional strain was partially accommodated through the deformation and subsequent emplacement of fault-bound metasedimentary packages.



Further details of geological products and maps produced by the Geological Survey of Western Australia are available from:

Information Centre  
Department of Mines and Petroleum  
100 Plain Street  
EAST PERTH WA 6004  
Phone: (08) 9222 3459 Fax: (08) 9222 3444  
[www.dmp.wa.gov.au/GSWApublications](http://www.dmp.wa.gov.au/GSWApublications)